Characterization of an Amphipathic Alpha-Helix in the Membrane Targeting and Viral Genome Replication of Brome Mosaic Virus

Preethi Sathanantham

Dissertation submitted to the faculty of the Virginia Polytechnic Institute and State University in partial fulfillment of the requirements for the degree of

Doctor of Philosophy

In

School of Plant and Environmental Sciences

Prof. Xiaofeng Wang, Chair

Prof. Boris Vinatzer

Prof. Xiang-Jin Meng

Prof. Daniel Capelluto

January 21, 2022

Blacksburg, VA

Keywords: Keywords: (+)RNA viruses, alphavirus-like superfamily, brome mosaic virus, membrane associations, amphipathic helices, viral genome replication

Characterization of an Amphipathic Alpha-Helix in the Membrane Targeting and Viral Genome Replication of Brome Mosaic Virus

Preethi Sathanantham

ABSTRACT

Positive-strand RNA viruses associate with specific organelle membranes of host cells to establish viral replication complexes. The replication protein 1a of brome mosaic virus associates strongly with the nuclear endoplasmic reticulum (ER) membranes, invaginates membranes into the lumen, and recruits various host proteins to establish replication complexes termed spherules. 1a has a strong affinity towards the perinuclear ER membrane, however, the structural features in 1a that dictate its membrane associations and thereby membrane remodeling activities are unclear. This study examined the possible role of an amphipathic α-helix, helix B, in BMV 1a's membrane association. Deletion or single substitution of multiple amino acids of helix B abolished BMV 1a's localization to nuclear ER membranes. Additional reporter-based, gain-of-function assays showed that helix B is sufficient in targeting several soluble proteins to the nuclear ER membranes. Furthermore, we found that the helix B-mediated organelle targeting is a functionally conserved feature among positive-strand RNA viruses of the alphavirus-like superfamily that includes notable human viruses such as Hepatitis E virus and Rubella virus as well as plant viruses such as cucumber mosaic virus and cowpea chlorotic mottle virus. Our results demonstrate a critical role for helix B across members of the alphavirus-like superfamily in anchoring viral replication complexes to the organelle membranes. We anticipate our findings to be a starting point for the development of sophisticated models to use helix B as a novel target for the development of antivirals for positive-strand RNA viruses that belong to the alphavirus-like superfamily.

Characterization of an Amphipathic Alpha-Helix in the Membrane Targeting and Viral Genome Replication of Brome Mosaic Virus

Preethi Sathanantham

GENERAL AUDIENCE ABSTRACT

Among the seven classes of viruses, the positive-strand RNA viruses dominate the domain of viral diseases of the world. Brome mosaic virus (BMV) is a positive-strand RNA virus that infects cereal crops such as wheat, barley, and rice. BMV has a simple genome organization and serves as a suitable model virus to study and characterize positive-strand RNA viruses. The replication of all positive-strand RNA viruses occurs at the organelle membranes of the host. Membrane association of the replication is one of the early steps and a crucial event in the life cycle of positive-strand RNA viruses. One of the proteins produced early on during BMV infection is the replication protein 1a, which is also the master regulator of viral replication; 1a recruits viral factors in addition to hijacking the necessary host factors at the membranous sites to initiate replication. Upon reaching the organelle membranes, 1a induces membrane rearrangements to form viral replication complexes that safeguard the recruited factors from the deleterious effects of the host cell. The structural determinants within 1a that are responsible for such membrane association are unknown. This study explored the potential roles of a short helical motif within the 1a protein for its ability to dictate such site-specific membrane associations. We show here that this helical region is necessary and sufficient for 1a's membrane-binding activity. We also discovered it to be a functionally conserved feature that is responsible for membrane associations in various viruses of the alphavirus-like superfamily that includes some of the notable human viruses such as Hepatitis E virus and Rubella virus in addition to plant viruses such as cucumber mosaic virus and cowpea chlorotic mottle virus.

“For Bella and O”

ACKNOWLEDGEMENTS

I wish to thank the following people for helping me throughout my research and in the preparation of this dissertation.

Dr. Xiaofeng Wang, my mentor, to whom I owe a deep sense of gratitude for giving me an opportunity to pursue research in his lab and also for providing intellectual guidance throughout this work. Thank you for your astounding editing and feedback during the manuscript preparation as well as dissertation. This research had me motivated and kept me curious throughout the research period.

My lab mates with whom I conducted research and who helped me get adjusted to the program while I was still new to the lab- Zhenlu Zhang, Guijuan He, Wenhao Zhao, and Haijie Liu.

Parkesh Suseendran, Xin Zhang, and Haijie Liu for collegiality of work, generosity, and their calming spirit in the lab.

Heartfelt thanks to my committee members, Dr. Boris Vinatzer, for his insightful thoughts and interesting questions during my preliminary examination that provoked an interest to understand the evolutionary aspect of viruses.

Dr. X. J. Meng, for awakening an interest in animal viruses and helping me understand my research in a broader context of viruses.

Dr. Daniel Capelluto, for his excellence in protein biochemistry and questions that helped me strengthen the basic and advanced concepts in the molecular biology of the cell which I did apply throughout my research in the lab.

My parents, Mallika Sathanantham, and Sathanantham Balaiyan, for perspective and will to strive.

Table of Contents

List of Figures

List of Tables

List of Abbreviations

(+)RNA:	positive-strand RNA
ACBP:	acyl coA binding protein
BMV:	*Brome mosaic virus*
CAP:	capping domain
CCMV:	*Cowpea chlorotic mottle virus*
Cho2p:	choline-requiring 2
CMs:	convoluted membranes
CMV:	*Cucumber mosaic virus*
COP II:	coat protein complex II
SARS-CoV:	severe acquired respiratory syndrome-coronavirus
DENV:	*Dengue virus*
DMV:	double membrane vesicle
dsRNA:	double strand RNA
ER:	endoplasmic reticulum
FHV:	*Flock house virus*
GFP:	green fluorescent protein
HA:	Helix A
HB:	Helix B
HCV:	*Hepatitis C virus*
HEL:	helicase domain
HEV:	*Hepatitis E virus*
HMGCR:	3-hydroxy-methylglutaryl-CoA reductase
L32:	32aa containing linker
m7G:	7-methylguanylate
mC:	mCherry
MW:	molecular weight
nER:	perinuclear endoplasmic reticulum
Pah1:	phosphatidate phosphatase
PhER:	peripheral endoplasmic reticulum

PC: phosphatidylcholine

PDR: pathogen-derived resistance

PE: phosphatidylethanolamine

PEMT: phosphatidylethanolamine methyltransferase

Pgk: phosphoglycerate kinase

PI4P: phosphatidylinositol-4phosphate

PMME: phosphatidyl-*N*-monomethylethanolamine

PVDF: polyvinylidene fluoride

RHD: reticulon homology domain

RTNs: reticulons

RuV: *Rubella virus*

SMV: single membrane vesicle

TBSV: *Tomato bushy stunt virus*

TMD: transmembrane domain

TMV: *Tobacco mosaic virus*

ToMV: *Tomato mosaic virus*

TuMV: *Turnip mosaic virus*

UTR: untranslated region

VIGS: virus-induced gene silencing

VRC: viral replication complex

WNV: *West Nile virus*

WT: wild type

YFP: yellow fluorescent protein

CHAPTER 1

INTRODUCTION

As obligate parasites, viruses require a host cell to reproduce. Once inside the host cell, they strategize on evading the immune responses of the host. Due to this parasitic nature, viruses have earned a special taxonomic position. There are seven classes of viruses based on the Baltimore classification system (Fig 1.1) (Baltimore, 1971), which categorizes viruses based on their messenger RNA (mRNA) synthesis.

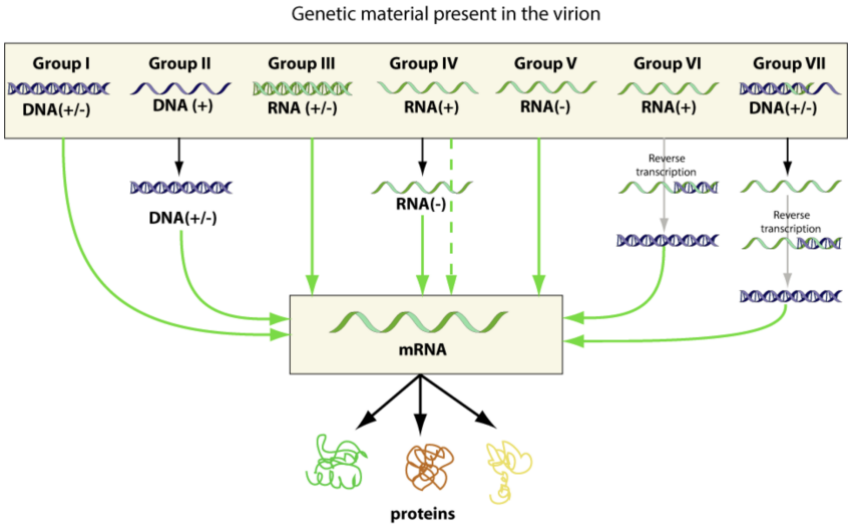

Fig. 1.1. The Baltimore classification of viruses

Solid and dotted green arrows represent the indirect and direct use of the viral genome as mRNA respectively. Adapted from ViralZone, Swiss Institute of Bioinformatics. www.expasy.ch/viralzone/

Among the different classes of viruses, positive-strand RNA [(+)RNA] viruses do not require any intermediate steps to synthesize a functional mRNA because their genomic RNA genome can be recognized by host ribosomes as a template for translation (Fig 1.2). This fitness has made

this class of viruses be, thus far, the most abundant as well as highly pathogenic class of viruses with 30 families (Lefkowitz et al., 2018).

Notable (+)RNA viruses include the members from families *Picornaviridae* (Poliovirus, Coxsackie, Rhinovirus), *Coronaviridae* (SARS-, MERS-coronavirus), *Flaviviridae* (Hepatitis C virus, Yellow fever virus, West Nile virus), *Bromoviridae* (Brome mosaic virus, Cucumber mosaic virus) and *Togaviridae* (Sindbis virus, Rubella virus, Equine encephalitis virus).

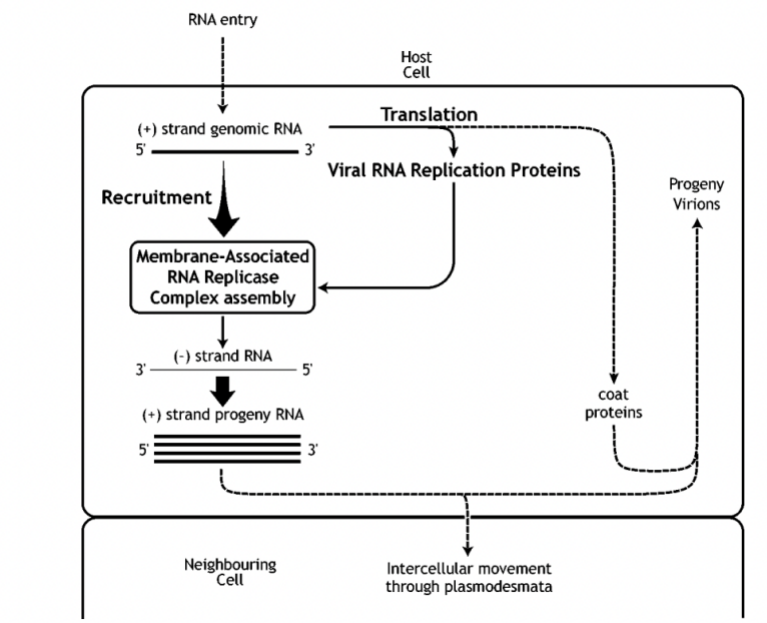

Fig. 1.2. A general scheme of positive-strand RNA virus replication

All steps specific to RNA replication are depicted with solid arrows, whereas steps in the virus lifecycle not involved in RNA replication are depicted with dotted arrows. In RNA replication, all steps where host factors have been implicated are in bold. (Adapted from Noueiry and Ahlquist, 2003).

1.1 The concept of superfamilies

Mutations, recombination events, and selection have given rise to members with a wide range of host preferences and divergence in terms of morphology. Grouping of viruses based on the genetic similarities indicating potential relationships between distantly related hosts, such as plants and animals has led to the concept of "superfamilies" (Goldbach, 1987; Koonin et al., 1993). Each superfamily includes many viruses infecting plant, fungal, and animal RNA viruses that differ in terms of their host range, transmission route, and serological cross-reactivity (Wolf et al., 2018). Recent phylogenetic reconstructions performed to consolidate the expanded RNA virome in terms of their replication complex morphology (Ahola, 2019) have further strengthened the concept.

Based on the genome organization and homology of RNA dependent RNA polymerase (RdRp), (+) RNA viruses are grouped into three superfamilies (Table 1.1).

Table 1.1 Characteristics of (+) RNA viral superfamilies

	domain type if present			
Supergroup	RdRp	Capping	Helicase	Protease
Picornavirus-like superfamily	I	VPg	3	Cysteine
Flavivirus-like superfamily	II	2	2	Serine
Alphavirus-like superfamily	III	1	1	Cysteine

(Adapted from (van der Heijden & Bol, 2002))

Picornavirus-like superfamily (superfamily I) express their genome by synthesizing polyprotein(s) that are proteolytically processed by viral proteinases. Most of the members in this superfamily, such as poliovirus, coxsackievirus, rhinovirus, etc., utilize a small VPg protein in

RNA replication, with no caps or protein domains involved in capping processes (Goodfellow, 2011; Koonin et al., 2008).

Flavivirus-like superfamily (superfamily II) includes viruses that express their genomes by synthesizing polyproteins that are processed by their serine-type protease domain. Examples include Dengue virus (DENV), West Nile virus (WNV), Zika virus, etc. This group contains distinct domains for methyltransferase as well as helicase-like activities (Koonin et al., 2015).

Alphavirus-like superfamily (superfamily III) do not necessarily produce polyprotein(s) and thus genomes of some members such as brome mosaic virus (BMV) and cucumber mosaic virus (CMV) are expressed as separate proteins without the requirement of proteolytic processing (He et al., 2021) or processed by self-encoded papain-like proteases if polyprotein is produced (Vasiljeva et al., 2003). Other features of this superfamily include the production of subgenomic RNA (sgRNA). The arrangement and conservation of methyltransferase, helicase-like, and polymerase domains together with the presence of conserved residues within these domains are noted among the members of this superfamily (Koonin et al., 1993, 2015).

1.2 Plant viruses: economic significance

Plant pathogens such as fungi, viruses, bacteria, and nematodes cause serious damages to crop worldwide and impact the overall crop yield and quality. The fungal or fungal-like pathogens dominate the domain of plant diseases and are the primary contributor to crop-yield loss. Viruses make up almost half of the plant disease-causing pathogens and are the second greatest contributor to crop-yield loss accounting for about $30 billion/year globally (Nicaise, 2014).

Many (+)RNA viruses (>500 species) (ICTV, 2021) are adapted to infect plant hosts including those that serve as model systems such as tobacco mosaic virus (TMV) and BMV (Elena et al., 2014). Unlike animal viruses, plant viruses cannot invade a plant cell via receptor-mediated endocytosis due to the presence of a thick cell wall composed of cellulose, therefore, they navigate into a plant cell either through mechanical wounds or via insects that provide an entry point.

Notable plant diseases caused by (+)RNA viruses arise from economically important families such as *Potyviridae, Bromoviridae,* and *Closteroviridae*, among others (German-Retana et al., 1999; López-Moya et al., 2009; Wang & Ahlquist, 2008). The *Potyviridae* family alone encompasses more than 30% of known plant viruses of economic significance (Riechmann et al., 1992). Noteworthy examples include the potato virus Y (PVY) that induces a wide variety of foliar and tuber necrosis in potato affecting the tuber quality (Karasev & Gray, 2013), Plum pox virus (PPV) that affects stone fruit crops such as peaches, plum, cherries, causing a reduction in yield and fruit quality. The worldwide distribution and the predominant transmission via many species of aphid impact crop and fruit production significantly (Levy et al., 2000). Members of *Bromoviridae* such as BMV and CMV are placed among the top 10 important viral pathogens in addition to PVY and PPV based on their use as scientific tools in global viral research (Scholthof et al., 2011).

One of the widely studied viral pathogens infecting a wide variety of crops is CMV. CMV is also a member of *Bromoviridae* and infects over 1200 host species of >100 plant families, including

economically important members of the Solanaceae family (tomato, tobacco) (Hosseinzadeh et al., 2012), Poaceae family (maize) (Wang et al., 2013), Fabaceae family (soybean, chickpea) (Hosseinzadeh et al., 2012), etc. Because of this very wide host range, and its efficient transmission by several aphid species, control measures including the strategies based on genetic resistance have been largely ineffective. Many of the reported instances of resistance or tolerance against CMV are effective for a limited number of CMV strains but not all.

Present disease control measures to combat plant viruses are based on three strategies:
1. development of resistant cultivars via conventional breeding approaches. Single dominant resistance genes in susceptible hosts have been identified in Arabidopsis, tomato, and pepper (Kang et al., 2010; Stamova & Chetelat, 2000; Takahashi et al., 2001), 2. pathogen-derived resistance (PDR) (Fitchen & Beachy, 1993), where part of the viral genome comprising of key genetic elements capable of conferring resistance to an otherwise susceptible host is overexpressed in transgenic plants. A validated concept of PDR could be traced to the tobacco plants that exhibited resistance to infection by TMV upon expressing the TMV coat protein gene (Abel et al., 1986). A successful commercial example is the control measures adopted for the papaya ringspot virus that started a viral epidemic resulting in almost 50% production loss in Hawaii (Tripathi et al., 2008). The approval of the genetically modified papaya, known as the Rainbow papaya, designed to be resistant to the virus, later accounted for about 90% of papaya production in Hawaii (Gonsalves et al., 2004; Tripathi et al., 2011), 3. adopting prophylactic control measures to restrict virus dispersion (Nicaise, 2014), such as removal of infected plants and control of natural vectors. Disease mitigation practices to limit virus dispersal consist of either removing all virus-infected crops that act as inoculum source or eliminating the virus from

a valuable cultivar when healthy plants are limited. Limiting vector populations by the use of pesticides and other additional means that interfere with the transmission process is also an important and commonly used practice (Rubio et al., 2020).

1.3 Positive-strand RNA virus-mediated membrane remodeling

Association with host specific organelle membranes and remodeling host membranes to induce the formation of viral replication complexes (VRCs) are characteristic features of replication of all (+)RNA viruses. The VRCs established by viral proteins serve as mini-organelles that synthesize offspring (+)RNA genomes, prevent viral RNA from RNase degradation, enrich critical viral and host proteins, and separate RNA synthesis from viral translation and viral particle packaging (Boon et al., 2010).

Viruses are able to distinguish and select specific organelle membranes for their replication (Fig. 1.3). For example, the ER membrane is preferentially used by several members of the *Flaviviridae* such as HCV and DENV (Romero-Brey et al., 2012; Welsch et al., 2009), the mitochondrial membranes by Flock House virus (FHV) (Miller et al., 2001; Miller & Ahlquist, 2002), and endosomes by Semliki Forest virus (SFV) (Lampio et al., 2000; Peränen et al., 1995).

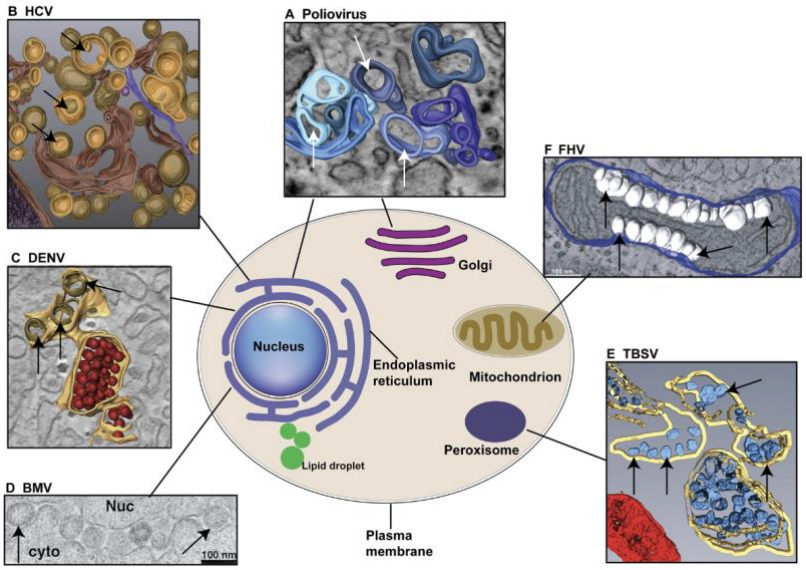

Fig. 1.3. Three-dimensional reconstructions of VRCs of different viruses

(A) The single membrane tubules formed at the early stages of poliovirus infection at the junctions of ER and Golgi membranes. (B) HCV DMVs at the ER regions (C) DENV DMVs at the ER membranes (yellow), VRCs (light brown) (D) BMV VRCs at the nuclear ER regions. Nuc: nucleus; cyto: cytoplasm. (E) TBSV in association with the peroxisomal membranes showing VRCs (blue) formed inside multivesicular bodies (MVB, yellow membranes). (F) FHV invaginations at the outer mitochondrial membranes (blue) showing VRCs (White). Arrows point to VRCs. Adapted from (Zhang et al., 2019).

There are at least two types of VRCs formed by (+)RNA viruses that have been documented: single-membrane vesicles (SMV) also known as spherules and double-membrane vesicles (DMVs) (Fig. 1.4). A typical single-membrane spherule is formed by invaginating an outer organelle membrane (the inner organelle membrane is not affected) into the luminal space and away from the cytoplasm, so the curvature is negative (Fig 1.4A). These invaginations are stabilized by the positive curvatures at the spherule neck that allow them to remain undetached from their membrane source (Fig 1.4A, pink arrow). When invaginated into the luminal space, VRCs have viral replication proteins and RNA templates inside the VRCs when RNAs are

separated from cellular mRNA and protected from cellular RNase. The VRCs formed at the perinuclear ER (nER) membranes by BMV, or at the peroxisomes and mitochondrial membranes by FHV and tomato bushy stunt virus are representative of SMVs (Fig 1.4A). (Kopek et al., 2007; Jonczyk et al., 2007; Schwartz et al., 2002).

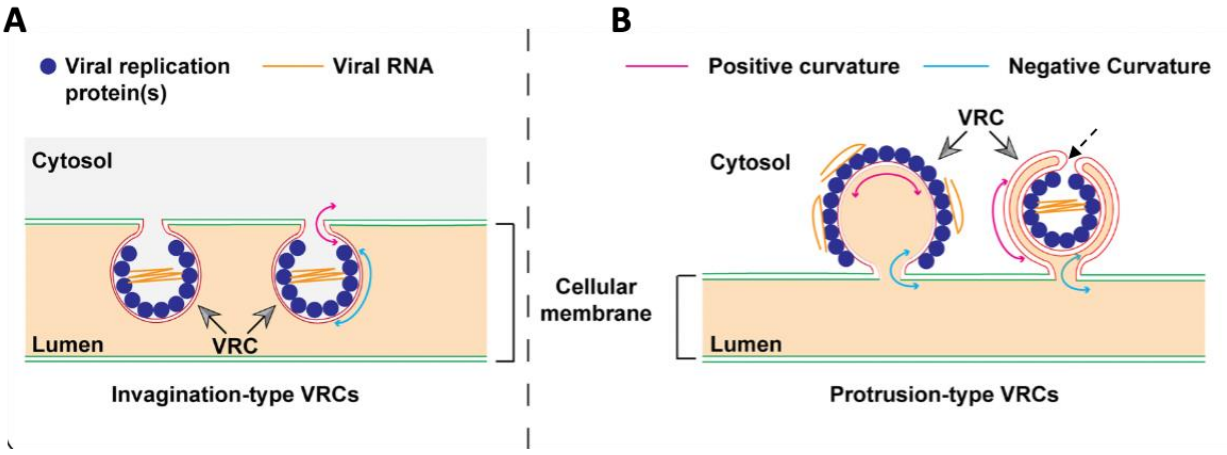

Fig. 1.4. The viral replication complexes depicting single and double-membrane vesicles
(A) Invaginated spherules as observed for BMV or FHV. A multimerizing viral protein (blue) is responsible for membrane alterations and forms a protein shell inside the spherules. (B) Protrusion-type replication complexes as observed for HCV. DMVs can arise from the protrusion of membranes into the cytosol accompanied by a secondary invagination event (dotted arrow), as has been suggested for HCV. Adapted from (Zhang et al., 2019).

When viral proteins induce the generation of positive curvature, such as by poliovirus, VRCs protrude into the cytoplasm. As shown Fig. 1.4B (the model on the left side), viral RNA synthesis will occur on the surface of VRCs. As such, extra protections are needed to maintain efficient viral RNA synthesis and RNA integrity. These protrusion VRCs further fold into DMVs (Fig. 1.4B, the model on the right side, dotted arrows). VRCs formed by poliovirus (Fig. 1.3A), HCV (Fig. 1.3B), and DENV (Fig. 1.3C) are typical DMVs.

1.4 Brome mosaic virus

Brome mosaic virus (BMV) is a non-enveloped (+)RNA virus that infects cereal crops such as barley, wheat, and rice, causing mosaic symptoms and stunting (Ding et al., 2006; Pocsai, 1987). Without an effective insect as a vector, BMV is not a big threat to agriculture production. However, a recent field study on a BMV isolate affecting wheat productivity in Ohio showed grain yield reduction of up to 60% (Hodge et al., 2018). The mechanism of BMV transmission in an agricultural field is currently unknown, even though it can be transmitted by beetles in the laboratory setting.

Among the six genera in the family *Bromoviridae*, BMV is the type member of the family and the genus *Bromovirus* (Lefkowitz et al., 2018) and serves as one of the best models for (+)RNA viruses to study viral replication, host interactions (Diaz et al., 2015; Diaz & Wang, 2014), RNA recombination events (Figlerowicz et al., 1998), gene expression, and virion assembly (Lucas et al., 2002). BMV also serves as a vector for virus-induced gene silencing for analysis of gene function (Ding et al., 2006). Extensive research on BMV has given valuable insights into many of the common features shared by (+)RNA viruses and also principles of general cellular biology. Some of the featured discoveries in BMV research include the first demonstration of template specificity of viral RdRp (Hardy et al., 1979), the infectious nature of viral transcripts from cDNA clones (Ahlquist et al., 1984), the synthesis of subgenomic mRNA synthesis via internal initiation (Miller et al., 1985), and the demonstration of eukaryotic viral replication in yeast (Janda & Ahlquist, 1993).

1.4.1 Genome

The 8.2 kb-long BMV RNA genome is divided among three genomic RNAs (Fig 1.3). BMV also has a subgenomic RNA, RNA4. All four RNAs are capped at the 5' end and contain a conserved t-RNA like structure at their 3' end. The segmented genome of BMV allows encapsidation of its RNAs into three separate virions that are homogeneous in size and morphology but heterogeneous in terms of density (Lane & Kaesberg, 1971).

For productive replication, RNA1 (3.2kb) and RNA2 (2.9kb) are required (Ishikawa et al., 1997; Janda & Ahlquist, 1993), whereas, for systemic infectivity, RNA3 is also required. RNA1 and RNA2 encode a replication protein 1a (109kDa), and an RdRp, $2a^{pol}$ (94kDa), respectively. Together, 1a and $2a^{pol}$ are necessary and sufficient for BMV RNA replication (He et al., 2021). RNA3 has a bicistronic architecture that encodes a movement protein, 3a (35kDa), from the 5' end and a coat protein (CP, 20kDa) from the 3' end. However, the CP is translated from the subgenomic RNA, RNA4 (Miller et al., 1985), which is, in addition to its role in encapsidation, implicated in regulating gene expression via translational inhibition of RNA1-3 (Shih & Kaesberg, 1976).

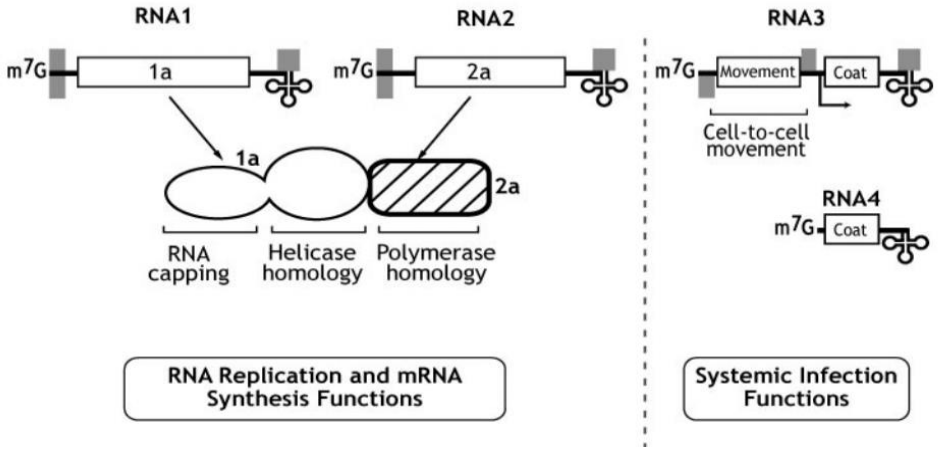

Fig. 1.5. Schematic diagram showing the BMV genome and the encoded proteins

Replication factors 1a and 2a and their domain-specific interactions are shown below RNA1 and RNA2. Open boxes represent the ORFs, single black lines represent the noncoding regions, tRNA-like 3' ends (cloverleaf), and subgenomic mRNA start site (bent arrow). Shaded boxes above noncoding regions represent replication and gene expression elements on positive strands. Gray boxes below noncoding regions represent replication elements on negative strands. Adapted from (Noueiry & Ahlquist, 2003).

1.4.2 The replication protein 1a

BMV 1a is a 109 kDa protein encoded by RNA1. BMV 1a has two major domains with designated functions, the N-terminal capping domain, and a C-terminal NTPase/helicase-like domain. As a multifunctional protein that adds the cap structure to all BMV RNAs, 1a also induces membrane remodeling at replication-site specific membranes and recognizes and recruits viral RNA templates, $2a^{pol}$, and certain host proteins to form functional VRCs.

BMV 1a localizes to the nER regions of the host cell. The expression of BMV 1a alone, in the absence of active viral RNA replication or any other viral proteins, can induce intracellular membrane modifications to establish spherules (Fig 1.4) that resembles those induced during

viral infections which strictly requires the presence of other viral factors (Restrepo-Hartwig & Ahlquist, 1999) and therefore, 1a is the master regulator of BMV viral replication (den Boon et al., 2001; Restrepo-Hartwig & Ahlquist, 1999).

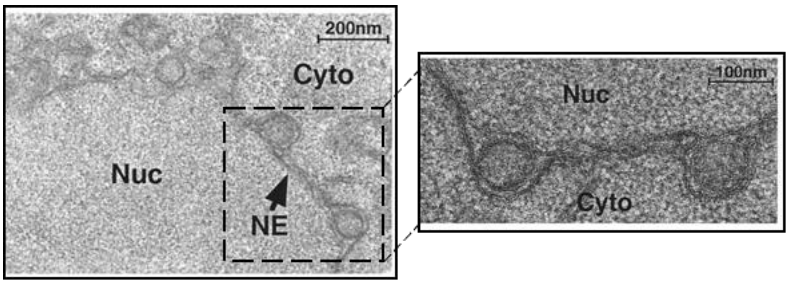

Fig. 1.6. BMV 1a induced spherules at the nER regions

The spherules are formed via the invagination of the nER membrane into the lumen. NE represents nuclear envelope, Nuc: nucleus; Cyto: cytoplasm. Adapted from (Lee & Ahlquist, 2003).

In the presence of viral factors, $2a^{pol}$ and RNA3, 1a interacts and recruits $2a^{pol}$ and RNA templates into the interior of the established spherules (Chen et al., 2001). BMV 1a is required for the synthesis of all viral RNA forms of BMV (Kroner et al., 1990) and provides template specificity during viral replication (Traynor & Ahlquist, 1990) by specifically recognizing the *cis*-acting elements present in viral genomic RNAs (Sullivan & Ahlquist, 1999). 1a selectively recruits viral genomic RNAs to the site of replication at the nER (Chen et al., 2001). The recruitment of RNAs away from translation and into the replication compartment requires the recognition of conserved replication enhancer elements present at the 5' untranslated regions of BMV RNAs (Janda & Ahlquist, 1998; Sullivan & Ahlquist, 1999), and host factors that act as chaperones in activating the replication complex or factors that enhance the transition of viral mRNA from translation to replication (Díez et al., 2000; Noueiry & Ahlquist, 2003).

1.4.3 RNA Capping domain of BMV 1a

All BMV RNAs, genomic RNA1, 2, and 3, as well as subgenomic mRNA, RNA4, have a 5' cap structure, $m^7G^{5'}ppp^{5'}Gp$ (He et al., 2021). Capped viral RNAs allow for efficient protein synthesis by utilizing the mRNA cap-dependent cellular translation machinery (Ferron et al., 2012). Since cellular RNA capping activities take place in the nucleus, viruses that replicate in the cytoplasm, such as BMV, encode their own capping enzyme that provides stability and protection from cellular degradation (Ahola & Ahlquist, 1999).

Unlike the cellular capping enzymes, viruses in the alphavirus-like superfamily have a unique type of RNA capping enzyme that has a combined methyltransferase and guanylyltransferase activity (MTase-GTase) (Ahola & Ahlquist, 1999; Ahola & Kääriäinen, 1995). The N-terminal region in 1a spanning aa 1- 561 is responsible for the 5' capping of RNAs of BMV (Kong et al., 1999). In contrast to the cellular mRNA capping process where methyltransferase methylates GTP only after it has been transferred to an mRNA molecule, the capping process of BMV RNAs involves GTP methylation before GTP gets linked to the mRNA molecule (Ahola & Kääriäinen, 1995; Decroly et al., 2011).

In addition to capping related activities, the capping domain of BMV 1a is implicated for 1a's intramolecular interactions (Diaz et al., 2012; O'Reilly et al., 1998) and also for the membrane binding activity (den Boon et al., 2001).

1.4.4 Helicase-like domain of BMV 1a

BMV 1a has a superfamily I nucleoside triphosphatase/helicase-like domain (NTPase/hel) at the C-terminus (aa 562 to 961) (Ahola et al., 2000; Kroner et al., 1990) with signature motifs of the DEAD-box containing helicases (Gorbalenya & Koonin, 1993; Koonin et al., 1993; Wang et al., 2005).

The C-terminal helicase-like domain possesses ATPase and GTPase activities involved in hydrolyzing ATPs and capping-related activities (Ahola & Ahlquist, 1999; Wang et al., 2005). Even though helicases unwind duplex RNA or DNA molecules, 1a's RNA-unwinding activity has not been experimentally verified. Similar to other members of this superfamily, the RNA 5' triphosphatase activity is essential for 5' cap synthesis since it initiates the capping processes by removing the 5′ γ-phosphate of nascent mRNA (Ahola & Ahlquist, 1999; Decroly et al., 2011; Karpe & Lole, 2010; Li et al., 2001).

In addition to their roles in hydrolyzing NTPs and possibly translocating viral genomic RNAs into VRCs (Wang et al., 2005), the helicase-like domain of BMV also indirectly contributes to regulating the viral infectivity by repressing translation of RNA1 and RNA2 since methyltransferase domain alone is not sufficient to inhibit translation (Yi et al., 2007).

BMV 1a's intermolecular interaction with $2a^{pol}$ involved in the RNA synthesis has been described for the helicase-like domain (Chen & Ahlquist, 2000; Kao & Ahlquist, 1992). Mutations in the helicase-like domain impact viral RNA replication (Ahola et al., 2000), their

ability to recruit and provide a nuclease resistant state for RNA3 (Wang et al., 2005), and also 1a's capacity to repress the RNA1 and RNA2 translation (Yi et al., 2007).

1.4.5 Disordered regions

Viral proteins, particularly those from RNA viruses were found to be enriched in disordered regions (Tokuriki et al., 2009). Intrinsically disordered regions (IDRs) in viruses allow for promiscuity in terms of interacting partners and function as a flexible linker between functional domains (Xue et al., 2014). Due to the presence of disordered regions enriched in polar residues and residues that are not involved in regular secondary structure elements, these regions (and the entire protein) are less affected by mutations, which in turn corresponds to their high evolvability (Tokuriki et al., 2009). Although many (+)RNA viruses contain disordered regions including NS5A of HCV (Hanoulle et al., 2010), polyprotein of SFV, and the Nucleocapsid protein of all coronaviruses (Mishra et al., 2020), an example of IDRs of BMV and HEV are discussed briefly. A proline-rich linker region that separates the methyltransferase and helicase-like domains in BMV 1a predicted to be intrinsically disordered is similar to the hypervariable region of HEV. A region of low amino acid complexity, rich in Ala, Gly, Pro, and Ser is present in HEV (Purdy et al., 2012). The HEV hypervariable region is rich in prolines that are known for forming structural randomness qualifying it to be an intrinsically disordered region (IDR). In BMV, the linker region is enriched with Ser, Pro, and Val. Mutations in the polyproline region (PPR) did not abolish the infectivity of HEV but resulted in attenuation when the PPR region was almost completely removed (Pudupakam et al., 2009). In BMV, the degree of flexibility in this hinge region tends to affect the interaction between 1a and 2a which then impacts viral replication (Kao & Ahlquist, 1992).

1.5 The engineered BMV-yeast system

The yeast *Saccharomyces cerevisiae* (baker's yeast) can act as a host for the replication of the BMV viral genome (Janda & Ahlquist, 1993). It is one of the best-characterized eukaryotes with a fully sequenced genome (Cherry et al., 2012). Amenable to classical genetics, multiple genomic systems, such as arrays of deletion, fluorescence protein-tagging, or overexpression strains, enable large-scale functional analysis of its ~6,000 genes.

Since viral RNA genomes can be manipulated at the cDNA level, the BMV-yeast system was developed to express BMV 1a and $2a^{pol}$ from either plasmid (Janda & Ahlquist, 1993) or chromosome (Ishikawa et al., 1997) and the transcribed RNA3 is used as the replication template. The yeast system only harbors the open reading frame (ORF) of 1a and $2a^{pol}$ but not the 5' and 3' UTR signals so that the replication of RNA1 and RNA2 is avoided and RNA3 replication can be studied on its own (since the transcripts of RNA3 derivatives have an intact 5' and 3' regions to allow initiation of replication).

Since CP is only required for viral packaging but not replication and the subgenomic RNA4 can be produced only after successful replication, the CP ORF in RNA3 can be replaced with reporter genes such as chloramphenicol acetyltransferase (CAT) or orotidine 5'-phosphate decarboxylase (URA3) to allow detection of viral replication in cells expressing 1a, 2a, and RNA3-derivatives. In the original system, when transcripts of RNA3 derivatives were transformed into yeast cells along with plasmids expressing BMV 1a and $2a^{pol}$, a strong expression of CAT or URA3 was detected, indicating yeast cells can support BMV replication (Janda & Ahlquist, 1993).

To further improve the assays and avoid loss of the RNA3 replicon in the absence of selection and to produce an authentic 3' viral RNA ends, plasmids carrying the coding sequence for RNA3 or RNA3 derivatives were introduced with a self-cleaving ribozyme sequence from hepatitis delta virus at the 3' UTR of RNA3. Upon transcription, the ribozyme cleaves itself and the poly-A tail off from the RNA3 transcripts, and thus, produces RNA3 with an authentic 3' end of RNA3 (Ishikawa et al., 1997). This replication-based yeast system allows screening of host proteins that are necessary for viral replication (Fig 1.5). By employing this system, many yeast genes have been identified as necessary for - or involved in - BMV replication (Ishikawa et al., 1997; Kushner et al., 2003).

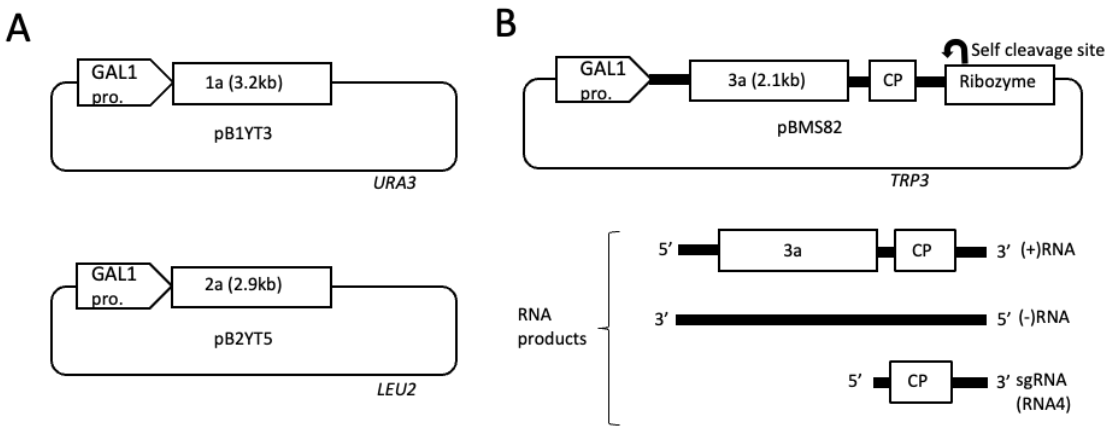

Fig. 1.7. The BMV yeast system

(A) The plasmid constructs are employed to express 1a and 2a proteins under the control of the *GAL1* promoter and with specific auxotrophic selections. (B) The plasmid construct to produce RNA3 transcripts. The RNA products of the construct are indicated below the construct. The bold region within the construct depicts the 5' and 3' ends required to produce authentic viral 5' and 3' ends. Ribozyme is at the end of RNAs to produce an authentic viral 3' end. Adapted and modified from (Ishikawa et al., 1997; Janda & Ahlquist, 1993).

Nearly all features of BMV RNA replication in plant cells are duplicated in the yeast system including 1a-2a^{pol} interaction, selective encapsidation of viral RNAs, production of RNA4, localization of 1a at the nER, site of VRC formation, etc. (Ishikawa et al., 1997; Janda & Ahlquist, 1993; Restrepo-Hartwig & Ahlquist, 1996; Restrepo-Hartwig & Ahlquist, 1999; Schwartz et al., 2002). Additional advantages of this host include shorter generation times, well-characterized genetics, and the availability of genetic tools for easy manipulations.

1.6 Host genes critical for BMV replication

(+)RNA viruses with their compact genomes depend on the host proteins for successful replication. To facilitate their replication, they establish protein-protein, RNA-protein, and/or protein-lipid interactions that subsequently subvert the host factors to sites of viral replication (Nagy & Pogany, 2011).

Some notable host proteins involved in BMV replication include the reticulon homology proteins (RHPs) (Diaz et al., 2010) known for their membrane shaping abilities, ESCRT (endosomal sorting complexes required for transport) family proteins (Diaz et al., 2015), Erv14, a cargo receptor of coat protein complex II (Li et al., 2016), enzymes of the lipid biosynthesis pathway such as Cho2p involved in the choline biosynthesis (He et al., 2019), the ER-localized Δ9 fatty acid desaturase, Ole1p of the unsaturated fatty acid synthesis (Lee & Ahlquist, 2003), pah1p involved in the conversion of phosphatidate (PA) to diacylglycerol (DAG) during the synthesis of storage lipids (Zhang et al., 2018), and Acyl coenzyme A binding protein (ACBP) of yeast that selectively binds to long-chain fatty acids (Zhang et al., 2012).

The role of membrane shaping proteins, RHPs, and some proteins involved in lipid biosynthesis are further discussed below.

1.6.1 The membrane shaping reticulon homology proteins

The endoplasmic reticulum (ER) is an important cellular organelle that not only houses resident membrane proteins, and chaperones, but is also actively involved in protein synthesis and secretion, as well as cellular lipid biogenesis (Jacquemyn et al., 2017). The expansive surface area of the ER also enables it to connect with several other organelles, which makes it an important organelle for many viruses such as BMV, CCMV, Polio, HCV, HEV, etc. (Patarroyo et al., 2013; Ravindran et al., 2016; Verchot, 2014).

The ER membrane undergoes substantial membrane modifications during viral infections. The membrane shaping reticulon homology proteins (RHPs) have been implicated in creating an appropriate topology that allows the modified ER membrane to support replication of the viral genome of many (+)RNA viruses (Aktepe et al., 2017; Diaz et al., 2010; Diaz & Ahlquist, 2012).

BMV recruits the ER membrane-shaping proteins, reticulon homology protein(s) (RHP), which are known to alter membrane curvature to the ER (Diaz et al., 2010). The reticulons (RTNs) have a reticulon homology domain that consists of two hairpin transmembrane (TM) regions separated by a hydrophilic loop (Zurek et al., 2011). The hairpin TM resides on the outer ER membrane and creates a positive curvature of the membrane toward the cytoplasm (Fig 1.8) (Yang & Strittmatter, 2007; Zurek et al., 2011).

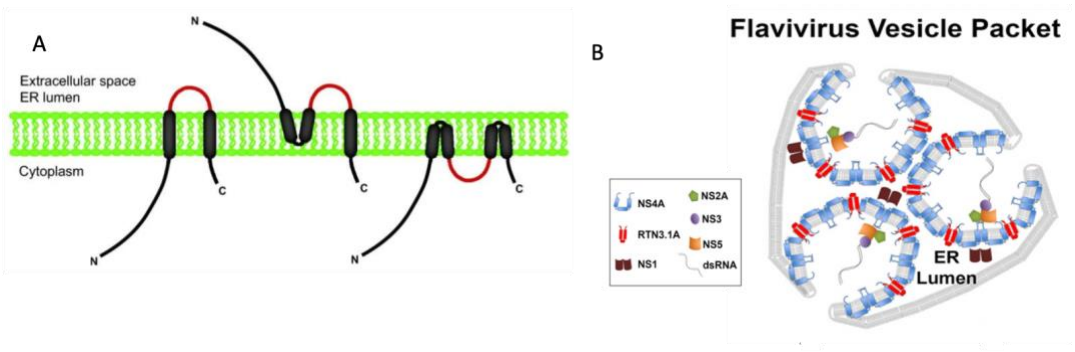

Fig. 1.8. The possible membrane topologies of reticulons and their role in membrane shaping

(A) Possible topologies of RTNs depending on the cell types and organelle membrane composition may enable reticulons to carry out diverse roles in the cell. (B) A pictoral representation of the FHV vesicle packet containing vesicles shaped by reticulons in red. Adapted from (Yang & Strittmatter, 2007) in (A), and (Aktepe et al., 2017) in (B).

BMV RNA replication is inhibited up to 90% in the absence of all three RHPs, Rtn1p, Rtn2p, and Yop1p in yeast (Diaz et al., 2010). The replication protein 1a fails to not only recruit RNA templates in the absence of RHPs but also fails to establish replication compartments while still localizing to the nER regions. The RHPs usually reside in the peripheral ER tubules (Voeltz et al., 2006), however, in the presence of 1a, >50% of RHPs are directed into the VRCs suggesting that 1a interacts with RHPs and utilizes their functionality in shaping the replication compartments (Diaz et al., 2010).

The reticulon proteins tend to modulate the diameter of the established replication compartments. Partial depletion of RTN proteins allowed the formation of functional replication compartments but reduced their diameter by 30–50% of the 1a induced replication compartments that range between 58-74nm in diameter (Diaz et al., 2010).

The proposed models for the potential mechanism for RHPs in spherule formation include their involvement in establishing and stabilizing the spherule neck of positive curvature alongside the negative curvature induced by 1a, and their involvement in the maintenance of the original spherule size (Diaz et al., 2010).

1.6.2 Proteins involved in lipid biosynthesis pathways play critical roles in the replication of BMV and other viruses

Cellular lipids play crucial roles in the replication of multiple (+)RNA viruses because lipids are vital components of organelle membranes (Zhang et al., 2019). Altering the phospholipid or sterol biosynthesis impacts the replication of BMV (Zhang et al., 2016), West Nile virus (Mackenzie et al., 2007), DENV (Rothwell et al., 2009), Poliovirus (Zhanga et al., 2016), enteroviruses (Ilnytska et al., 2013) and many others (Romero-Brey & Bartenschlager, 2014).

Several host genes of the lipid biosynthetic pathway have been characterized for their roles in BMV replication. The host phosphatidate phosphatase, Pah1p, limits viral replication by regulating phospholipid synthesis. In the absence of Pah1p, the nuclear ER membrane expands due to the enhanced production of PA and other phospholipids that supports viral replication significantly higher than those in the presence of Pah1p (Zhang et al., 2018).

Deletion of the Acyl-CoA-binding protein (ACBP) and mutation in Δ9 fatty acid desaturase in yeast also inhibits BMV RNA replication (Lee et al., 2001; Zhang et al., 2012). ACBP, involved in lipid biosynthesis has a profound effect on spherule formation. In addition to a 30-fold

decrease in viral replication, the established spherule sizes were ~50% smaller and ~4-fold more abundant in mutant cells than those in wild type cells.

Phospholipids such as phosphatidylcholine (PC) make up more than 50% of the total phospholipids in eukaryotic cells (van Meer et al., 2008). Many (+)RNA viruses increase specific phospholipid levels during replication. For example, BMV increases PC content in yeast and barley cells upon infection and enriches PC at the nER regions by interacting with and recruiting Cho2p, which is a phosphatidylethanolamine (PE) methyltransferase (PEMT) that converts PE to monomethyl PE (PMME) (Zhang et al., 2016). Polio and Rhinovirus promote the enrichment of free cholesterol at the sites of their replication (Roulin et al., 2014; Vance et al., 1980) whereas DENV creates a unique lipid repertoire during infection by enriching selective PC species (Perera et al., 2012).

The lipid enrichment at the replication sites involves either transport of the necessary lipids or recruitment of the proteins necessary for their biosynthesis. For example, the red clover necrotic mosaic virus, WNV, and BMV promote PC, and cholesterol production by hijacking phospholipase D (Hyodo et al., 2015), 3-hydroxy-methylglutaryl-CoA reductase (HMGCR) (Mackenzie et al., 2007), and choline-requiring 2 (Cho2p) (Zhang et al., 2016) respectively to the sites of replication whereas TBSV and carnation Italian ringspot virus transport PE by hijacking the Rab5-positive endosomes to viral replication sites to build the PE-enriched VRCs (Xu & Nagy, 2016).

Due to their dependence on cellular lipids, lipid biosynthetic genes serve to be a possible target for developing antiviral strategies, however, since modifying lipid biosynthetic genes could also

impact the host cell growth and viability, mutants that specifically inhibit only the viral growth without altering the cellular metabolism provide a new avenue for antivirals. A study by He et al., 2019 showed that a mutant Cho2p could support normal yeast cell growth but significantly inhibited BMV replication, localization of 1a, and the formation of VRCs at the nER regions (He et al., 2019).

1.7 Objectives and significance of research

The primary aim of this research was to understand the role of an amphipathic helix, Helix B, present at the N-terminal capping domain of BMV replication protein 1a. To test the function of this amphipathic helix, a mutational approach was adopted, and localization studies were performed. The significance of several amino acid residues within helix B was tested and their impact on the overall membrane targeting and thereby viral replication was studied.

This work sought to decipher the structural feature(s) or motif(s) within BMV 1a that shows organelle membrane specificity to establish VRCs. Membrane associations are the first step towards viral replication, and a key feature across all (+) RNA viruses to assemble VRCs. Some notable plant viruses such as BMV, cowpea chlorotic mottle virus, and beet black scotch virus replicate at the ER membranes whereas Cucumber mosaic virus, Tomato bushy stunt virus, Barley stripe mosaic virus, and Turnip crinkle virus prefer membranes of the tonoplast, peroxisome, chloroplast, and mitochondria, respectively (Blake et al., 2007; Cao et al., 2015; Hatta & Francki, 1981; McCartney et al., 2005; Restrepo-Hartwig & Ahlquist, 1999; Wang et al., 2021). It is believed that the membrane lipid compositions dictate the choice of organelle membranes for specific viruses, however, it is still unclear what structural determinant within the

viral protein is responsible for targeting these viruses to their specific site of replication especially when transmembrane domains (TMDs) are absent.

The knowledge of the structural features/motifs that are responsible for such specific membrane targeting activities would be useful for moving towards the development of antiviral strategies to control viral infection since all positive-strand RNA viruses invariably associate with cellular membranes.

1.8 References

Abel, P. P., Nelson, R. S., De, B., Hoffmann, N., Rogers, S. G., Fraley, R. T., & Beachy, R. N. (1986). Delay of Disease Development in Transgenic Plants That Express the Tobacco Mosaic Virus Coat Protein Gene. *Science*, *232*(4751), 738–743.

Ahlquist, P., French, R., Janda, M., & Loesch-Fries, L. S. (1984). Multicomponent RNA plant virus infection derived from cloned viral cDNA. *Proceedings of the National Academy of Sciences*, *81*(22), 7066–7070.

Ahola, T. (2019). New phylogenetic grouping of positive-sense RNA viruses is concordant with replication complex morphology. *MBio*, *10*(4):e01402-19.

Ahola, T., & Ahlquist, P. (1999). Putative RNA capping activities encoded by brome mosaic virus: methylation and covalent binding of guanylate by replicase protein 1a. *Journal of Virology*, *73*(12), 10061–10069.

Ahola, T., den Boon, J. A., & Ahlquist, P. (2000). Helicase and Capping Enzyme Active Site Mutations in Brome Mosaic Virus Protein 1a Cause Defects in Template Recruitment, Negative-Strand RNA Synthesis, and Viral RNA Capping. *Journal of Virology*, *74*(19), 8803–8811.

Ahola, T., & Kääriäinen, L. (1995). Reaction in alphavirus mRNA capping: formation of a covalent complex of nonstructural protein nsP1 with 7-methyl-GMP. *Proceedings of the National Academy of Sciences of the United States of America*, *92*(2), 507.

Aktepe, T. E., Liebscher, S., Prier, J. E., Simmons, C. P., & Mackenzie, J. M. (2017). The Host Protein Reticulon 3.1A Is Utilized by Flaviviruses to Facilitate Membrane Remodelling. *Cell Reports*, *21*(6), 1639–1654.

Baltimore, D. (1971). Expression of animal virus genomes. *Bacteriological Reviews*, *35*(3), 235–241.

Blake, J. A., Lee, K. W., Morris, T. J., & Elthon, T. E. (2007). Effects of turnip crinkle virus infection on the structure and function of mitochondria and expression of stress proteins in turnips. *Physiologia Plantarum*, *129*(4), 698–706.

Boon, J. A. den, Diaz, A., & Ahlquist, P. (2010). Cytoplasmic Viral Replication Complexes. *Cell Host & Microbe*, *8*(1), 77–85.

Cao, X., Jin, X., Zhang, X., Li, Y., Wang, C., Wang, X., Hong, J., Wang, X., Li, D., & Zhang, Y. (2015). Morphogenesis of Endoplasmic Reticulum Membrane-Invaginated Vesicles during Beet Black Scorch Virus Infection: Role of Auxiliary Replication Protein and New Implications of Three-Dimensional Architecture. *Journal of Virology*, *89*(12), 6184.

Chen, J., & Ahlquist, P. (2000). Brome Mosaic Virus Polymerase-Like Protein 2a Is Directed to the Endoplasmic Reticulum by Helicase-Like Viral Protein 1a. *Journal of Virology*, *74*(9), 4310–4318.

Chen, J., Noueiry, A., & Ahlquist, P. (2001). Brome Mosaic Virus Protein 1a Recruits Viral RNA2 to RNA Replication through a 5′ Proximal RNA2 Signal. *Journal of Virology*, *75*(7), 3207–3219.

Cherry, J. M., Hong, E. L., Amundsen, C., Balakrishnan, R., Binkley, G., Chan, E. T., Christie, K. R., Costanzo, M. C., Dwight, S. S., Engel, S. R., Fisk, D. G., Hirschman, J. E., Hitz, B. C., Karra, K., Krieger, C. J., Miyasato, S. R., Nash, R. S., Park, J., Skrzypek, M. S., … Wong, E. D. (2012). Saccharomyces Genome Database: the genomics resource of budding yeast. *Nucleic Acids Research*, *40*(Database issue), D700-D705.

Decroly, E., Ferron, F., Lescar, J., & Canard, B. (2011). Conventional and unconventional mechanisms for capping viral mRNA. *Nature Reviews. Microbiology*, *10*(1), 51–65.

den Boon, J. A., Chen, J., & Ahlquist, P. (2001). Identification of Sequences in Brome Mosaic Virus Replicase Protein 1a That Mediate Association with Endoplasmic Reticulum Membranes. *Journal of Virology*, *75*(24), 12370–12381.

Diaz, A., & Ahlquist, P. (2012). Role of host reticulon proteins in rearranging membranes for positive-strand RNA virus replication. *Current Opinion in Microbiology*, *15*(4), 519–524.

Diaz, A., Gallei, A., & Ahlquist, P. (2012). Bromovirus RNA Replication Compartment Formation Requires Concerted Action of 1a's Self-Interacting RNA Capping and Helicase Domains. *Journal of Virology*, *86*(2), 821–834.

Diaz, A., & Wang, X. (2014). Bromovirus-induced remodeling of host membranes during viral RNA replication. *Current Opinion in Virology*, *9*, 104–110.

Diaz, A., Wang, X., & Ahlquist, P. (2010). Membrane-shaping host reticulon proteins play crucial roles in viral RNA replication compartment formation and function. *Proceedings of the National Academy of Sciences of the United States of America*, *107*(37), 16291–16296.

Diaz, A., Zhang, J., Ollwerther, A., Wang, X., & Ahlquist, P. (2015). Host ESCRT Proteins Are Required for Bromovirus RNA Replication Compartment Assembly and Function. *PLOS Pathogens*, *11*(3), e1004742.

Díez, J., Ishikawa, M., Kaido, M., & Ahlquist, P. (2000). Identification and characterization of a host protein required for efficient template selection in viral RNA replication. *Proceedings of the National Academy of Sciences of the United States of America*, *97*(8), 3913.

Ding, X. S., Schneider, W. L., Chaluvadi, S. R., Rouf Mian, M. A., & Nelson, R. S. (2006). Characterization of a Brome mosaic virus strain and its use as a vector for gene silencing in monocotyledonous hosts. *Molecular Plant-Microbe Interactions*, *19*(11), 1229–1239.

Elena, S. F., Fraile, A., & García-Arenal, F. (2014). Evolution and Emergence of Plant Viruses. *Advances in Virus Research*, *88*, 161–191.

Ferron, F., Decroly, E., Selisko, B., & Canard, B. (2012). The viral RNA capping machinery as a target for antiviral drugs. *Antiviral Research*, *96*(1), 21.

Figlerowicz, M., Nagy, P. D., Tang, N., Kao, C. C., & Bujarski, J. J. (1998). Mutations in the N Terminus of the Brome Mosaic Virus Polymerase Affect Genetic RNA-RNA Recombination. *Journal of Virology*, *72*(11), 9192–9200.

Fitchen, J. H., & Beachy, R. N. (1993). Genetically engineered protection against viruses in transgenic plants. *Annual Review of Microbiology*, *47*, 739–764.

German-Retana, S., Candresse, T., & Martelli, G. (1999). CLOSTEROVIRUSES (CLOSTEROVIRIDAE). *Encyclopedia of Virology*, 266-273.

Goldbach, R. (1987). Genome similarities between plant and animal RNA viruses. Microbiological Sciences, 4(7), 197—202.

Gonsalves, D., Gonsalves, C., Ferreira, C., & Fitch, M. (2004). Transgenic Virus-Resistant Papaya: From Hope to Reality in Controlling Papaya Ringspot Virus in Hawaii. *APSnet Feature Articles*.

Goodfellow, I. (2011). The genome-linked protein VPg of vertebrate viruses - a multifaceted protein. *Current Opinion in Virology*, *1*(5), 355.

Gorbalenya, A. E., & Koonin, E. v. (1993). Helicases: amino acid sequence comparisons and structure-function relationships. *Current Opinion in Structural Biology*, *3*(3), 419–429.

Hanoulle, X., Badillo, A., Verdegem, D., Penin, F., & Lippens, G. (2010). The Domain 2 of the HCV NS5A Protein Is Intrinsically Unstructured. *Protein & Peptide Letters*, *17*(8), 1012–1018.

Hardy, S. F., German, T. L., Loesch-Fries, L. S., & Hall, T. C. (1979). Highly active template-specific RNA-dependent RNA polymerase from barley leaves infected with brome mosaic virus. *Proceedings of the National Academy of Sciences*, *76*(10), 4956–4960.

Hatta, T., & Francki, R. I. B. (1981). Cytopathic Structures Associated with Tonoplasts of Plant Cells Infected with Cucumber Mosaic and Tomato Aspermy Viruses. *Journal of General Virology*, *53*(2), 343–346.

He, G., Zhang, Z., Sathanantham, P., Diaz, A., & Wang, X. (2021). Brome Mosaic Virus (Bromoviridae). *Encyclopedia of Virology*, 252–259.

He, G., Zhang, Z., Sathanantham, P., Zhang, X., Wu, Z., Xie, L., & Wang, X. (2019). An engineered mutant of a host phospholipid synthesis gene inhibits viral replication without compromising host fitness. *Journal of Biological Chemistry*, *294*(38), 13973–13982.

Hodge, B. A., Salgado, J. D., Paul, P. A., & Stewart, L. R. (2018). Characterization of an Ohio isolate of Brome Mosaic Virus and its Impact on the Development and Yield of Soft Red Winter Wheat. *Plant Disease*, *103*(6), 1101-1111.

Hosseinzadeh, H., Nasrollanejad, S., & Khateri, H. (2012). Serological detection of Cucumber mosaic virus on some important host crops in the north region of Iran. *Archives of Phytopathology and Plant Protection*, *45*(16), 1884–1890.

Hyodo, K., Taniguchi, T., Manabe, Y., Kaido, M., Mise, K., Sugawara, T., Taniguchi, H., & Okuno, T. (2015). Phosphatidic Acid Produced by Phospholipase D Promotes RNA Replication of a Plant RNA Virus. *PLOS Pathogens*, *11*(5), e1004909.

ICTV (International Committee on Taxonomy of Viruses). Retrieved March 17, 2021, from https://talk.ictvonline.org/taxonomy

Ilnytska, O., Santiana, M., Hsu, N. Y., Du, W. L., Chen, Y. H., Viktorova, E. G., Belov, G., Brinker, A., Storch, J., Moore, C., Dixon, J. L., & Altan-Bonnet, N. (2013). Enteroviruses Harness the Cellular Endocytic Machinery to Remodel the Host Cell Cholesterol Landscape for Effective Viral Replication. *Cell Host & Microbe*, *14*(3), 281–293.

Ishikawa, M., Janda, M., Krol, M. A., & Ahlquist, P. (1997). In vivo DNA expression of functional brome mosaic virus RNA replicons in Saccharomyces cerevisiae. *Journal of Virology*, *71*(10), 7781–7790.

Jacquemyn, J., Cascalho, A., & Goodchild, R. E. (2017). The ins and outs of endoplasmic reticulum-controlled lipid biosynthesis. *EMBO Reports*, *18*(11), 1905.

Janda, M., & Ahlquist, P. (1993). RNA-dependent replication, transcription, and persistence of brome mosaic virus RNA replicons in S. cerevisiae. *Cell*, *72*(6), 961–970.

Janda, M., & Ahlquist, P. (1998). Brome mosaic virus RNA replication protein 1a dramatically increases in vivo stability but not translation of viral genomic RNA3. *Proceedings of the National Academy of Sciences*, *95*(5), 2227–2232.

Jonczyk, M., Pathak, K. B., Sharma, M., & Nagy, P. D. (2007). Exploiting alternative subcellular location for replication: Tombusvirus replication switches to the endoplasmic reticulum in the absence of peroxisomes. *Virology*, *362*(2), 320–330.

Kang, H., Hoang, N. H., Yang, H.-B., Kwon, J.-K., Jo, S.-H., Seo, J.-K., Kim, K.-H., Choi, D., & Kang, B.-C. (2010). Molecular mapping and characterization of a single dominant gene controlling CMV resistance in peppers (Capsicum annuum L.). *Theor Appl Genet*, *120*(8), 1587–1596.

Kao, C. C., & Ahlquist, P. (1992). Identification of the domains required for direct interaction of the helicase-like and polymerase-like RNA replication proteins of brome mosaic virus. *Journal of Virology*, *66*(12), 7293-7302.

Karasev, A. v, & Gray, S. M. (2013). Continuous and Emerging Challenges of Potato virus Y in Potato. *Annual Review of Phytopathology*, *51*(1), 571–586.

Karpe, Y. A., & Lole, K. S. (2010). RNA 5′-Triphosphatase Activity of the Hepatitis E Virus Helicase Domain. *Journal of Virology*, *84*(18), 9637 LP – 9641.

Kong, F., Sivakumaran, K., & Kao, C. (1999). The N-Terminal Half of the Brome Mosaic Virus 1a Protein Has RNA Capping-Associated Activities: Specificity for GTP and S-Adenosylmethionine. *Virology*, *259*(1), 200–210.

Koonin, E. v., Dolja, V. v., & Krupovic, M. (2015). Origins and evolution of viruses of eukaryotes: The ultimate modularity. *Virology*, *479–480*, 2–25.

Koonin, E. v., Dolja, V. v., & Morris, T. J. (1993). Evolution and taxonomy of positive-Strand RNA viruses: Implications of comparative analysis of amino acid sequences. *Critical Reviews in Biochemistry and Molecular Biology*, *28*(5), 375–430.

Koonin, E. v., Wolf, Y. I., Nagasaki, K., & Dolja, V. v. (2008). The Big Bang of picorna-like virus evolution antedates the radiation of eukaryotic supergroups. *Nature Reviews Microbiology 2008 6:12*, *6*(12), 925–939.

Kopek, B. G., Perkins, G., Miller, D. J., Ellisman, M. H., & Ahlquist, P. (2007). Three-Dimensional Analysis of a Viral RNA Replication Complex Reveals a Virus-Induced Mini-Organelle. *PLOS Biology*, *5*(9), e220.

Kroner, P. A., Young, B. M., & Ahlquist, P. (1990). Analysis of the role of brome mosaic virus 1a protein domains in RNA replication, using linker insertion mutagenesis. *Journal of Virology*, *64*(12), 6110–6120.

Kushner, D. B., Lindenbach, B. D., Grdzelishvili, V. Z., Noueiry, A. O., Paul, S. M., & Ahlquist, P. (2003). Systematic, genome-wide identification of host genes affecting replication of a positive-strand RNA virus. *Proceedings of the National Academy of Sciences*, *100*(26), 15764–15769.

Lampio, A., Kilpeläinen, I., Pesonen, S., Karhi, K., Auvinen, P., Somerharju, P., & Kääriäinen, L. (2000). Membrane Binding Mechanism of an RNA Virus-capping Enzyme *. *Journal of Biological Chemistry*, *275*(48), 37853–37859.

Lane, L. C., & Kaesberg, P. (1971). Multiple genetic components in bromegrass mosaic virus. *Nature New Biology*, *232*(28), 40–43.

Lee, W.-M., & Ahlquist, P. (2003). Membrane Synthesis, Specific Lipid Requirements, and Localized Lipid Composition Changes Associated with a Positive-Strand RNA Virus RNA Replication Protein. *Journal of Virology*, *77*(23), 12819–12828.

Lee, W.-M., Ishikawa, M., & Ahlquist, P. (2001). Mutation of Host Δ9 Fatty Acid Desaturase Inhibits Brome Mosaic Virus RNA Replication between Template Recognition and RNA Synthesis. *Journal of Virology*, *75*(5), 2097–2106.

Lefkowitz, E. J., Dempsey, D. M., Hendrickson, R. C., Orton, R. J., Siddell, S. G., & Smith, D. B. (2018). Virus taxonomy: the database of the International Committee on Taxonomy of Viruses (ICTV). *Nucleic Acids Research*, *46*(D1), D708–D717.

Levy, L., Damsteegt, V., Scorza, R., & Kolber, M. (2000). Plum Pox Potyvirus Disease of Stone Fruits. *APSnet*. Available online: http://www.apsnet.org/online/feature/PlumPox/.

Li, J., Fuchs, S., Zhang, J., Wellford, S., Schuldiner, M., & Wang, X. (2016). An unrecognized function for COPII components in recruiting the viral replication protein BMV 1a to the perinuclear ER. *Journal of Cell Science*, *129*(19), 3597–3608.

López-Moya, J. J., Valli, A., & García, J. A. (2009). Potyviridae. *Encyclopedia of Life Sciences*.

Lucas, R. W., Larson, S. B., & McPherson, A. (2002). The crystallographic structure of brome mosaic virus. *Journal of Molecular Biology*, *317*(1), 95–108.

Mackenzie, J. M., Khromykh, A. A., & Parton, R. G. (2007). Cholesterol Manipulation by West Nile Virus Perturbs the Cellular Immune Response. *Cell Host & Microbe*, *2*(4), 229–239.

McCartney, A. W., Greenwood, J. S., Fabian, M. R., White, K. A., & Mullen, R. T. (2005). Localization of the Tomato Bushy Stunt Virus Replication Protein p33 Reveals a Peroxisome-to-Endoplasmic Reticulum Sorting Pathway. *The Plant Cell*, *17*(12), 3513–3531.

Miller, D. J., & Ahlquist, P. (2002). Flock House Virus RNA Polymerase Is a Transmembrane Protein with Amino-Terminal Sequences Sufficient for Mitochondrial Localization and Membrane Insertion. *Journal of Virology*, *76*(19), 9856–9867.

Miller, D. J., Schwartz, M. D., & Ahlquist, P. (2001). Flock House Virus RNA Replicates on Outer Mitochondrial Membranes in Drosophila Cells. *Journal of Virology*, *75*(23), 11664.

Miller, W. A., Dreher, T. W., & Hall, T. C. (1985). Synthesis of brome mosaic virus subgenomic RNA in vitro by internal initiation on (−)-sense genomic RNA. *Nature 1985 313:5997*, *313*(5997), 68–70.

Mishra, P. M., Verma, N. C., Rao, C., Uversky, V. N., & Nandi, C. K. (2020). Intrinsically disordered proteins of viruses: Involvement in the mechanism of cell regulation and pathogenesis. *Progress in Molecular Biology and Translational Science*, *174*, 1-78.

Miyanari, Y., Atsuzawa, K., Usuda, N., Watashi, K., Hishiki, T., Zayas, M., Bartenschlager, R., Wakita, T., Hijikata, M., & Shimotohno, K. (2007). The lipid droplet is an important organelle for hepatitis C virus production. *Nature Cell Biology*, *9*(9), 1089–1097.

Nagy, P. D., & Pogany, J. (2011). The dependence of viral RNA replication on co-opted host factors. *Nature Reviews Microbiology 2012 10:2*, *10*(2), 137–149.

Nicaise, V. (2014). Crop immunity against viruses: Outcomes and future challenges. *Frontiers in Plant Science*, *5*, 660.

Noueiry, A. O., & Ahlquist, P. (2003). Brome Mosaic Virus RNA Replication: Revealing the Role of the Host in RNA Virus Replication. In *Annual Review of Phytopathology*, *41*, 77-98.

O'Reilly, E. K., Wang, Z., French, R., & Kao, C. C. (1998). Interactions between the Structural Domains of the RNA Replication Proteins of Plant-Infecting RNA Viruses. *Journal of Virology*, *72*(9), 7160–7169.

Patarroyo, C., Laliberté, J. F., & Zheng, H. (2013). Hijack it, change it: How do plant viruses utilize the host secretory pathway for efficient viral replication and spread? *Frontiers in Plant Science*, *3*, 308.

Peränen, J., Laakkonen, P., Hyvönen, M., & Kääriäinen, L. (1995). The Alphavirus Replicase Protein nsP1 Is Membrane-Associated and Has Affinity to Endocytic Organelles. *Virology*, *208*(2), 610–620.

Perera, R., Riley, C., Isaac, G., Hopf-Jannasch, A. S., Moore, R. J., Weitz, K. W., Pasa-Tolic, L., Metz, T. O., Adamec, J., & Kuhn, R. J. (2012). Dengue Virus Infection Perturbs Lipid Homeostasis in Infected Mosquito Cells. *PLOS Pathogens*, *8*(3), e1002584.

Pocsai, E. (1987). Effect of brome mosaic virus infection on the plant height and weight of cereals at their early stages of growth. *Cereal Research Communications*, *15*(2/3), 167–174.

Pudupakam, R. S., Huang, Y. W., Opriessnig, T., Halbur, P. G., Pierson, F. W., & Meng, X. J. (2009). Deletions of the Hypervariable Region (HVR) in Open Reading Frame 1 of Hepatitis E Virus Do Not Abolish Virus Infectivity: Evidence for Attenuation of HVR Deletion Mutants In Vivo. *Journal of Virology*, *83*(1), 384–395.

Purdy, M. A., Lara, J., & Khudyakov, Y. E. (2012). The Hepatitis E Virus Polyproline Region Is Involved in Viral Adaptation. *PLOS ONE*, *7*(4), e35974.

Ravindran, M. S., Bagchi, P., Cunningham, C. N., & Tsai, B. (2016). Opportunistic intruders: how viruses orchestrate ER functions to infect cells. *Nature Reviews Microbiology*, *14*(7), 407–420.

Restrepo-Hartwig, M. A., & Ahlquist, P. (1996). Brome mosaic virus helicase- and polymerase-like proteins colocalize on the endoplasmic reticulum at sites of viral RNA synthesis. *Journal of Virology*, *70*(12), 8908–8916.

Restrepo-Hartwig, M., & Ahlquist, P. (1999). Brome mosaic virus RNA replication proteins 1a and 2a colocalize and 1a independently localizes on the yeast endoplasmic reticulum. *Journal of Virology*, *73*(12), 10303–10309.

Riechmann, J. L., Laín, S., & García, J. A. (1992). Highlights and prospects of potyvirus molecular biology. *Journal of General Virology*, *73*(1), 1–16.

Romero-Brey, I., & Bartenschlager, R. (2014). Membranous Replication Factories Induced by Plus-Strand RNA Viruses. *Viruses 2014, Vol. 6, Pages 2826-2857*, *6*(7), 2826–2857.

Romero-Brey, I., Merz, A., Chiramel, A., Lee, J. Y., Chlanda, P., Haselman, U., Santarella-Mellwig, R., Habermann, A., Hoppe, S., Kallis, S., Walther, P., Antony, C., Krijnse-Locker, J., & Bartenschlager, R. (2012). Three-Dimensional Architecture and Biogenesis of Membrane Structures Associated with Hepatitis C Virus Replication. *PLOS Pathogens*, *8*(12), e1003056.

Rothwell, C., LeBreton, A., Young Ng, C., Lim, J. Y. H., Liu, W., Vasudevan, S., Labow, M., Gu, F., & Gaither, L. A. (2009). Cholesterol biosynthesis modulation regulates dengue viral replication. *Virology*, *389*(1–2), 8–19.

Roulin, P. S., Lötzerich, M., Torta, F., Tanner, L. B., van Kuppeveld, F. J. M., Wenk, M. R., & Greber, U. F. (2014). Rhinovirus Uses a Phosphatidylinositol 4-Phosphate/Cholesterol Counter-Current for the Formation of Replication Compartments at the ER-Golgi Interface. *Cell Host & Microbe*, *16*(5), 677–690.

Rubio, L., Galipienso, L., & Ferriol, I. (2020). Detection of Plant Viruses and Disease Management: Relevance of Genetic Diversity and Evolution. *Frontiers in Plant Science*, *11*, 1092.

Scholthof, K.-B. G., Adkins, S., CzosNEK, H., Palukaitis, P., Jacquot, E., Hohn, T., HohN, B., Saunders, K., Candresse, T., Ahlquist, P., Hemenway, C., & Foster, G. D. (2011). Top 10 plant viruses in molecular plant pathology. *Molecular Plant Pathology*, *12*(9), 938–954.

Schwartz, M., Chen, J., Janda, M., Sullivan, M., den Boon, J., & Ahlquist, P. (2002). A positive-strand RNA virus replication complex parallels form and function of retrovirus capsids. *Molecular Cell*, *9*(3), 505–514.

Shih, D. S., & Kaesberg, P. (1976). Translation of the RNAs of brome mosaic virus: The monocistronic nature of RNA1 and RNA2. *Journal of Molecular Biology*, *103*(1), 77–88.

Stamova, B. S., & Chetelat, R. T. (2000). Inheritance and genetic mapping of cucumber mosaic virus resistance introgressed from Lycopersicon chilense into tomato. *Theoretical and Applied Genetics 2000 101:4*, *101*(4), 527–537.

Sullivan, M. L., & Ahlquist, P. (1999). A brome mosaic virus intergenic RNA3 replication signal functions with viral replication protein 1a to dramatically stabilize RNA in vivo. *Journal of Virology*, *73*(4), 2622–2632.

Takahashi, H., Suzuki, M., Natsuaki, K., Shigyo, T., Hino, K., Teraoka, T., Hosokawa, D., & Ehara, Y. (2001). Mapping the Virus and Host Genes Involved in the Resistance Response in Cucumber Mosaic Virus-Infected Arabidopsis thaliana. *Plant and Cell Physiology*, *42*(3), 340–347.

Tokuriki, N., Oldfield, C. J., Uversky, V. N., Berezovsky, I. N., & Tawfik, D. S. (2009). Do viral proteins possess unique biophysical features? *Trends in Biochemical Sciences*, *34*(2), 53–59.

Traynor, P., & Ahlquist, P. (1990). Use of bromovirus RNA2 hybrids to map cis- and trans-acting functions in a conserved RNA replication gene. *Journal of Virology*, *64*(1), 69–77.

Tripathi, S., Suzuki, J. Y., Carr, J. B., McQuate, G. T., Ferreira, S. A., Manshardt, R. M., Pitz, K. Y., Wall, M. M., & Gonsalves, D. (2011). Nutritional composition of Rainbow papaya, the first commercialized transgenic fruit crop. *Journal of Food Composition and Analysis*, *24*(2), 140–147.

Tripathi, S., Suzuki, J. Y., Ferreira, S. A., & Gonsalves, D. (2008). Papaya ringspot virus-P: Characteristics, pathogenicity, sequence variability and control. *Molecular Plant Pathology*, *9*(3), 269–280.

van der Heijden, M. W., & Bol, J. F. (2002). Composition of alphavirus-like replication complexes: involvement of virus and host encoded proteins Brief Review. *Arch Virol*, *147*, 875–898.

van Meer, G., Voelker, D. R., & Feigenson, G. W. (2008). Membrane lipids: where they are and how they behave. *Nature Reviews Molecular Cell Biology*, *9*(2), 112–124.

Vance, D. E., Trip, E. M., & Paddon, H. B. (1980). Poliovirus increases phosphatidylcholine biosynthesis in HeLa cells by stimulation of the rate-limiting reaction catalyzed by CTP: phosphocholine cytidylyltransferase. *Journal of Biological Chemistry*, *255*(3), 106–1069.

Vasiljeva, L., Merits, A., Golubtsov, A., Sizemskaja, V., Kääriäinen, L., & Ahola, T. (2003). Regulation of the Sequential Processing of Semliki Forest Virus Replicase Polyprotein *. *Journal of Biological Chemistry*, *278*(43), 41636–41645.

Verchot, J. (2014). The ER quality control and ER associated degradation machineries are vital for viral pathogenesis. *Frontiers in Plant Science*, *5*, 66.

Voeltz, G. K., Prinz, W. A., Shibata, Y., Rist, J. M., & Rapoport, T. A. (2006). A Class of Membrane Proteins Shaping the Tubular Endoplasmic Reticulum. *Cell*, *124*(3), 573–586.

Wang, R., Wang, N., Ye, T., Chen, H., Fan, Z., & Zhou, T. (2013). Natural Infection of Maize by Cucumber Mosaic Virus in China. *Journal of Phytopathology*, *161*(11–12), 880–883.

Wang, X., & Ahlquist, P. (2008). Brome Mosaic Virus. *Encyclopedia of Virology*, 381–386.

Wang, X., Jiang, Z., Yue, N., Jin, X., Zhang, X., Li, Z., Zhang, Y., Wang, X.-B., Han, C., Yu, J., & Li, D. (2021). Barley stripe mosaic virus γb protein disrupts chloroplast antioxidant defenses to optimize viral replication. *The EMBO Journal*, *40*(16), e107660.

Wang, X., Lee, W.-M., Watanabe, T., Schwartz, M., Janda, M., & Ahlquist, P. (2005). Brome Mosaic Virus 1a Nucleoside Triphosphatase/Helicase Domain Plays Crucial Roles in Recruiting RNA Replication Templates. *Journal of Virology*, *79*(21), 13747–13758.

Welsch, S., Miller, S., Romero-Brey, I., Merz, A., Bleck, C. K. E., Walther, P., Fuller, S. D., Antony, C., Krijnse-Locker, J., & Bartenschlager, R. (2009). Composition and Three-Dimensional Architecture of the Dengue Virus Replication and Assembly Sites. *Cell Host & Microbe*, *5*(4), 365–375.

Wolf, Y. I., Kazlauskas, D., Iranzo, J., Lucía-Sanz, A., Kuhn, J. H., Krupovic, M., Dolja, V. v., & Koonin, E. v. (2018). Origins and Evolution of the Global RNA Virome. *mBio*, *9*(6), e02329-18.

Xu, K., & Nagy, P. D. (2016). Enrichment of Phosphatidylethanolamine in Viral Replication Compartments via Co-opting the Endosomal Rab5 Small GTPase by a Positive-Strand RNA Virus. *PLOS Biology*, *14*(10), e2000128.

Xue, B., Blocquel, D., Habchi, J., Uversky, A. v., Kurgan, L., Uversky, V. N., & Longhi, S. (2014). Structural Disorder in Viral Proteins. *Chemical Reviews*, *114*(13), 6880–6911.

Yang, Y. S., & Strittmatter, S. M. (2007). The reticulons: A family of proteins with diverse functions. *Genome Biology*, *8*(12), 1–10.

Yi, G., Gopinath, K., & Kao, C. C. (2007). Selective Repression of Translation by the Brome Mosaic Virus 1a RNA Replication Protein. *Journal of Virology*, *81*(4), 1601–1609.

Zhang, J., Diaz, A., Mao, L., Ahlquist, P., & Wang, X. (2012). Host Acyl Coenzyme A Binding Protein Regulates Replication Complex Assembly and Activity of a Positive-Strand RNA Virus. *Journal of Virology*, *86*(9), 5110–5121.

Zhang, J., Zhang, Z., Chukkapalli, V., Nchoutmboube, J. A., Li, J., Randall, G., Belov, G. A., & Wang, X. (2016). Positive-strand RNA viruses stimulate host phosphatidylcholine synthesis at viral replication sites. *Proceedings of the National Academy of Sciences*, *113*(8), E1064–E1073.

Zhang, Z., He, G., Filipowicz, N. A., Randall, G., Belov, G. A., Kopek, B. G., & Wang, X. (2019). Host Lipids in Positive-Strand RNA Virus Genome Replication. *Frontiers in Microbiology*, *10*, 286.

Zhang, Z., He, G., Han, G. S., Zhang, J., Catanzaro, N., Diaz, A., Wu, Z., Carman, G. M., Xie, L., & Wang, X. (2018). Host Pah1p phosphatidate phosphatase limits viral replication by regulating phospholipid synthesis. *PLoS Pathogens*, *14*(4), e1006988.

Zhanga, J., Zhang, Z., Chukkapalli, V., Nchoutmboube, J. A., Li, J., Randall, G., Belov, G. A., & Wang, X. (2016). Positive-strand RNA viruses stimulate host phosphatidylcholine synthesis at viral replication sites. *Proceedings of the National Academy of Sciences of the United States of America*, *113*(8), E1064–E1073.

Zurek, N., Sparks, L., & Voeltz, G. (2011). Reticulon Short Hairpin Transmembrane Domains Are Used to Shape ER Tubules. *Traffic*, *12*(1), 28–41.

CHAPTER 2

A Conserved Viral Amphipathic Helix Governs the Replication Site-Specific Membrane Association

A preprint version of this chapter is available at bioRxiv. The full citation detail is: Preethi Sathanantham, Wenhao Zhao, Guijuan He, Austin Murray, Emma Fenech, Arturo Diaz, Maya Schuldiner, Xiaofeng Wang (2021). A conserved viral amphipathic helix governs the replication site-specific membrane association. https://doi.org/10.1101/2021.12.09.472036

2.1 Abstract

Positive-strand RNA viruses assemble their viral replication complexes (VRCs) on specific host organelle membranes, yet it is unclear how viral replication proteins recognize, and what motifs or domains in viral replication proteins determine, their localizations. We show here that an amphipathic helix, helix B in replication protein 1a of brome mosaic virus (BMV), is necessary for 1a's localization to the nuclear endoplasmic reticulum (ER) membrane where BMV assembles its VRCs. Helix B is also sufficient to target soluble proteins to the nuclear ER membrane in yeast and plant cells. We further show that an equivalent helix in several plant- and human-infecting viruses of the alphavirus-like superfamily targets fluorescent proteins to the organelle membranes where they form their VRCs, including ER, vacuole, and Golgi membranes. Our work reveals a conserved helix that governs the localization of VRCs among a large group of viruses and points to a possible target for developing broad-spectrum antiviral strategies.

Keywords: amphipathic helix/membrane binding/viral replication complexes

2.2 Summary

Positive-strand RNA viruses [(+)RNA viruses] constitute the largest viral class and include numerous pathogens causing important diseases in humans, animals, and plants. During infection, (+)RNA viruses assemble their viral replication complexes (VRCs), where they multiply at specific organelle membranes. An initial step to form VRCs is to target viral replication proteins to the designated organelle membranes. For brome mosaic virus (BMV), its replication protein 1a is responsible for the VRC formation at the nuclear endoplasmic reticulum (ER) membrane. We show that an amphipathic alpha-helix, helix B, in BMV 1a is necessary for the association of BMV 1a with the nuclear ER membrane, and for BMV genome amplification. In addition, Helix B is sufficient to target several soluble proteins to the nuclear ER membrane in yeast and plant cells. BMV belongs to the alphavirus-like superfamily that includes viruses infecting humans, animals, and plants. We further show that the helix B across members of the alphavirus-like superfamily is sufficient to target fluorescence proteins to the designated organelle membrane. Our results reveal a conserved feature among a large group of viruses in governing their associations with replication site-specific organelle membranes and point to a target to develop broad-spectrum antivirals.

2.3 Introduction

Positive-strand RNA viruses [(+)RNA viruses] are the largest viral class and include many important human and animal pathogens as well as the great majority of plant viruses. Just a few examples include SARS-COV-2 that has infected more than 200 million and led to the death of >4.6 million people in the world (*COVID Live Update: Worldometer*, 2021); foot and mouth disease virus, the most economically important animal virus; and cucumber mosaic virus (CMV),

which infects more than 1,200 plant species. Despite very different host ranges, (+)RNA viruses are only grouped into three superfamilies (alphavirus-, flavivirus-, and picornavirus-like superfamilies) based on their genome organization and homology of RNA-dependent RNA polymerase (Koonin et al., 2015). Each superfamily includes viruses infecting humans, animals, and plants.

A universal feature of (+)RNA viruses is that they assemble their viral replication complexes (VRCs) or replication organelles on specific cellular organelle membranes (Paul & Bartenschlager, 2013; Wang, 2015). This membrane specificity is attributed to membrane lipid composition (Belov & Kuppeveld, 2012; Chukkapalli et al., 2012; Zhang et al., 2019), among others. The viral replication proteins that commence membrane associations can either be a true integral membrane protein with transmembrane domain(s) (TMDs), such as protein A of Flock House virus (FHV) (Miller et al., 2001; Miller & Ahlquist, 2002) or peripheral membrane-associated proteins such as 2C of poliovirus (Teterina et al., 2006) and nSP1 of Semliki Forest virus (Lampio et al., 2000). Targeting viral replication proteins to the designated organelle membranes is the initial step towards viral replication, and therefore, the knowledge of structural features responsible for protein targeting will not only lead to a better understanding of viral replication mechanisms but may also take us closer to developing new ways for viral control.

Brome mosaic virus (BMV) shares replication features with (+)RNA viruses from many other families and therefore has been useful to investigate fundamental aspects of viral replication and associated processes (Diaz & Wang, 2014; Schwartz et al., 2002). BMV is the type-member of the family *Bromoviridae* and a member of the alphavirus-like superfamily (Diaz & Wang, 2014; He et al., 2021). BMV has a tripartite genome where genomic RNA1 encodes replication protein

1a (1a herein) and RNA2 encodes 2a ($2a^{pol}$ herein) that has a conserved RNA-dependent RNA polymerase domain. RNA3 encodes the movement protein, 3a, and coat protein, which is expressed from RNA4, a subgenomic mRNA that is a replication product of RNA3 (He et al., 2021; Wang & Ahlquist, 2008). BMV assembles its spherular VRCs at perinuclear ER (nER) membranes (Schwartz et al., 2002). Independent of other viral components, 1a localizes to the nER membranes where it induces the invaginations of the outer nER member into the lumen to form spherules (Schwartz et al., 2002), which become VRCs when $2a^{pol}$ and viral genomic RNA templates are recruited by BMV 1a (Schwartz et al., 2002).

BMV 1a has a capping domain at the N-terminus, a helicase-like domain at the C-terminus with a demonstrated NTPase activity (Wang et al., 2005), and a linker region enriched in prolines between two domains (He et al., 2021). It has been previously revealed that a 113-amino acid region in 1a, region E [amino acids (aa) 367-480], is necessary for its nER membrane association (den Boon et al., 2001). Further studies have identified an amphipathic α-helix, helix A (aa 392-409, Fig 2.1A) within region E, that regulates 1a's membrane association, as well as the size and frequency of VRCs, among others (Liu et al., 2009) Although helix A was shown to be sufficient to target GFP to membrane fractions, it remained unclear whether helix A is sufficient to target proteins specifically to the nER membrane (Liu et al., 2009). A second amphipathic α-helix, helix B (aa 416-433, Fig 2.1B), which is within region E and immediately downstream of helix A (Ahola & Karlin, 2015), has been shown to play a crucial role in membrane permeabilization to release the oxidizing potential of the ER lumen, and thus, maintain efficient BMV genome replication (Nishikiori & Ahlquist, 2018).

We report here that helix B is necessary for 1a's nER membrane association and is sufficient to target several soluble proteins to the nER membrane, extending our understanding of the roles of helix B in targeting 1a to the designated organelle for the VRC formation. Furthermore, we show that also the predicted helix B motifs from replication proteins of cowpea chlorotic mottle virus (CCMV), CMV, hepatitis E virus (HEV), and Rubella virus (RuV) direct soluble fluorescent protein(s) to specific organelles where these viruses replicate, revealing a functionally conserved motif across the alphavirus-like superfamily and pointing out a potential antiviral strategy to control a large group of viruses.

2.4 Results

2.4.1 Helix B of 1a is necessary for BMV RNA replication

For many membrane-associated proteins without TMDs, shallow insertion of amphipathic helices into membranes promotes membrane binding and remodeling (Drin & Antonny, 2010; Martyna et al., 2017). BMV 1a does not have any TMD but is tightly associated with the membrane (den Boon et al., 2001) at the nER. It has been previously reported that helix A was able to target GFP to membranes based on a membrane flotation assay (Liu et al., 2009), however, it was unclear whether helix A is sufficient for 1a's association with the nER membrane. We tested whether helix B is involved in targeting 1a to the nER membrane or whether a concerted action by both helices is required.

We first tested whether helix B is necessary for viral replication by deleting the entire sequence of helix B to make the 1a-ΔB mutant. In cells expressing $2a^{pol}$, RNA3, and wild-type (WT) 1a, strong signals were detected for both (-)RNA3 and (+)RNA4, which can only be produced after a full round of replication (Fig 2.1C). In parallel with the previous report that deleting helix A

blocked BMV replication (Liu et al., 2009), no (-)RNA3 or (+)RNA4 band was detected with the 1a-ΔB mutant, indicating that helix B is necessary for BMV replication (Table 2.1).

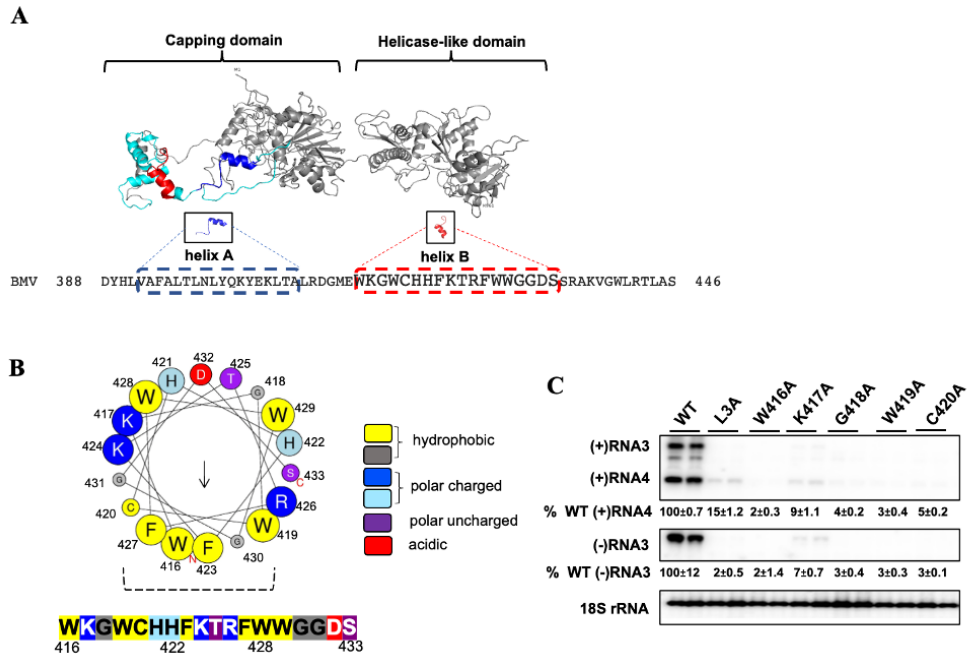

Fig. 2.1. Mutations in BMV 1a helix B inhibit viral genome replication

(A) The predicted model for BMV 1a generated using the resolved crystal structure of tomato mosaic virus helicase-like domain as the template (PDB-3VKW). Helix A and helix B are highlighted in blue and red respectively and their amino acid sequences are shown. Note region E highlighted in cyan includes helix A and B. (B) Helical wheel projection generated using an 18 aa analysis window in Heliquest. The predicted hydrophobic face is formed by W419, G430, F423, W416, F427, and C420, as indicated by the dotted lines. The size of each residue in the helical wheel represents the bulkiness of their sidechain and the arrow in the helical wheel corresponds to the hydrophobic moment. (C) BMV genomic replication was measured by using Northern blotting for WT and various 1a mutants. Positive- and negative-strand viral RNAs were detected using BMV strand-specific probes. 18S rRNA served as a loading control. Band intensities were measured using Adobe Photoshop. Note: L3A has 3 Leu residues replaced by Ala in helix A and serves as a negative control.

We net substituted every amino acid in helix B with alanine and characterized each mutant on their ability to support BMV RNA replication. Most mutants failed to support genome replication, producing (-)RNA3 at levels less than 10% of that with WT 1a (Table 2.1 and Fig 2.1C). These mutants were comparable to that of a helix A mutant, L3A, which has 3 leucine residues replaced by alanine, is not associated with the nER membrane, and is defective in supporting the viral replication (Fig 2.1C) (Liu et al., 2009). Only 5 mutants in Group C (F423A, T425A, F427A, W428A, and S433A) produced (-)RNA3 that were higher than 25% of WT levels. The inhibited BMV RNA replication was not due to the affected expression and/or stability by each mutation, because each mutant accumulated at similar levels to WT 1a (Table 2.1). These data indicated that helix B is necessary for viral replication processes.

Table 2.1. Characteristics of 1a helix B mutants

	1a or 1a mutants	(-)RNA3 accumulation (% of WT)	1a-mediated RNA3 protection (% of WT)	1a accumulation (% of WT)	1a-mC localization	The nER-localized 1a-mC (% of total)
	WT	100	100	100	nER*	>87
Group A	1a-ΔB	0	5	104	C+phER†	0
	W416A	2	9	113	C+phER	7
	G418A	3	13	98	C+phER	0
	W419A	3	11	100	C+phER	2
	C420A	3	22	118	C+phER	0
	H422A	1	10	123	C+phER	0
	K424A	6	23	92	C+phER	0
	R426A	0	0	101	C+PhER	12
	G431A	3	14	168	C+phER	7
Group B	K417A	7	56	98	nER	36
	H421A	3	13	96	nER	28
	W429A	3	49	94	nER	21
	G430A	3	7	89	nER	31
	D432A	4	8	164	nER	17
Group C	F423A	69	83	102	nER	57
	T425A	29	58	112	nER	62
	F427A	33	17	112	nER	21
	W428A	43	54	100	nER	27
	S433A	85	88	96	nER	71

[*]nER represents nuclear ER for all mutants tested. However, the percentage of cells showing nER-localization across mutants was consistently low with respect to cells expressing WT 1a.

[†]cytosolic (C) and peripheral ER (phER) associated mutants.

Mutants are categorized into three groups, A, B, and C, based on their localization, and replicating capacity. Note that only those mutants with >15% cells displaying nER localization are designated as nER.

2.4.2 Helix B is necessary for the nER membrane association of BMV 1a

To assess the impact of each mutation on 1a's membrane association, we performed a membrane flotation assay by an iodixanol density gradient. Membrane flotation assays distinguish membrane-associated or -integral proteins from those that are soluble or cytoplasmic. Using the established conditions where membranes and membrane-proteins float atop the gradient, and soluble fractions sink to the bottom (den Boon et al., 2001), we confirmed that WT 1a and membrane-protein dolichol-phosphate mannosyltransferase (Dpm1) were both detected primarily in the top two fractions, and the soluble protein phosphoglycerate kinase (Pgk1) was in the bottom two fractions (Fig 2.2A). Membrane association was determined as the percentage of a protein in the top three fractions against the sum of all 6 fractions (Fig 2.2A). About 88% of WT 1a, 96% of Dpm1, and 6% of Pgk1 were detected in the top 3 fractions (Fig 2.2A).

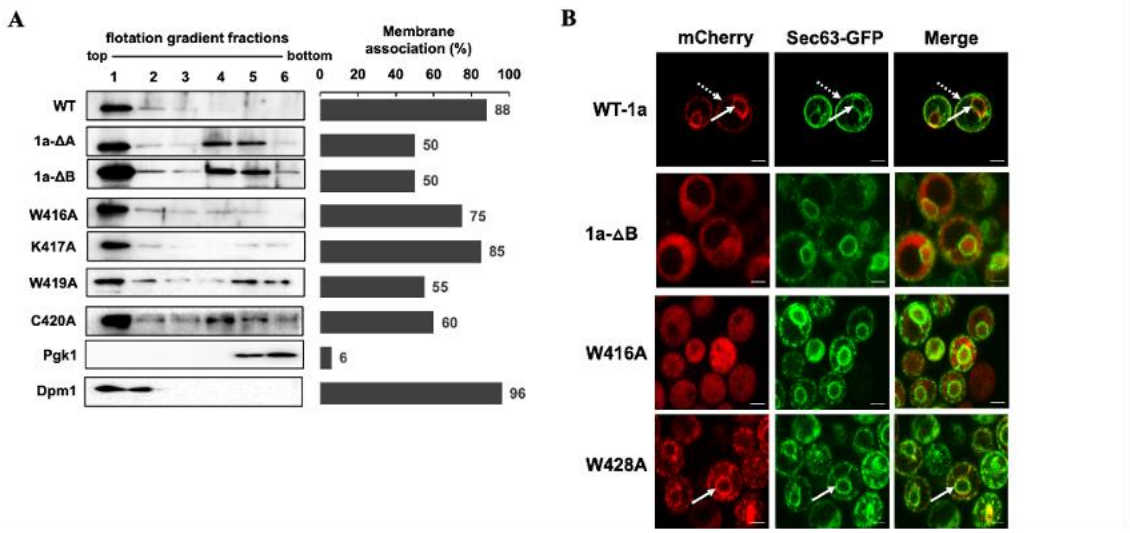

Fig. 2.2. Mutations in BMV 1a helix B inhibit the nuclear ER membrane association of BMV 1a

(A) Membrane association of BMV 1a mutants was determined via a membrane flotation assay. Histograms represent the percentage of membrane-associated proteins as determined by the

signal intensity of each protein segregated into the top three membrane fractions compared to the sum of all six fractions. Lysates of yeast cells expressing WT or mutant 1a were subjected to an iodixanol density gradient and analyzed by Western blotting using antibodies against ER membrane protein Dpm1, soluble protein Pgk1, or His6 for His6-tagged BMV 1a derivatives. **(B)** Localization of mCherry-tagged 1a mutants in yeast cells co-expressing Sec63-GFP as examined using confocal microscopy. Nuclear ER and peripheral ER associations are indicated by solid and dotted arrows, respectively. The yellow signal in the merge panel is representative of colocalization of mCherry-tagged WT or mutant 1a with Sec63-GFP. Scale bars: 2μm.

We chose five replication defective mutants for the membrane flotational analysis, including 1a-ΔB with helix B deleted, W416A, W419A, C420A, and K417A. The mutants W416A, W419A, and C420A form the predicted hydrophobic face of the amphipathic helix (Fig 2.1B) and are also present at the beginning of the helix sequence. The mutant K417A was chosen due to its charged nature and potential contribution to membrane association. The 1a-ΔB mutant showed a 50% accumulation in the membrane fractions. The other 50% accumulated in the cytosolic fractions, with most accumulated in fractions 4 and 5, similar to the previously characterized deletion mutant, 1a-ΔA (Liu et al., 2009). Mutants W416A and K417A showed a strong membrane association with 75% and 85% of total protein in the membrane fractions, whereas W419A and C420A showed membrane association of about 55% and 60%, respectively (Fig 2.2A).
Since membrane flotation results are not informative in terms of specific organelle membranes where target proteins reside, we checked the localization for all 1a mutants using fluorescence and/or confocal microscopy. Since 1a predominantly localizes to the nER membrane when expressed alone (Restrepo-Hartwig & Ahlquist, 1999), we expressed 1a helix B mutants with a C-terminally fused mCherry (mC) in yeast cells along with an ER protein marker, Sec63, with a C-terminally fused GFP. Since proteins could obtain distinct conformation due to the presence of

an additional protein moiety (Argos, 1990; Chen et al., 2013), we incorporated a 32 amino acid linker (herein L32) (Finnigan et al., 2016) with desirable small polar amino acids, such as Thr, Ser, and Gly, between the carboxy-terminal of the protein and mC. The mC-tagged WT 1a protein was efficiently localized to the nER (the inner ring pointed by solid arrows in Fig 2.2B) and the peripheral ER regions (the outer ring as pointed by dotted arrows). When helix B was deleted from 1a, the mC signal was throughout the cytoplasm, indicating that helix B was necessary for 1a's association with the nER membrane (Fig 2.2B). Helix B mutants with single substitutions that were defective in replication were segregated into two sets based on their ability to localize to the nER membrane, as shown for a representative mutant for each set in Fig 2.2B. Mutants in Group A (W416A, G418A, W419A, C420A, H422A, K424A, R426A, and G431) were detected mostly throughout the cytosol (Fig 2.2B, Table 2.1). Group B comprised of mutants that could partially localize to the nER membrane, including K417A, H421A, F423A, T425A, F427A, W428A, W429A, G430A, D432A, and S433A. Although Group B mutants retained their ability to associate with the nER membrane, there were not as many cells showing nER localization as observed in cells expressing WT 1a protein (Table 2.1). We also noticed puncta in mutants F423A, T425A, and W429A (Supplemental Fig 2.5 C).

2.4.3 Mutations in helix B inhibit 1a-mediated RNA3 protection

BMV 1a, in the absence of other viral components, induces the formation of spherules in yeast cells. 1a also recognizes and recruits viral genomic RNA and $2a^{pol}$ into spherules, which become VRCs (Schwartz et al., 2002). When expressed alone, RNA3 is unstable in yeast cells with a half-life of 3-10 minutes, whereas in the presence of 1a, the half-life of RNA3 increases to more than 3 hours, and the accumulated RNA3 increases 5-20 folds, depending on the levels of

expressed 1a (Janda & Ahlquist, 1998; Wang et al., 2005). As shown in Fig 2.3, an 11-fold increase of RNA3 was observed in the presence of WT 1a but not in the 1a-ΔB mutant, indicating the importance of helix B in 1a-mediated RNA3 protection. In addition, the majority of helix B mutants with a single substitution showed a comparatively lower amount of protected RNA3 than WT 1a (Fig 2.3, Table1). As shown in Fig 2.3 for W416A, W418A, W419A, and C420A, all mutants in Group A showed <25% levels of the accumulated RNA3 in cells expressing WT 1a (Table 2.1), consistent with the fact that all mutants in Group A failed to associate with the nER (Table 2.1), and thus, these mutations may have substantially interfered with 1a's ability to form spherules. However, this note should be confirmed in the future with electron microscopy. The accumulated RNA was widely varied among mutants in Group B and C, which were partially associated with the nER membrane, from 17% to 88% of WT levels (Table 2.1), as represented by K417A at 56% of WT 1a levels (Fig 2.3).

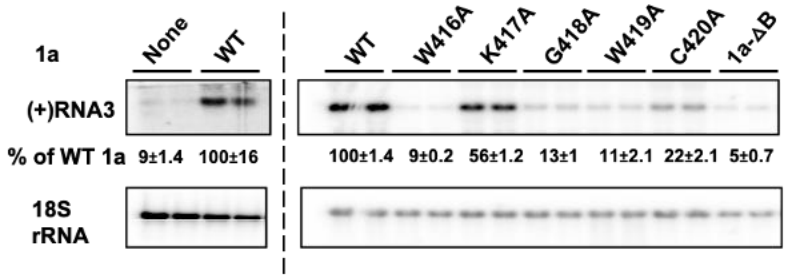

Fig. 2.3. Mutations in BMV 1a helix B inhibit the 1a-mediated RNA3 protection

RNA3 accumulation in the presence of WT or mutant 1a. Total RNA was isolated from cells expressing RNA3 alone or in the presence of WT or mutant 1a. Viral (+)RNA3 was detected using a BMV positive-strand-specific probe. 18S rRNA served as a loading control. Band intensities were measured using Adobe Photoshop. Note Northern blot on the left for WT and the control was done independently from the blot on the right.

2.4.4 Helix B is sufficient to target soluble proteins to the nER membrane

It was previously reported that helix A alone or the entire region E is capable of targeting GFP to the membrane fractions based on membrane flotation assays (Liu et al., 2009). To estimate the membrane association capacity of helix B in comparison to the entire region E or helix A, we performed a membrane flotation assay using lysates from cells expressing GFP-tagged region E, helix A, helix B, or helices A and B.

Consistent with previous studies, when fused to region E or helix A, 54% and 40% of GFP were detected in the membrane fractions compared to the sum of GFP signal across all fractions, respectively (den Boon et al., 2001; Liu et al., 2009). Cells expressing both helices showed 46% of GFP in the membrane fractions but GFP was detected across all the collected fractions, similar to cells expressing region E-GFP. Surprisingly, 68% of helix B-GFP was associated with the membrane fractions, suggesting that helix B is critical in targeting 1a to membranes (Fig 2.4A).

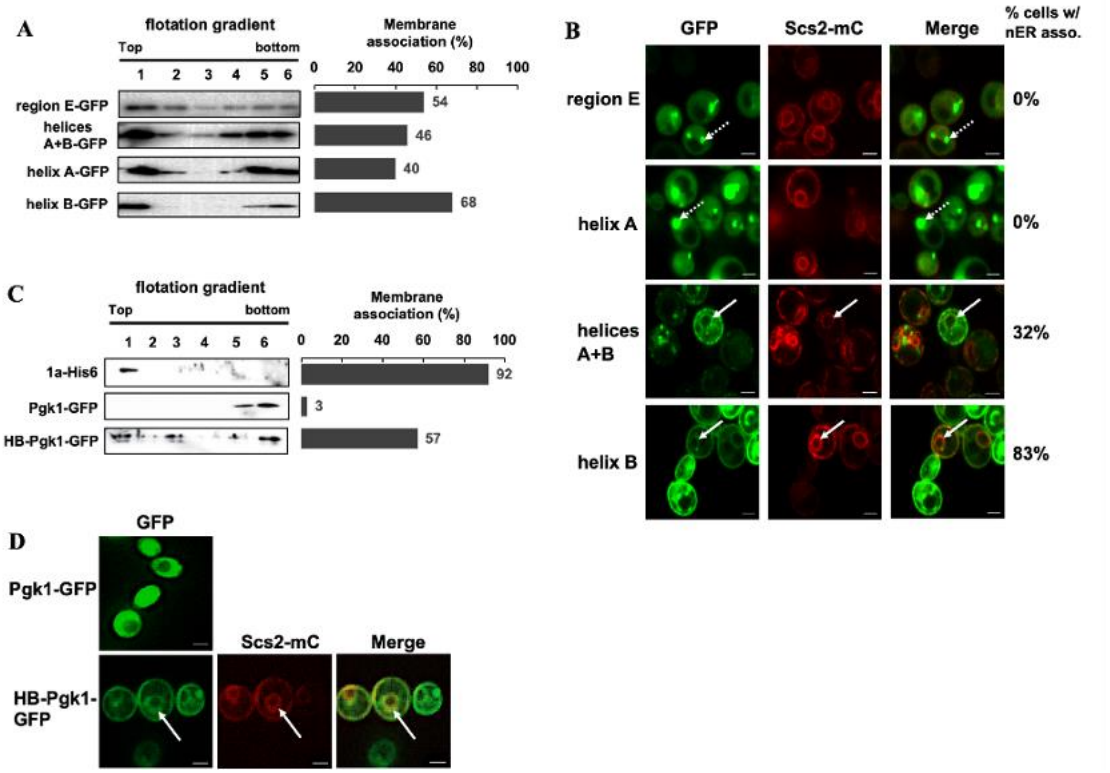

Fig. 2.4. Helix B is capable of targeting soluble proteins to the nuclear ER membrane

(A) Membrane flotation analysis of GFP-fused region E, helices A+B, helix A, and helix B. Histograms represent the percentage of proteins detected in the top three fractions of the flotation gradient. A representative western blot is shown, with bands corresponding to respective 1a fragments detected using an anti-GFP antibody. **(B)** Localization of GFP-tagged region E, helices A+B, helix A, or helix B co-expressed with a mCherry-tagged ER marker protein Scs2. Dotted arrows point to punctate structures and solid arrows point to the nER membrane. Images were obtained using a confocal microscope. **(C)** Membrane flotation analysis for Pgk1-GFP and HB-Pgk1-GFP, using 1a-His6 as a positive control. **(D)** Localization of HB-PGK-GFP at the nER membranes with an ER marker Scs2. Solid arrows point to the nER membrane. Images are obtained using a fluorescence microscope. Scale bars: 2μm.

Since membrane fractions represent many cellular organelle membranes, we turned to microscopy to determine whether helix B-GFP is associated with the nER membrane specifically. To assess whether helix B-GFP is associated with the nER association, we expressed helix B-GFP along with a mCherry-tagged ER marker Scs2. We also included helix A and region E for comparative analysis. Each was expressed under the control of the *GAL1* promoter, and the cells were harvested across various time points post induction when the carbon source was switched from raffinose to galactose. Region E did not localize GFP to the nER membrane across various time points but aggregated as puncta in cells, consistent with the previous report (den Boon et al., 2001). These punctate structures that were observed at 6-7 hours post-induction became more diffused into the cytosolic region at 12h post-induction. Helix A-GFP primarily showed a rather peripheral and dispersed localization along with strong puncta (Fig 2.4B). Cells expressing a 1a fragment encompassing both helices A and B showed a partial nER association in ~32% of the cells. Helix B-GFP, agreeing well with the membrane flotation results (Fig 2.4A), was detected as a two-ring pattern typical of nER and peripheral ER association in nearly 83% of the cells (Fig 2.4B). On the contrary, none of the cells expressing either region E-GFP or helix A-GFP showed the fluorescent signal in the nER membrane (Fig 2.4B), suggesting that helix B is not only sufficient for the nER targeting but also represents the strongest targeting information in region E. Shorter helix B sequences spanning only the first seven (W416-H422) or eleven (W416-R426) amino acids of the alpha-helix B failed to associate with the nER (Fig 2.5 B), suggesting that the amphipathicity is governed by more than the first eleven residues of helix B.

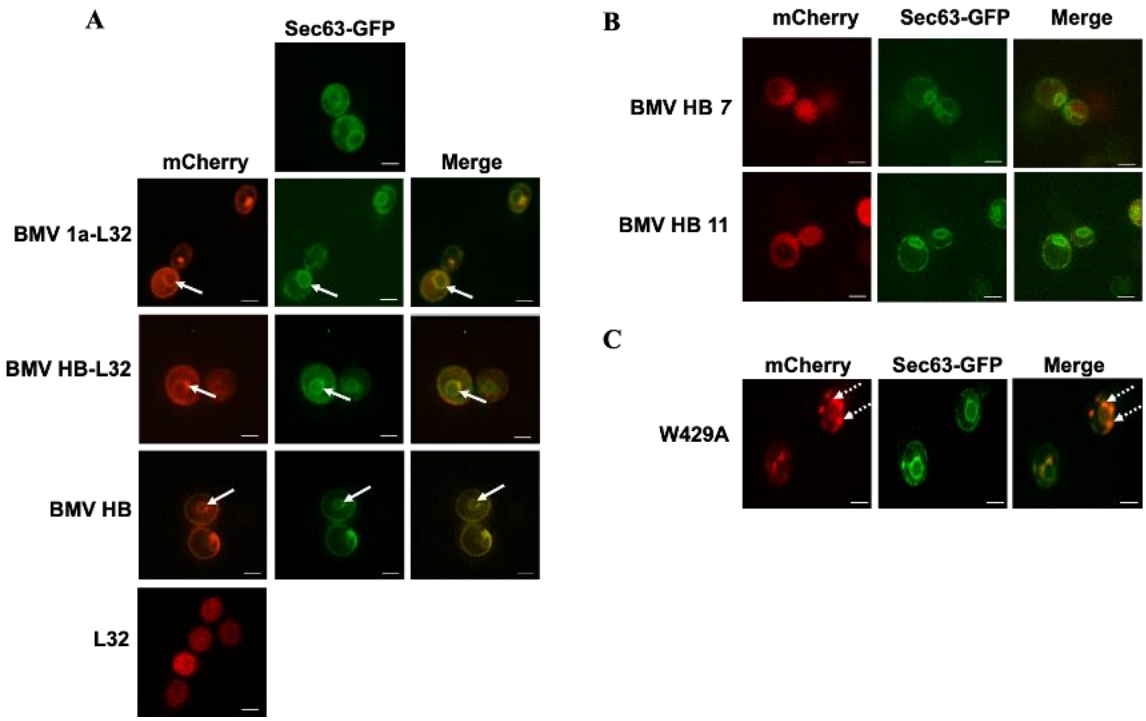

Fig. 2.5. The 32 amino acid-long linker is not required for the correct localization of fluorescent protein-tagged 1a or helix B

(A) Fluorescence microscopic images showing that mCherry-tagged BMV 1a or helix B with or without the 32 aa-long linker is colocalized with an ER marker Sec63-GFP. L32-mC, which is not fused to BMV 1a or helix B, is localized in the cytosol (bottom panel). **(B)** Truncated versions of helix B spanning W416-H422 (BMV HB 7) or W416-R426 (BMV HB 11) fail to target mCherry to ER membranes. **(C)** Localization of a representative mutant, W429A, that formed puncta similar to mutants F423A and T425A (shown in dotted arrows) in cells co-expressing Sec63-GFP. Scale bars: 2μm.

To further determine the capacity of helix B in targeting other soluble proteins to the nER membrane, we fused helix B at the N-terminus of an endogenous yeast cytosolic protein. We chose yeast Pgk1, a soluble protein that is primarily detected in the cytoplasm when fused with GFP (Fig 2.4D) and readily detected at the bottom-most fractions in our flotational analysis in the absence (Fig 2.2A) or presence of GFP (Fig 2.4C). The fusion protein, HB-Pgk1-GFP gained

the ability to associate with membranes and 57% of the protein was detected at the top three fractions (Fig 2.4C). In agreement with the membrane flotation results, it could also be seen localized to the nER and peripheral ER regions, colocalizing with Scs2-mC (Fig 2.4D), similar to WT-1a protein that brought mCherry to the nER membrane (Fig 2.2B). Collectively, our results indicated that Helix B acted as a dominant targeting peptide that directed soluble proteins to the nER membrane.

2.4.5 The amphipathic α-helix represented by helix B is functionally conserved among viruses in the alphavirus-like superfamily

BMV is a representative member of the alphavirus-like superfamily. Viruses in this superfamily contain a methyltransferase-guanylyltransferase (MTase-GTase) domain whose activity has been experimentally confirmed in the nsP1 of SFV (Laakkonen et al., 1994; Scheidel et al., 1989), 1a of BMV (Kong et al., 1999), and open reading frame 1 (ORF1) of hepatitis E virus (HEV) (Magden et al., 2001). Among the alphavirus-like superfamily, a conserved "Iceberg" region has been identified at the C-terminus of the viral MTase-GTase domains with the presence of two amphipathic helices (Ahola & Karlin, 2015), similar to the helices A and B of 1a.

Since amphipathic helix B is a predicted secondary structure conserved across the alphavirus-like superfamily (Ahola & Karlin, 2015) with the actual predicted boundary of each helix varying across the superfamily, we wanted to test whether the predicted helix B from other members is also functionally conserved in terms of targeting the replication protein to specific organelle membranes. We noticed that the primary sequence conservation is retained for members in the same genus, such as BMV and CCMV (Sibert et al., 2018), whereas the conservation is not high across members of a family, including BMV and CMV, where BMV is a type member of the

genus Bromovirus and CMV is of the genus Cucumovirus (Fig 2.6). The primary sequence conservation of helix B was even lower for human viruses such as HEV and RuV when compared against BMV helix B (Ahola & Karlin, 2015).

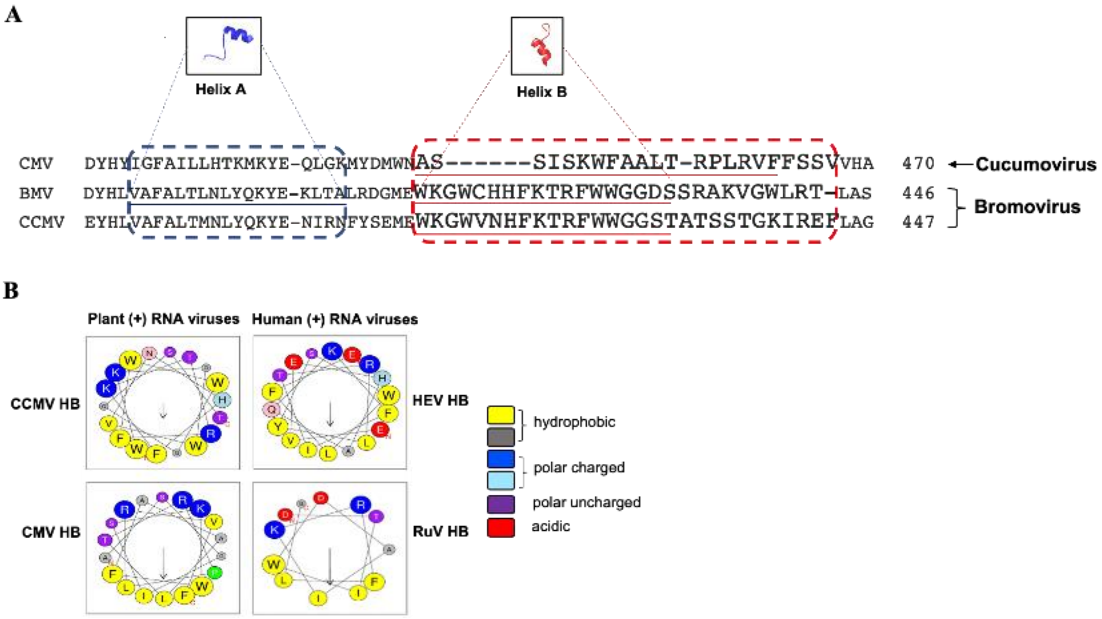

Fig. 2.6. Two amphipathic alpha-helices are present in the replication proteins from members of the alphavirus-like superfamily

(A) Multiple sequence alignment shown for a short stretch of region encompassing helix A and helix B across plant viruses, BMV, CCMV, and CMV. The members of a genus share higher identity in helix A and helix B (CCMV and BMV) than members from higher ranks such as family (BMV and CMV). **(B)** Helical wheel projections of amphipathic helix B of plant (CMV, CCMV) and animal viruses (HEV, RuV) using the predicted helix B regions. Amphipathic faces for CCMV, CMV as predicted by HeliQuest are WGFWFV and PWFLILFA and for HEV and RuV are LALIVY and AFIILW respectively. The arrow in helical wheels corresponds to the hydrophobic moment.

We fused the predicted helix B of CCMV, CMV, HEV, and RuV to the N-terminus of fluorescent proteins and tested the localization of each recombinant protein in yeast cells, along with an ER marker, Scs2-mC or Sec63-GFP. The CCMV helix B, when fused to GFP (CCMV-HB-GFP), was capable of targeting GFP to the nER membrane and colocalized with Scs2-mC (Fig 2.7A). This agreed well with the previous report that CCMV replicates in the nER membranes (Kim, 1977; Sibert et al., 2018) and CCMV 1a when expressed in yeast cells in the absence of other viral proteins, induces the formation of spherular invaginations at the outer nER membranes (Sibert et al., 2018).

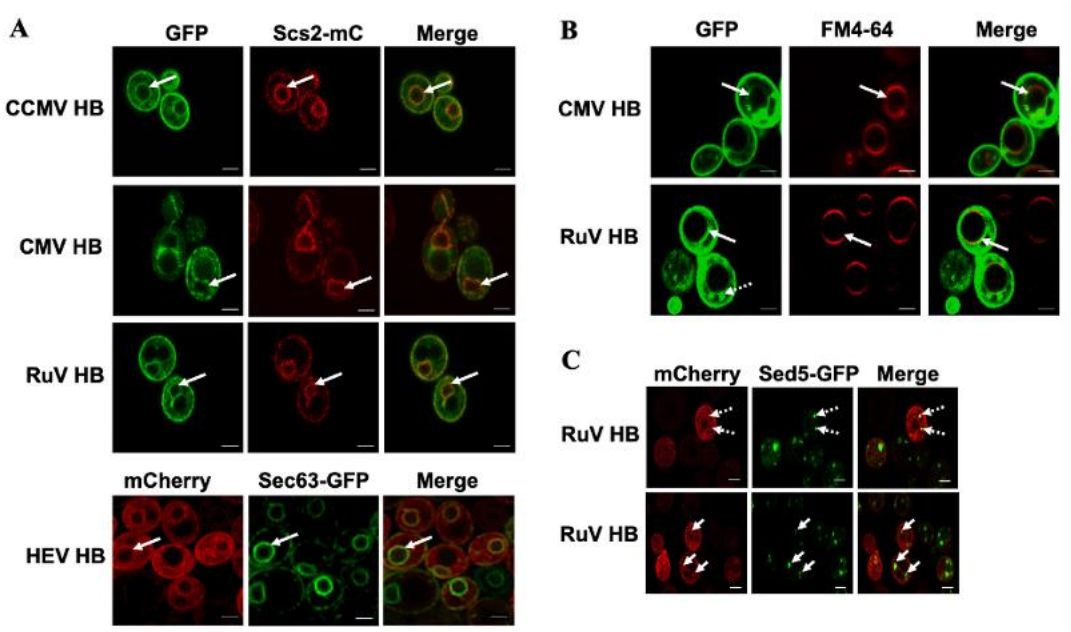

Fig. 2.7. Helix B-mediated organelle targeting is conserved across members of the alphavirus-like superfamily

(A) Colocalization of GFP-tagged HB of CCMV, CMV, or RuV with an ER marker Scs2-mC, and colocalization of the mCherry-tagged HEV HB and Sec63-GFP at the nER membrane. Solid arrows point to the nER membrane. Note arrows in second and third rows (CMV and RuV) distinguish the nER membrane from other membranous regions present in the cells. **(B)**

Colocalization observed for CMV HB and RuV HB with vacuolar membranes stained by a lipophilic dye, FM4-64. The solid arrows in both panels point to vacuolar membranes. The dotted arrow in the RuV-HB panel shows punctate structures. **(C)** Colocalization of RuV HB-mC with Sed5-GFP, a marker for vesicles that traffic from the ER to the Golgi. Images were obtained using a confocal microscope. Scale bars: 2µm.

Unlike BMV and CCMV, CMV replicates in the vacuolar membrane (Hatta & Francki, 1981; Wang, Ma, et al., 2021). Interestingly, CMV helix B targeted GFP to the nER and vacuolar membranes in yeast cells (Fig 2.7A). At 6-7 hours post induction of its expression, CMV-HB-GFP localized at the nER in 64% of cells and at vacuoles in 77% of cells, 12% of cells showed both nER as well as vacuolar localization (n=175). Vacuolar localization of CMV-HB-GFP dominated when grown beyond 7 hours in induction media. It is possible that CMV HB-GFP was localized first to ER membranes, following the protein secretory pathway, before reaching vacuolar membranes.

HEV is a non-enveloped (+)RNA virus in the family of *Hepeviridae* (Kenney & Meng, 2019). It is one of the leading viral pathogens causing acute hepatitis. HEV encodes 3 major ORFs. ORF1 is a polypeptide that is processed by viral encoded proteases. Two amphipathic alpha-helices, helix A (aa 362-380) and B (aa 399-417), are also present in the Y domain (aa 216-442) of ORF1. When fused to GFP, Helix B of HEV ORF1 also colocalized with the ER marker Sec63 at the nER membrane (Fig 2.7A), which is the purported site of HEV replication (Kenney & Meng, 2019). However, mCherry signal was also found between the nER and peripheral ER, similar to tubular ERs that connect the nER and peripheral ER.

RuV is known to utilize multiple organelle membrane sites for its replication. These membranes include those of Golgi, endosomes, vesicles, and vacuoles of endolysosomal origin in addition to ER (Fontana et al., 2007). The viral NS protein P150 is sufficient for organelle targeting (Kujala et al., 1999) and also contains a Y domain similar to HEV with the presence of two amphipathic helices. We expressed RuV helix B with a C-terminally fused GFP and confirmed its localization at the vacuolar regions using a lipophilic dye, FM4-64 that stains the vacuolar membrane (Fig 2.7B), and its localization at the nER by using the ER marker Scs2-mC (Fig 2.7A). We also fused RuV HB (aa 423-434) to mC and coexpressed RuV-HB-mC along with an early Golgi compartment marker Sed5 that was fused with GFP. As shown in Fig 2.7C, RuV-HB-mC did colocalize with the punctate structures seen throughout the cytoplasm labeled by Sed5-GFP.

2.4.6 Helix B from BMV and CMV target fluorescent proteins to ER membranes and tonoplast in plant cells

The ability of BMV and CMV helix B to target GFP to the nER and/or vacuole membranes in yeast cells prompted us to check whether these helices could do the same *in planta*. To do this, we fused BMV or CMV helix B to the N-terminus of YFP in a T-DNA binary vector under the control of the cauliflower mosaic virus (CaMV) 35S promoter (Zhao et al., 2020) and expressed by agroinfiltration in histone 2B-RFP (H2B-RFP) transgenic *Nicotiana benthamiana* plants (Martin et al., 2009). The localization of the YFP signal in *N. benthamiana* cells was observed under a laser confocal microscope at 40 hours post agroinfiltration (hpai), which is the commonly used time point to observe transiently expressed proteins (Zhao et al., 2020). While free YFP was observed in the cytoplasm and the nucleus, BMV HB-YFP signal was observed at the nER membranes, surrounding the histone 2B-RFP-represented nucleus (Fig 2.8A). To

confirm BMV HB-YFP was associated with the nER membrane, we co-expressed BMV HB-YFP and an mC-tagged ER marker (Nelson et al., 2007). The YFP signal was co-localized with the mC signal in the nER and peripheral ER (Fig 2.8B). In addition, we have observed multiple ER-localized aggregates that were not present in cells expressing YFP (Fig 2.8A). Surprisingly, we also observed small vesicle-like structures that contain both signals of YFP and mC (arrowheads in Fig 2.8B), indicating the ER origin of these vesicles. However, the possible functions of these vesicle-like structures are unclear.

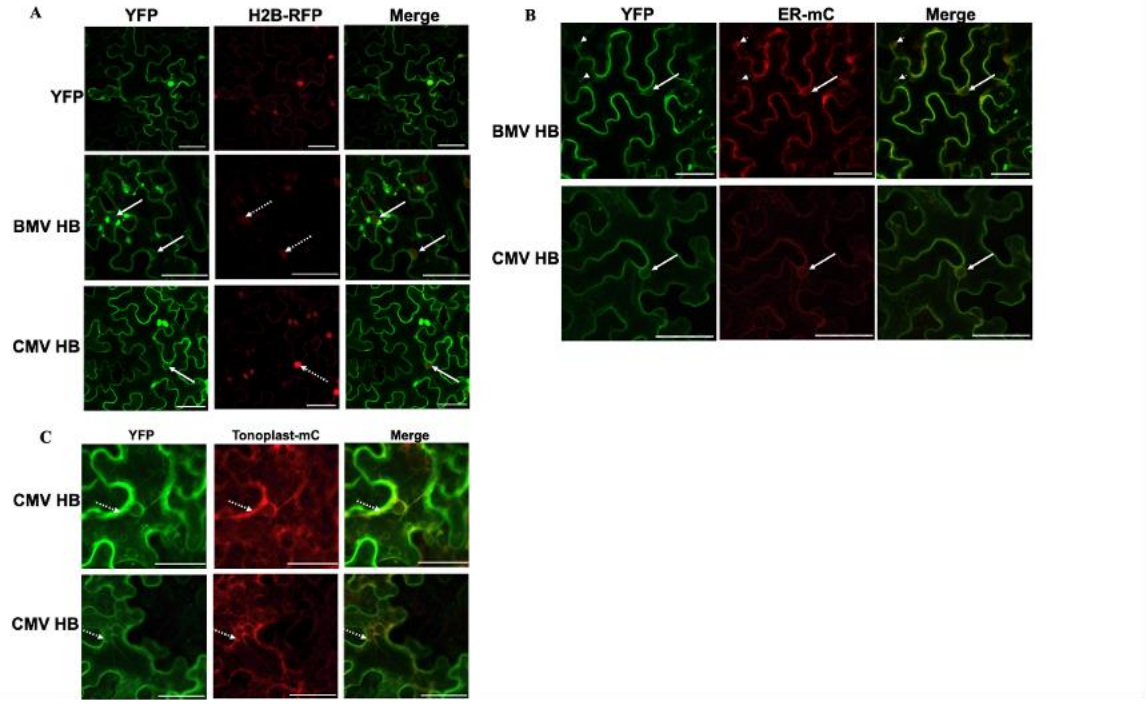

Fig. 2.8. Localizations of BMV and CMV helix B in *N. benthamiana* cells parallel those in yeast cells

(A) YFP-tagged Helix B from BMV or CMV was expressed in histone 2B-RFP transgenic *Nicotiana benthamiana* plants via agroinfiltration. Solid and dotted arrows point to the nER membrane and the nucleus, respectively. (B) BMV HB-YFP was co-expressed with a mCherry-tagged ER marker. Arrows point to the nER membrane and arrowheads point to small vesicles

that are colocalized with the ER marker. (C) Colocalization of CMV HB-YFP with a mCherry-tagged tonoplast marker as indicated by dotted arrows. The fluorescence signal was observed under laser confocal microscopy at 40 hpai. Scale bars: 50μm.

We next tested the localization of YFP-tagged CMV HB in H2B-RFP-transgenic *N. benthamiana* cells. Similar to what we have observed in yeast cells, CMV HB-YFP was localized at the nER membrane surrounding the nucleus and co-localized with the ER marker (Fig 2.8A and B). Agreeing well with the report that CMV 1a, when expressed alone, localizes to vacuolar membranes (Wang, Ma, et al., 2021), CMV HB-RFP was detected primarily at the tonoplasts as it colocalized with an mC-tagged tonoplast marker (Fig 2.8C). These results confirmed the results observed in yeast that CMV HB can target YFP to both ER and vacuolar membranes. We also included YFP-tagged CCMV HB in our study and found nER localization in these cells (Fig 2.9), agreeing well with the results in yeast cells (Fig 2.7A).

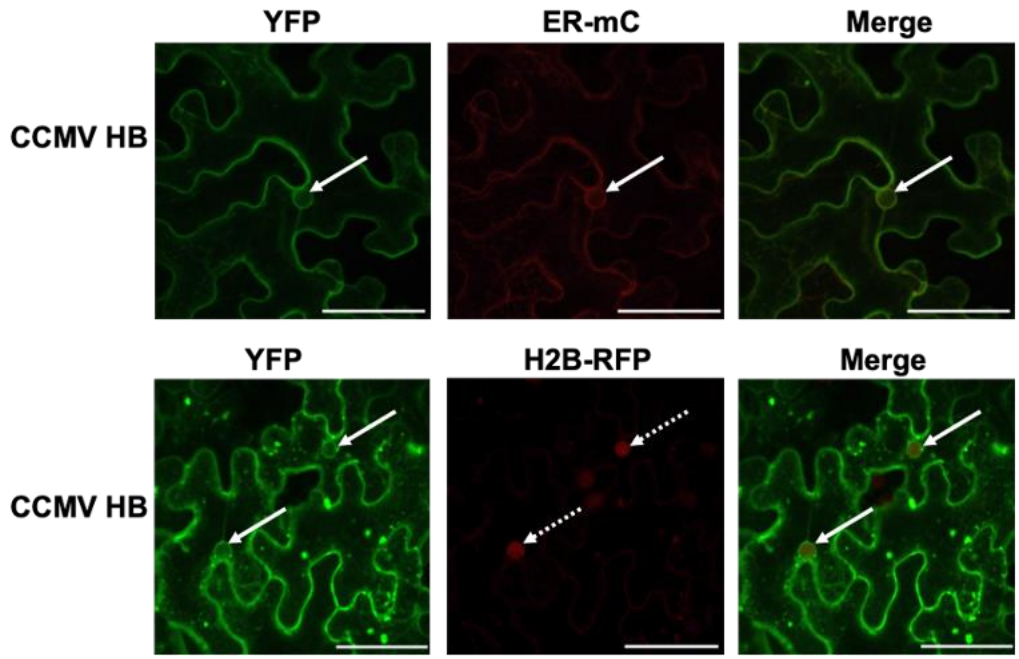

Fig. 2.9. CCMV HB directs yellow fluorescent protein to ER membranes
Confocal microscope images showing YFP-tagged CCMV HB with an ER-mC marker (top row). The bottom panel shows colocalization of YFP-tagged CCMV HB expressed in histone 2B-RFP transgenic plant background. Solid arrows denote the nER localization and dotted arrows represent the nucleus. Scale bars: 50µm.

2.5 Discussion

The membrane association of viral replication complexes is a key feature across all (+)RNA viruses. Different (+)RNA viruses replicate in specific organelle membranes. BMV, CCMV, and beet black scotch virus replicate on ER membranes, whereas CMV, tomato bushy stunt virus, barley stripe mosaic virus, and turnip crinkle virus prefer membranes of the tonoplast, peroxisome, chloroplast, and mitochondria, respectively (Blake et al., 2007; Cao et al., 2015; Hatta & Francki, 1981; Kim, 1977; McCartney et al., 2005; Restrepo-Hartwig & Ahlquist, 1996; Wang, Jiang, et al., 2021). Some plausible reasons for the varied preference of membranes are believed to be due to the membrane lipids and/or protein compositions (Lee et al., 2001; Lee &

Ahlquist, 2003; Zhang et al., 2012, 2016, 2018). However, it is still unclear what structural determinant(s) within the viral replication proteins are responsible for targeting these proteins to specific organelles, especially for those that lack TMDs, such as BMV 1a. We report here that a single amphipathic α-helix in 1a, helix B, plays a key role in determining 1a's association with the nER membrane. Helix B is necessary for 1a's nER membrane association and is sufficient to target several soluble proteins to the nER membrane, extending our understanding beyond its role as to regulate the oxidizing potential of the ER lumen (Nishikiori & Ahlquist, 2018). We further show that a similar helix in the replication proteins of CCMV, CMV, HEV, and RuV can target fluorescent proteins to the specific organelles where their VRCs are formed, revealing a conserved feature among members of the alphavirus-like superfamily.

2.5.1 BMV 1a helix B is necessary and sufficient for 1a's association with the nuclear ER membrane

Many viral replication proteins from (+)RNA viruses contain TMDs that target them to the designated organelle membranes for initiating the VRC formation. Protein A of FHV, when expressed alone, is targeted to the outer mitochondrial membrane where FHV forms VRCs (Ertel et al., 2017; Miller & Ahlquist, 2002). Protein A has an N-terminal TMD (aa 1-46) that is sufficient to target GFP to mitochondrial membranes (Miller & Ahlquist, 2002). Replication proteins of some (+)RNA viruses lack a TMD but possess amphipathic α-helix or helices, includes BMV 1a (helix A, aa 392-407 and helix B aa 416-433) (Ahola & Karlin, 2015; Liu et al., 2009; Nishikiori & Ahlquist, 2018), Chikungunya virus nsP1 (aa 244-263) (Gottipati et al., 2020), poliovirus 2C (aa 19-36) (Laufman et al., 2019; Teterina et al., 2006), Hepatitis C virus 5A (aa 7-28) (Elazar et al., 2003), and SFV nsP1 (aa 245-264) (Spuul et al., 2007), among others.

Amphipathic α-helices have long been recognized as generators and/or sensors of membrane curvature (Drin & Antonny, 2010; Shen et al., 2012). Residues on the hydrophobic face of the helix insert into the fatty acid tails while polar residues are involved in electrostatic interactions with the polar head of phospholipids (Jensen et al., 2011). It has long been understood that the amphipathic α-helix serves as an anchor, inserting TMD-lacking viral proteins shallowly into the membranes. Our recent data indicated that the helix of poliovirus 2C played an active role in remodeling membranes. In an *in vitro* tubulation assay, the synthesized peptide representing the helix of poliovirus 2C converted large spherical liposomes into tubules and smaller vesicles that were stable for a week (Varkey et al., 2020). In addition, mutations disrupting the helicity of the 2C helix inhibited membrane remodeling *in vitro* when expressed as a peptide and blocked viral replication when incorporated into the full-length viral genome (Varkey et al., 2020).

Helix B of BMV 1a was first predicted by Ahola and Karlin while analyzing BMV 1a, SFV nSP1, and equivalent replication proteins among the alphavirus-like superfamily (Ahola & Karlin, 2015). The predicted helix B was further characterized for its amphipathicity and its viroporin activity that allows oxidizing environment within BMV VRCs (Nishikiori & Ahlquist, 2018). In this study, we determined that helix B is necessary and sufficient for BMV 1a's association with nER membrane, and thus, essential for BMV genomic replication (Table 2.1). The vast majority of the helix B mutants (group A and B) with an Ala substitution either failed or supported no more than 10% of WT 1a genomic replication (Table 2.1), indicating a crucial role for helix B in this process. This also aligns with the reported helix B mutants K424G and R426K for selectively lacking viroporin activity that failed to replicate (Nishikiori & Ahlquist, 2018). The 19 helix B mutants generated in this study can be divided into three groups based on genomic replication and their localization. Group A contains nine mutants, including the helix B

deletion mutant, and eight Ala-replacement mutants (W416A, G418A, W419A, C420A, H422A, K424A, R426A, and G431A), which were primarily detected in the cytoplasm and possibly peripheral ER membranes (Table 2.1). Future experiments will further address to which organelle(s), other than the nER, these 1a mutants were targeted. Group B includes five mutants that were associated with the nER at lower efficiency than WT, ranging from 17% to 36% of cells (Table 2.1). For instance, K417A was detected in the nER membrane in 36% of cells, compared to 87% of cells with WT 1a (Table 2.1). Mutants in both Groups A and B supported less than 10% of viral genomic replication compared to WT 1a. Another five mutants supporting partial replication and inefficiently localized at the nER membrane are assigned to group C. It is possible that some mutants were only transiently associated with the nER. Given the fact that these mutants accumulated at a similar level to WT (Table 2.1), we concluded that helix B is necessary for BMV 1a's nER membrane association and thus, genome replication.

Soluble proteins, GFP (Fig 2.4B), mC (Supplemental Fig 2.5 A), and Pgk1 (Fig 2.4D), were targeted primarily to the nER and also peripheral ER membrane when fused to helix B at their N-terminus. However, helix A-tagged GFP did not (Fig 2.4B), indicating that BMV 1a helix B is responsible for 1a's targeting to the nER membrane. We are unable to determine whether helix B-mediated nER targeting is due to the specific lipid composition of the organelle membranes or whether it interacts with a specific host protein that localizes to the nER (Li et al., 2016). It will be exciting to study in the future whether targeting is an active process requiring host machinery in trans or whether it is a passive process relying on cis-elements within the helix and their internal propensity to bind the lipid bilayer.

2.5.2 Helix B-mediated organelle targeting is a conserved feature across members within the alphavirus-like superfamily

The initial step for a successful viral infection is to assemble functional VRCs at the target organelle. This starts with targeting viral replication proteins to the organelle where VRCs will be established. Disruption of this step will block viral replication at its early stage. For instance, we have reported a mutant of yeast protein Cho2p (choline requiring 2), *Cho2p-aia*, that retargeted BMV 1a away from the nER and ended as peripheral ER-localized puncta, and thus, significantly inhibited BMV replication (He et al., 2019).

Knowing that helix B of 1a is sufficient to target soluble proteins to the site of BMV replication, we tested the conservation of this feature across the members of the alphavirus-like superfamily, given the fact that two similar amphipathic α-helices have been identified based on sequence analysis with helix B immediately downstream of helix A (Ahola & Karlin, 2015). Helix B from CCMV, which is in the same genus as BMV and replicates in the nER membrane (Sibert et al., 2018), targeted mC to the nER membrane, as hypothesized (Fig 2.7A). Helix B from CMV 1a targeted GFP to vacuolar membranes, similar to the tonoplast where CMV replicates in plant cells (Hatta & Francki, 1981; Wang, Ma, et al., 2021). Importantly, the results for the helices from BMV, CMV, and CCMV were similar in both yeast and plant cells (Figs. 2.7, 2.8 and 2.9). We further demonstrated that predicted amphipathic α-helices in HEV and RuV were able to target mCherry to the sites of replication, the ER membrane for HEV, and Golgi, ER, and vacuolar membranes for RuV (Fontana et al., 2007; Kenney & Meng, 2019) (Fig 2.7). Our work, therefore, demonstrates that helix B in the replication proteins of a group of diverse viruses in the alphavirus-like superfamily is indeed a conserved determinant for targeting the viral replication proteins to their specific sites of replication.

It has been reported that the amphipathic α-helix (aa 7-28) in HCV 5A was able to target GFP to ER membranes, where HCV assembles its VRCs (Wang & Tai, 2016). For poliovirus 2C, a 38 amino acid long fragment (amino acid 1-38) encompassing the amphipathic α-helix (amino acid 19-36) was able to associate with lipid droplets, where poliovirus VRCs acquire fatty acids for VRC formation (Laufman et al., 2019). With two amphipathic helices (αA and αB) that are separated by several amino acids, the 41 amino acid-long chloroplast targeting domain (CTD) of the 140K/98K replication protein from turnip yellow mosaic virus (TYMV), another virus from the alphavirus-like superfamily, targets GFP to the outer chloroplast membranes (Moriceau et al., 2017). These results have pointed out the role of amphipathic α-helix from individual viruses in targeting specific organelles. Our work, going further, systematically analyzed a range of helices from replication proteins of viruses in the alphavirus-like superfamily and confirmed a conserved role of these helices in targeting viral replication proteins to specific organelle membranes where VRCs are formed.

2.5.3 Different BMV 1a helices may play different roles in the VRC formation

The helix A peptide of 1a becomes helical when incubated with lipid bilayer-mimicking micelles (Liu et al., 2009). Mutations in helix A generated two groups of mutants that were all defective in supporting BMV genome replication. Group I mutants did not associate with the nER membrane, indicating a necessary role of helix A in 1a's nER association. Mutants in group II induced the formation of VRCs that were more abundant but smaller in size compared to those induced by WT 1a, pointing out a possible role in generating or facilitating the remodeling of membranes into VRCs (Liu et al., 2009). Helix A was able to target GFP to membrane fractions in the membrane flotation assay (Liu et al., 2009), however, our data showed that helix A was

not able to target proteins to the nER on its own (Fig 2.4B). Further, helix A and B helices together were not as effective as helix B alone in targeting GFP to the nER membrane (Fig 2.4B). It is possible that the presence of helix A might affect the conformation of helix B. Based on the data from Liu et al (Liu et al., 2009) and our results, we propose that helix A may participate in membrane remodeling but not 1a targeting and helix B is responsible for 1a's targeting to the nER membrane.

In this regard, the roles of BMV 1a helix A and B are different from αA and αB in the CTD of TYMV 140K/98K replication protein. TYMV is in the Tymo group of the alphavirus-like superfamily, different from the Alto group that includes BMV, CCMV, CMV, HEV, and RuV (Ahola & Karlin, 2015). TYMV replicates at the outer membrane of chloroplasts and its replication protein 140K/98K is responsible for targeting and remodeling the chloroplast membranes (Moriceau et al., 2017), similar to the roles of BMV 1a. The CTD is able to target GFP to the chloroplast membranes. However, it has been clearly demonstrated that disrupting the helicity of either αA or αB does not affect the CTD's ability to target GFP to the chloroplast membrane, indicating either helix is sufficient when present in the CTD. This is in contrast to the BMV 1a helices A+B domain that showed much reduced efficiency in targeting GFP to the membrane fraction (Fig 2.4A) and the nER membrane (Fig 2.4B). It should be noted that it is unclear whether αA or αB is sufficient to target GFP to chloroplast membranes when either of them is fused to GFP independent of the CTD.

2.5.4 Possible mechanisms governing the amphipathic helix-mediated membrane targeting

It is not yet clear how each replication protein is targeted uniquely to a specific organelle membrane. There exist at least two potential nonexclusive mechanisms by which viral proteins

target specific membranes: the viral proteins associate with specific lipids enriched on those membranes, or there are host proteins on those membranes that act as receptors for the viral proteins. For cellular amphipathic α-helices that have been extensively studied, some can sense and bind specific lipids, and some are involved in inducing curvatures (Giménez-Andrés et al., 2018). For instance, the amphipathic α-helix in yeast transcription repressor Opi1 (overproduction of inositol 1) binds preferentially to phosphatidic acid (PA) over phosphatidylserine (PS) *in vitro* (Hofbauer et al., 2018). On the contrary, the amphipathic α-helix in yeast protein Spo2 (sporulation 20) prefers charged lipids and binds PA and PS with similar affinity (Horchani et al., 2014). Given that organelle membranes have different lipid compositions (van Meer et al., 2008; Zhang et al., 2019), it is possible that amphipathic α-helices from BMV 1a, CCMV 1a, and HEV ORF1 may recognize certain lipids present in ER membranes while helix B in CMV 1a and RuV 1a prefer lipids enriched in the vacuole membranes. In the future, the binding properties of these peptides to different organelle membranes can be examined by using *in vitro* assays (Varkey et al., 2020) with liposomes composed of different lipids.

We showed that CMV HB-GFP was at both ER and vacuolar membranes, suggesting that CMV HB-GFP was likely transported to the vacuolar membrane first before reaching the ER via the cellular protein secretory pathway. Of note, we have previously found that several components of the cellular COPII (coat protein complex II) pathway were required for BMV 1a's association with the nER membrane (Li et al., 2016), supporting our idea that the protein secretory and protein trafficking pathway is needed for these helix-mediated protein targeting.

In conclusion, we have demonstrated that helix B of BMV 1a is necessary and sufficient for 1a's targeting to nER membranes, and thus, plays a critical role in initiating BMV VRC formation at

the site of viral replication. The conclusion that an amphipathic helix dictates the targeting of a viral replication protein can be extended to several viruses belonging to the alphavirus-like superfamily, revealing a conserved feature among the superfamily encompassing viruses infecting plants, animals, and humans. Given that targeting viral replication proteins to the designated organelle is the initial step to form functional VRCs for genomic replication, a better understanding will provide opportunities to develop antiviral strategies for virus control.

2.6 Materials and Methods

2.6.1 Yeast strain

The *Saccharomyces cerevisiae* strain YPH500 (*MATα ura3–52, lys2–801, ade2–101, trp1-Δ63, his3-Δ200, leu2-Δ1*) were used in all experiments. Yeast cells were grown at 30 °C in a synthetic defined medium containing 2% raffinose or galactose as the carbon source. Histidine, tryptophan, uracil, leucine, or combinations of them were omitted from the medium to maintain selection for different plasmid combinations. Cells were harvested as described previously (He et al., 2019) when the optical density at 600 nm (OD_{600}) reached between 0.6 and 1.0. Except for the localization studies and membrane flotation assay for 1a fragments (region E, helix A, helix B, and helix A+B), all other experiments were carried out using His6-tagged BMV1a and WT $2a^{pol}$.

2.6.2 Plant Materials and Growth Conditions

All agroinfiltration experiments were performed in WT or H2B-RFP (red fluorescent protein fused to the C terminus of histone 2B) transgenic *N. benthamiana*. Plants were grown in a growth chamber with temperatures at 26°C (16 h, light) and 22°C (8 h, dark) for 4-6 weeks

before being infiltrated with agrobacterium cultures. After infiltration, the plants were kept under the same growth conditions.

2.6.3 Plasmids

BMV 1a, mutant derivatives, and $2a^{Pol}$ were expressed under the control of the *GAL1* promoter, using pB1YT3-cH6 (with a His6 tag at the C-terminus of BMV 1a) or derivatives, and pB2YT5, respectively (Ahola et al., 2000). BMV RNA3 was expressed from pB3MS82, where an RNA3 derivative with an abolished coat protein was under the *GAL1* promoter (Sullivan & Ahlquist, 1999). pB1YT3-mC was used as a vector to incorporate a 32 amino acids linker (-DVGGGGSEGGGSGGPGSGGEGSAGGGSAGGGS-) between 1a and mCherry. pB1YT3-L32-mC or pB1YT3-L32-GFP was used as the vector to introduce mutations in helix B by an overlapping PCR approach using specific primers to introduce mutations and to replace BMV 1a with region E, helix A+B, helix A, or helix B to make pE-, pHAB- pHA-, or pHB-L32-GFP. Organelle markers Scs2-mC, Sec63-GFP, GFP-Sed5 were expressed under the control of an endogenous promoter from a low-copy-number plasmid.

BMV or CMV HB was amplified from yeast plasmid pHB-L32-GFP-BMV or pHB-L32-GFP-CMV and inserted into the *Bam*HI-digested p1300-YFP vector (Zhao et al., 2020, 2021) in frame with and upstream of YFP and under the control of the Cauliflower mosaic virus 35S promoter to generate BMV HB-YFP and CMV HB-YFP.

2.6.4 RNA extraction and northern blotting

For RNA extraction, yeast cells were harvested between OD_{600} 0.6-1.0, and total RNA was extracted by a hot phenol method (Köhrer & Domdey, 1991). Equal amounts of total RNA were used for Northern blot analysis. ^{32}P-Labeled probes specific to BMV positive- or negative-strand RNAs or 18S rRNA were used for the hybridization. 18S rRNA was used as a loading control to eliminate loading variations. Radioactive signals of BMV positive-, negative-strand, and 18S rRNA were scanned using a Typhoon FLA 7000 phosphorimaging system, and the intensity of signals was quantified using Adobe Photoshop.

2.6.5 Protein extraction and western blotting

For protein analysis, two OD_{600} units of yeast cells were harvested and frozen prior to extraction. Total proteins were extracted as described previously (Li et al., 2016). Equal volumes of total lysates were analyzed using SDS-PAGE and transferred to a polyvinylidene difluoride (PVDF) membrane (Merck Millipore). Rabbit anti-BMV 1a antiserum (1:10,000 dilution, a gift from Dr. Paul Ahlquist at the University of Wisconsin-Madison), mouse anti-BMV $2a^{pol}$ (1:3000 dilution, a gift from Dr. Paul Ahlquist at the University of Wisconsin-Madison), mouse anti-Pgk1 (1:10,000 dilution; Thermo Fisher Scientific), anti-GFP (1:5000 dilution), and anti-RFP (1:3000 dilution, GenScript), anti-Dpm1 (1:3,000 dilution, Thermo Fisher Scientific) was used as the primary antibody. Horseradish peroxidase conjugated anti-rabbit or anti-mouse antibody (1:10,000 dilution, Thermo Fisher Scientific) together with the Supersignal West Femto maximum sensitivity substrate (Thermo Fisher Scientific) was used to detect target proteins. Band intensities were quantified using Adobe Photoshop.

2.6.6 Membrane flotation assays

Flotation assays were performed as described previously (Zhang et al., 2012, 2016). Briefly, spheroplasts prepared from ten OD_{600} units of yeast cells expressing His6-tagged helix B point mutants, and deletion mutants 1a-ΔA, and 1a-ΔB, and fragments spanning GFP fused region E, helix A+B, helix A, and helix B were resuspended in 350 µl of TNE buffer (50 mM Tris-HCl [pH 8], 150 mM NaCl, 5 mM EDTA) containing 1:100 dilution of yeast/fungal protease arrest from G biosciences. The resulting cell lysate was centrifuged for 5 min at 500 x *g* to remove cell debris. The supernatant was adjusted to 40% iodixanol by the addition of 60% iodixanol (Axis-Shield, Oslo, Norway). A 600 µl of the mixture was placed at the bottom of a Beckman TLS55 centrifuge tube and overlaid with 1.4 ml of 30% iodixanol in TNE and 100 µl of TNE. The gradients were centrifuged at 201,000 x *g* at 4°C for 5 h. The gradients were divided into 6 fractions (360 µl for the top two fractions and 320 µl for the rest) and analyzed by Western blotting for specific proteins.

2.6.7 Vacuolar membrane staining

To stain yeast vacuolar membranes, a lipophilic dye, FM4-64 (Thermo Fisher) that selectively stains the vacuolar membranes was used. A stock concentration of 1.6 µM in DMSO was made and staining was performed as described previously (Vida & Emr, 1995). Yeast cells at an OD_{600} of 0.6-0.8 were collected and centrifuged at 5000 x *g* for 5 minutes at RT. The pellet was suspended in 50 µl YAPD and mixed with 1µl of the stock dye. The cells were incubated in a water bath maintained at 30°C for 30 minutes. After the incubation, 1 ml YAPD was added, and the mixture was centrifuged at 5000 x *g* for 5 minutes at RT. The cell pellet was collected and resuspended in 5 ml YAPD and transferred to culture tubes and grown for 2.5 hours. The cells

were harvested by centrifugation at 5000 x *g* for 5 minutes and fluorescence was detected at an excitation/emission maximum of ~515/640 nm.

2.6.8 Structure prediction

RaptorX protein prediction platform was used for obtaining the pdb files for the 1a protein. The solved crystal structure of the tomato mosaic virus helicase-like domain (PDB-3VKW) was automatically chosen as a template by the program to generate the data files. The obtained pdb file was visualized using PyMol.

2.6.9 Fluorescence and confocal imaging

For all localization studies, yeast cells co-expressing mC- and eGFP-tagged proteins were grown overnight in a synthetic defined medium containing 2% raffinose as a carbon source at 30°C. From this starter culture, a subculture with an OD_{600} of 0.3 was initiated and grown in 2% galactose as a carbon source for the defined hours for microscopic analysis.

For confocal microscopy in plants, the expression vectors p1300-YFP, -BMV HB-YFP, -CMV HB-YFP, and CCMV HB-YFP were individually introduced into *A. tumefaciens* strain GV3101. After overnight growth and activation, Agrobacterium cultures were harvested and resuspended in the induction buffer (10 mM MgSO4, 100 mM 2-N-morpholino ethanesulfonic acid [pH 5.7], 2 mM acetosyringone), and incubated for at least 2 h at room temperature. The suspensions were then adjusted to OD600=1.0 and infiltrated into WT or H2B-RFP transgenic *N. benthamiana* plants. After agroinfiltration, *N. benthamiana* were grown in a growth chamber with a 16 h light/8 h dark cycle. At 40 hpai, leaves were excised and YFP fluorescence was examined in

epidermal cells using confocal microscopy (ZEISS LSM 710). The microscope was configured with a 458–515 nm dichroic mirror for dual excitation and a 488-nm beam splitter to help separate YFP fluorescence. Photographic images were prepared using ZEN 2011SP1.

2.7 References

Ahola, T., den Boon, J. A., & Ahlquist, P. (2000). Helicase and Capping Enzyme Active Site Mutations in Brome Mosaic Virus Protein 1a Cause Defects in Template Recruitment, Negative-Strand RNA Synthesis, and Viral RNA Capping. *Journal of Virology*, *74*(19), 8803–8811.

Ahola, T., & Karlin, D. G. (2015). Sequence analysis reveals a conserved extension in the capping enzyme of the alphavirus supergroup, and a homologous domain in nodaviruses. *Biology Direct*, *10*(1), 16.

Argos, P. (1990). An investigation of oligopeptides linking domains in protein tertiary structures and possible candidates for general gene fusion. *Journal of Molecular Biology*, *211*(4), 943–958.

Belov, G. A., & Kuppeveld, F. J. van. (2012). (+)RNA viruses rewire cellular pathways to build replication organelles. *Current Opinion in Virology*, *2*(6), 740.

Blake, J. A., Lee, K. W., Morris, T. J., & Elthon, T. E. (2007). Effects of turnip crinkle virus infection on the structure and function of mitochondria and expression of stress proteins in turnips. *Physiologia Plantarum*, *129*(4), 698–706.

Cao, X., Jin, X., Zhang, X., Li, Y., Wang, C., Wang, X., Hong, J., Wang, X., Li, D., & Zhang, Y. (2015). Morphogenesis of Endoplasmic Reticulum Membrane-Invaginated Vesicles during Beet Black Scorch Virus Infection: Role of Auxiliary Replication Protein and New Implications of Three-Dimensional Architecture. *Journal of Virology*, *89*(12), 6184.

Chen, X., Zaro, J., & Shen, W.-C. (2013). Fusion Protein Linkers: Property, Design and Functionality. *Advanced Drug Delivery Reviews*, *65*(10), 1357.

Chukkapalli, V., Heaton, N. S., & Randall, G. (2012). Lipids at the interface of virus-host interactions. *Current Opinion in Microbiology*, *15*(4), 512.

COVID Live Update: 229,431,285 Cases and 4,708,052 Deaths from the Coronavirus - Worldometer. Retrieved September 19, 2021, from https://www.worldometers.info/coronavirus/

den Boon, J. A., Chen, J., & Ahlquist, P. (2001). Identification of Sequences in Brome Mosaic Virus Replicase Protein 1a That Mediate Association with Endoplasmic Reticulum Membranes. *Journal of Virology*, *75*(24), 12370–12381.

Diaz, A., & Wang, X. (2014). Bromovirus-induced remodeling of host membranes during viral RNA replication. *Current Opinion in Virology*, *9*, 104–110.

Drin, G., & Antonny, B. (2010). Amphipathic helices and membrane curvature. *FEBS Letters*, *584*(9), 1840–1847.

Elazar, M., Cheong, K. H., Liu, P., Greenberg, H. B., Rice, C. M., & Glenn, J. S. (2003). Amphipathic Helix-Dependent Localization of NS5A Mediates Hepatitis C Virus RNA Replication. *Journal of Virology*, *77*(10), 6055–6061.

Ertel, K. J., Benefield, D., Castaño-Diez, D., Pennington, J. G., Horswill, M., den Boon, J. A., Otegui, M. S., & Ahlquist, P. (2017). Cryo-electron tomography reveals novel features of a viral RNA replication compartment. *ELife*, *6*, e25940.

Finnigan, G. C., Duvalyan, A., Liao, E. N., Sargsyan, A., & Thorner, J. (2016). Detection of protein-protein interactions at the septin collar in Saccharomyces cerevisiae using a tripartite split-GFP system. *Molecular Biology of the Cell*, *27*(17), 2708–2725.

Fontana, J., Tzeng, W., Calderita, G., Fraile-Ramos, A., Frey, T. K., & Risco, C. (2007). Novel replication complex architecture in rubella replicon-transfected cells. *Cellular Microbiology*, *9*(4), 875.

Giménez-Andrés, M., Čopič, A., & Antonny, B. (2018). The Many Faces of Amphipathic Helices. *Biomolecules*, *8*(3), 45.

Gottipati, K., Woodson, M., & Choi, K. H. (2020). Membrane binding and rearrangement by chikungunya virus capping enzyme nsP1. *Virology*, *544*, 31–41.

Hatta, T., & Francki, R. I. B. (1981). Cytopathic Structures Associated with Tonoplasts of Plant Cells Infected with Cucumber Mosaic and Tomato Aspermy Viruses. *Journal of General Virology*, *53*(2), 343–346.

He, G., Zhang, Z., Sathanantham, P., Diaz, A., & Wang, X. (2021). Brome Mosaic Virus (Bromoviridae). *Encyclopedia of Virology*, 252–259.

He, G., Zhang, Z., Sathanantham, P., Zhang, X., Wu, Z., Xie, L., & Wang, X. (2019). An engineered mutant of a host phospholipid synthesis gene inhibits viral replication without compromising host fitness. *Journal of Biological Chemistry*, *294*(38), 13973–13982.

Hofbauer, H. F., Gecht, M., Fischer, S. C., Seybert, A., Frangakis, A. S., Stelzer, E. H. K., Covino, R., Hummer, G., & Ernst, R. (2018). The molecular recognition of phosphatidic acid by an amphipathic helix in Opi1. *Journal of Cell Biology*, *217*(9), 3109–3126.

Horchani, H., Saint-Jean, M. de, Barelli, H., & Antonny, B. (2014). Interaction of the Spo20 Membrane-Sensor Motif with Phosphatidic Acid and Other Anionic Lipids, and Influence of the Membrane Environment. *PLOS ONE*, *9*(11), e113484.

Janda, M., & Ahlquist, P. (1998). Brome mosaic virus RNA replication protein 1a dramatically increases in vivo stability but not translation of viral genomic RNA3. *Proceedings of the National Academy of Sciences*, *95*(5), 2227–2232.

Jensen, M. B., Bhatia, V. K., Jao, C. C., Rasmussen, J. E., Pedersen, S. L., Jensen, K. J., Langen, R., & Stamou, D. (2011). Membrane Curvature Sensing by Amphipathic Helices: A Single Liposome Study Using α-Synuclein and Annexin B12. *Journal of Biological Chemistry*, *286*(49), 42603–42614.

Kenney, S. P., & Meng, X.-J. (2019). Hepatitis E Virus Genome Structure and Replication Strategy. *Cold Spring Harbor Perspectives in Medicine*, *9*(1), a031724.

Kim, K. S. (1977). An Ultrastructural Study of Inclusions and Disease Development in Plant Cells Infected by Cowpea Chlorotic Mottle Virus. *Journal of General Virology*, *35*(3), 535–543.

Köhrer, K., & Domdey, H. (1991). [27] Preparation of high molecular weight RNA. *Methods in Enzymology*, *194*(C), 398–405.

Kong, F., Sivakumaran, K., & Kao, C. (1999). The N-Terminal Half of the Brome Mosaic Virus 1a Protein Has RNA Capping-Associated Activities: Specificity for GTP and S-Adenosylmethionine. *Virology*, *259*(1), 200–210.

Koonin, E. v., Dolja, V. v., & Krupovic, M. (2015). Origins and evolution of viruses of eukaryotes: The ultimate modularity. *Virology*, *479–480*, 2–25.

Kujala, P., Ahola, T., Ehsani, N., Auvinen, P., Vihinen, H., & Kääriäinen, L. (1999). Intracellular Distribution of Rubella Virus Nonstructural Protein P150. *Journal of Virology*, *73*(9), 7805–7811.

Laakkonen, P., Hyvönen, M., Peränen, J., & Kääriäinen, L. (1994). Expression of Semliki Forest virus nsP1-specific methyltransferase in insect cells and in Escherichia coli. *Journal of Virology*, *68*(11), 7418–7425.

Lampio, A., Kilpeläinen, I., Pesonen, S., Karhi, K., Auvinen, P., Somerharju, P., & Kääriäinen, L. (2000). Membrane Binding Mechanism of an RNA Virus-capping Enzyme *. *Journal of Biological Chemistry*, *275*(48), 37853–37859.

Laufman, O., Perrino, J., & Andino, R. (2019). Viral Generated Inter-Organelle Contacts Redirect Lipid Flux for Genome Replication. *Cell*, *178*(2), 275-289.e16.

Lee, W.-M., & Ahlquist, P. (2003). Membrane Synthesis, Specific Lipid Requirements, and Localized Lipid Composition Changes Associated with a Positive-Strand RNA Virus RNA Replication Protein. *Journal of Virology*, *77*(23), 12819–12828.

Lee, W.-M., Ishikawa, M., & Ahlquist, P. (2001). Mutation of Host Δ9 Fatty Acid Desaturase Inhibits Brome Mosaic Virus RNA Replication between Template Recognition and RNA Synthesis. *Journal of Virology*, *75*(5), 2097–2106.

Li, J., Fuchs, S., Zhang, J., Wellford, S., Schuldiner, M., & Wang, X. (2016). An unrecognized function for COPII components in recruiting the viral replication protein BMV 1a to the perinuclear ER. *Journal of Cell Science*, *129*(19), 3597–3608.

Liu, L., Westler, W. M., den Boon, J. A., Wang, X., Diaz, A., Steinberg, H. A., & Ahlquist, P. (2009). An Amphipathic α-Helix Controls Multiple Roles of Brome Mosaic Virus Protein 1a in RNA Replication Complex Assembly and Function. *PLOS Pathogens*, *5*(3), e1000351.

Magden, J., Takeda, N., Li, T., Auvinen, P., Ahola, T., Miyamura, T., Merits, A., & Kääriäinen, L. (2001). Virus-Specific mRNA Capping Enzyme Encoded by Hepatitis E Virus. *Journal of Virology*, *75*(14), 6249–6255.

Martin, K., Kopperud, K., Chakrabarty, R., Banerjee, R., Brooks, R., & Goodin, M. M. (2009). Transient expression in Nicotiana benthamiana fluorescent marker lines provides enhanced definition of protein localization, movement and interactions in planta. *The Plant Journal*, *59*(1), 150–162.

Martyna, A., Bahsoun, B., Badham, M. D., Srinivasan, S., Howard, M. J., & Rossman, J. S. (2017). Membrane remodeling by the M2 amphipathic helix drives influenza virus membrane scission. *Scientific Reports 2017 7:1*, *7*(1), 1–12.

McCartney, A. W., Greenwood, J. S., Fabian, M. R., White, K. A., & Mullen, R. T. (2005). Localization of the Tomato Bushy Stunt Virus Replication Protein p33 Reveals a Peroxisome-to-Endoplasmic Reticulum Sorting Pathway. *The Plant Cell*, *17*(12), 3513–3531.

Miller, D. J., & Ahlquist, P. (2002). Flock House Virus RNA Polymerase Is a Transmembrane Protein with Amino-Terminal Sequences Sufficient for Mitochondrial Localization and Membrane Insertion. *Journal of Virology*, *76*(19), 9856–9867.

Miller, D. J., Schwartz, M. D., & Ahlquist, P. (2001). Flock House Virus RNA Replicates on Outer Mitochondrial Membranes in Drosophila Cells. *Journal of Virology*, *75*(23), 11664.

Moriceau, L., Jomat, L., Bressanelli, S., Alcaide-Loridan, C., & Jupin, I. (2017). Identification and molecular characterization of the chloroplast targeting domain of turnip yellow mosaic virus replication proteins. *Frontiers in Plant Science*, *8*.

Nelson, B. K., Cai, X., & Nebenführ, A. (2007). A multicolored set of in vivo organelle markers for co-localization studies in Arabidopsis and other plants. *Plant Journal*, *51*(6), 1126–1136.

Nishikiori, M., & Ahlquist, P. (2018). Organelle luminal dependence of (+)strand RNA virus replication reveals a hidden druggable target. *Science Advances*, *4*(1), eaap8258.

Paul, D., & Bartenschlager, R. (2013). Architecture and biogenesis of plus-strand RNA virus replication factories. *World Journal of Virology*, *2*(2), 32.

Restrepo-Hartwig, M. A., & Ahlquist, P. (1996). Brome mosaic virus helicase- and polymerase-like proteins colocalize on the endoplasmic reticulum at sites of viral RNA synthesis. *Journal of Virology*, *70*(12), 8908–8916.

Restrepo-Hartwig, M., & Ahlquist, P. (1999). Brome mosaic virus RNA replication proteins 1a and 2a colocalize and 1a independently localizes on the yeast endoplasmic reticulum. *Journal of Virology*, *73*(12), 10303–10309.

Scheidel, L. M., Durbin, R. K., & Stollar, V. (1989). SVLM21, a Sindbis virus mutant resistant to methionine deprivation, encodes an altered methyltransferase. *Virology*, *173*(2), 408–414.

Schwartz, M., Chen, J., Janda, M., Sullivan, M., den Boon, J., & Ahlquist, P. (2002). A positive-strand RNA virus replication complex parallels form and function of retrovirus capsids. *Molecular Cell*, *9*(3), 505–514.

Shen, H., Pirruccello, M., & de Camilli, P. (2012). SnapShot: Membrane Curvature Sensors and Generators. *Cell*, *150*(6), 1300-1300.e2.

Sibert, B. S., Navine, A. K., Pennington, J., Wang, X., & Ahlquist, P. (2018). Cowpea chlorotic mottle bromovirus replication proteins support template-selective RNA replication in Saccharomyces cerevisiae. *PLOS ONE*, *13*(12), e0208743.

Spuul, P., Salonen, A., Merits, A., Jokitalo, E., Kääriäinen, L., & Ahola, T. (2007). Role of the Amphipathic Peptide of Semliki Forest Virus Replicase Protein nsP1 in Membrane Association and Virus Replication. *Journal of Virology*, *81*(2), 872–883.

Sullivan, M. L., & Ahlquist, P. (1999). A brome mosaic virus intergenic RNA3 replication signal functions with viral replication protein 1a to dramatically stabilize RNA in vivo. *Journal of Virology*, *73*(4), 2622–2632.

Teterina, N. L., Gorbalenya, A. E., Egger, D., Bienz, K., Rinaudo, M. S., & Ehrenfeld, E. (2006). Testing the modularity of the N-terminal amphipathic helix conserved in picornavirus 2C proteins and hepatitis C NS5A protein. *Virology*, *344*(2), 453–467.

van Meer, G., Voelker, D. R., & Feigenson, G. W. (2008). Membrane lipids: where they are and how they behave. *Nature Reviews Molecular Cell Biology 2008 9:2*, *9*(2), 112–124.

Varkey, J., Zhang, J., Kim, J., George, G., He, G., Belov, G., Langen, R., & Wang, X. (2020). An Amphipathic Alpha-Helix Domain from Poliovirus 2C Protein Tubulate Lipid Vesicles. *Viruses 2020, Vol. 12, Page 1466*, *12*(12), 1466.

Vida, T. A., & Emr, S. D. (1995). A new vital stain for visualizing vacuolar membrane dynamics and endocytosis in yeast. *Journal of Cell Biology*, *128*(5), 779–792.

Wang, A. (2015). Dissecting the Molecular Network of Virus-Plant Interactions: The Complex Roles of Host Factors. *Annual Review of Phytopathology*, *53*(1), 45–66.

Wang, H., & Tai, A. W. (2016). Mechanisms of Cellular Membrane Reorganization to Support Hepatitis C Virus Replication. *Viruses*, *8*(5).

Wang, X., & Ahlquist, P. (2008). Brome Mosaic Virus. *Encyclopedia of Virology*, 381–386.

Wang, X., Jiang, Z., Yue, N., Jin, X., Zhang, X., Li, Z., Zhang, Y., Wang, X.-B., Han, C., Yu, J., & Li, D. (2021). Barley stripe mosaic virus γb protein disrupts chloroplast antioxidant defenses to optimize viral replication. *The EMBO Journal*, *40*(16), e107660.

Wang, X., Lee, W.-M., Watanabe, T., Schwartz, M., Janda, M., & Ahlquist, P. (2005). Brome Mosaic Virus 1a Nucleoside Triphosphatase/Helicase Domain Plays Crucial Roles in Recruiting RNA Replication Templates. *Journal of Virology*, *79*(21), 13747 LP – 13758.

Wang, X., Ma, J., Jin, X., Yue, N., Gao, P., Mai, K. K. K., Wang, X.-B., Li, D., Kang, B.-H., & Zhang, Y. (2021). Three-dimensional reconstruction and comparison of vacuolar membranes in response to viral infection. *Journal of Integrative Plant Biology*, *63*(2), 353–364.

Zhang, J., Diaz, A., Mao, L., Ahlquist, P., & Wang, X. (2012). Host Acyl Coenzyme A Binding Protein Regulates Replication Complex Assembly and Activity of a Positive-Strand RNA Virus. *Journal of Virology*, *86*(9), 5110–5121.

Zhang, J., Zhang, Z., Chukkapalli, V., Nchoutmboube, J. A., Li, J., Randall, G., Belov, G. A., & Wang, X. (2016). Positive-strand RNA viruses stimulate host phosphatidylcholine synthesis at viral replication sites. *Proceedings of the National Academy of Sciences*, *113*(8), E1064–E1073.

Zhang, Z., He, G., Filipowicz, N. A., Randall, G., Belov, G. A., Kopek, B. G., & Wang, X. (2019). Host Lipids in Positive-Strand RNA Virus Genome Replication. *Frontiers in Microbiology*, *10*(FEB), 286.

Zhang, Z., He, G., Han, G. S., Zhang, J., Catanzaro, N., Diaz, A., Wu, Z., Carman, G. M., Xie, L., & Wang, X. (2018). Host Pah1p phosphatidate phosphatase limits viral replication by regulating phospholipid synthesis. *PLOS Pathogens*, *14*(4), e1006988.

Zhao, W., Wu, S., Barton, E., Fan, Y., Ji, Y., Wang, X., & Zhou, Y. (2020). Tomato Yellow Leaf Curl Virus V2 Protein Plays a Critical Role in the Nuclear Export of V1 Protein and Viral Systemic Infection. *Frontiers in Microbiology*, *11*, 1243.

Zhao, W., Zhou, Y., Zhou, X., Wang, X., & Ji, Y. (2021). Host GRXC6 restricts Tomato yellow leaf curl virus infection by inhibiting the nuclear export of the V2 protein. *PLOS Pathogens*, *17*(8), e1009844.

CHAPTER 3

Targeting BMV 1a ATPase/helicase-like domain to ER membranes

3.1 Abstract

The replication protein 1a of brome mosaic virus contains two functionally separable domains responsible for 1a's capping-related activities and helicase-like activities respectively. Both capping and helicase-like domains are responsible for recruiting necessary viral factors to sufficiently support viral replication. Although the capping domain alone is sufficient for establishing membrane remodeling activities, neither the capping domain nor the helicase-like domain alone is sufficient to induce spherules that are typically formed by the full length 1a protein at the sites of replication. When the two domains are expressed separately, only the capping domain associates with the nuclear ER membranes. The preliminary data from this work shows that even when the helicase-like domain is targeted specifically to the nuclear ER regions via the addition of helix B motif, the replicating capacity is not reconstituted. Additionally, no significant role of the linker region that functionally separates the two 1a domains was observed when these domains were expressed separately.

Keywords: capping domain/helicase-like domain/ linker region

3.2 Introduction

The majority of higher eukaryotic viruses organize their genome into a single open reading frame to produce a precursor polyprotein that upon proteolytic processing yields multiple proteins of

various functional domains. This widely employed mechanism occurs in a highly regulated manner (Hellen et al., 2002; Spall et al., 1997) and allows for carrying a compact genome that eliminates the need for additional genetic features, such as promoter or enhancer elements, that otherwise would be necessary to express each protein individually.

Proteolytic processing enables the functionally different domains to be separated and transported to different cellular compartments (Spall et al., 1997). In addition to this, some viral proteins perform alternative functions in their precursor forms compared to their mature forms. For example, the alphavirus P23, along with alphavirus nsP1, and nsP4 preferentially use the genomic RNA to synthesize an intermediate RNA of negative sense (A.lemm et al., 1994; Shirako & Strauss, 1994). Whereas, after the cleavage event of P23, mature nonstructural proteins, nsP2 and nsP3 begin the replication process by switching the template to the negative-sense RNA to synthesize positive-sense genomic and subgenomic RNAs. Similarly, poliovirus 3CD polyprotein preferentially presumes a role of protease towards the precursor polyprotein, P1 by inhibiting the 3D pol activity (Jore et al., 1988; Ypma-Wong et al., 1988; Harris et al., 1992). These activities highlight the importance of polyprotein cleavage as a mechanism of gene regulation.

The members of the alphavirus-like superfamily, such as Semliki Forest virus and Sindbis virus have proteolytic processing of a single polyprotein that yields separate proteins for capping and helicase activities (Ahola & Kääriäinen, 1995; Gomez De Cedrón et al., 1999; Vasiljeva et al., 2000). Some members, such as the tobacco mosaic virus (TMV), bamboo mosaic virus (BaMV), beet yellow Virus (BYV), etc. produce a polyprotein that after getting processed, yields a protein

with fused capping and helicase domains. Some members that have a segmented genome that generally lacks proteolytic processing, such as CMV, CCMV, and BMV, also encode proteins with both capping and helicase domains (Ali et al., 2011; Kong et al., 1999; Nouri et al., 2014; Wang et al., 2005).

BMV replication protein 1a is a multifunctional protein with key roles in the assembly and function of viral RNA replication complexes (VRCs). 1a contains two functionally linked domains, an N-proximal RNA capping domain (aa 1-557) with methyltransferase/guanylyltransferase activity (CAP domain herein) that has been experimentally demonstrated (Ahola & Ahlquist, 1999; Kong et al., 1999), and a C-terminal NTPase/RNA helicase-like domain (HEL domain herein, aa 557-961) (Wang et al., 2005). 1a also contains an intriguing region (aa 487-572) that separates the two functional domains of 1a and is termed the linker region (den Boon et al., 2001) (Fig 3.1). The region is proline-rich, and its function is unknown. Both CAP and HEL domains are required for 1a's roles in recruiting necessary viral factors to the site of replication, interaction with host as well as viral factors, multimerization of 1a on the ER membranes, and establishment of VRCs (Diaz et al., 2012; O'Reilly et al., 1998).

BMV CAP domain alone is sufficient for establishing membrane contacts and inducing membrane remodeling that was different from what full-length 1a induced (Diaz et al., 2012). The C-terminal HEL domain interacts with the $2a^{pol}$ and is necessary for viral replication (Kao & Ahlquist, 1992). Linked RNA capping and helicase-like domains homologous to those of 1a are common across the alphavirus-like superfamily with essential roles in genome replication, and

establishment of VRCs (Ali et al., 2011; Kong et al., 1999; Nouri et al., 2014; Wang et al., 2005).

Although the capping domain alone is sufficient for nuclear ER (nER) targeting, this domain by itself fails to form spherules. Instead, the capping domain induced the formation of extended layers of ER membranes forming hexagonal lattices in yeast (Diaz et al., 2012). These structures did not support replication in the presence of the other viral factors, suggesting that the fused domains of both CAP and HEL-like domains are necessary for the formation of spherules and viral replication.

The HEL domain is not associated with the nER membrane but found in the cytoplasm when expressed on its own (den Boon et al., 2001). It was hypothesized that the HEL domain would be brought to the nER membrane *via* its interaction with the CAP domain given the interaction between the two domains (O'Reilly et al., 1998). However, the HEL domain was not localized to the nER regions in the presence of CAP domain (Diaz et al., 2012).

In O'Reilly et al (O'Reilly et al., 1998), the interaction was tested in the yeast two-hybrid system, where both domains were specifically targeted to the yeast nucleus. It is possible that the CAP and HEL domains were not able to encounter each other when expressed (Diaz et al., 2012). Given the fact that helix B is able to target several soluble proteins to the nER membrane (Fig 2.4, Chapter 2), I hypothesized that the helix B-tagged HEL domain is targeted to the nER membrane where CAP and HEL domain interact and support BMV replication. Another reason that the CAP failed to recruit HEL-like domains is that the linker region, which is upstream of

the HEL domain, may be included in the HEL-like domain. I hypothesized that the addition of the disordered region may facilitate the interaction between CAP and HEL-like domains. This work validated the above-described hypothesis.

3.3 Methods

3.3.1 Yeast strain

The *Saccharomyces cerevisiae* strain YPH500 (*MATα ura3–52, lys2–801, ade2–101, trp1-*Δ*63, his3-*Δ*200, leu2-*Δ*1*) were used in all experiments. Yeast cells were grown at 30 °C in a synthetic defined medium containing 2% galactose as the carbon source. Histidine, tryptophan, uracil, leucine, or combinations of them were omitted from the medium to maintain selection for different plasmid combinations. Cells were harvested as described previously (He et al., 2019) when the optical density at 600 nm (OD_{600}) reached between 0.6 and 1.0.

3.3.2 Plasmids

BMV 1a, CAP-domain, HEL-domain variants, and BMV $2a^{Pol}$ were expressed under the control of the *GAL1* promoter, using pB1YT3-cH6 (with a His6 tag at the C-terminus of BMV 1a) and $2a^{pol}$ expressed from pB2YT5 (Ahola et al., 2000). BMV RNA3 was expressed from pB3MS82, where an RNA3 derivative with an abolished coat protein was under the *GAL1* promoter (Sullivan & Ahlquist, 1999). For localization studies, the HEL-domain variants [HEL *1*-mC, HEL *2*-mC, and HEL *3*-mC] were expressed from pB1YT3-L32-mC and Sec63-GFP was expressed under the control of an endogenous promoter from a low-copy-number plasmid. All analysis involving the CAP domain was performed using a C-terminally Flag-tagged CAP domain.

The HEL-like domain variants, HEL *1*, HEL *2*, and HEL *3* spanning aa 557-961, aa 487-961, aa 597-961 respectively (Fig. 3.1) were made using primers designed to specifically amplify the region of interest (Table 3.1). The HB was amplified followed by homologous recombination into the HEL-like domain variants to make the HB-fused constructs.

3.3.3 RNA extraction and northern blotting

For RNA extraction, yeast cells were harvested between OD_{600} 0.6-1.0, and total RNA was extracted by a hot phenol method (Köhrer & Domdey, 1991). Equal amounts of total RNA were used for Northern blot analysis. ^{32}P-Labeled probes specific to BMV positive- or negative-strand RNAs or 18S rRNA were used for the hybridization. 18S rRNA was used as a loading control to eliminate loading variations. Radioactive signals of BMV positive-, negative-strand or 18S rRNA were scanned using a Typhoon FLA 7000 phosphorimaging system.

3.3.4 Protein extraction and western blotting

For protein analysis, two OD_{600} units of yeast cells were harvested and frozen prior to extraction. Total proteins were extracted as described previously (Li et al., 2016). Equal volumes of total lysates were analyzed using SDS-PAGE and transferred to a polyvinylidene difluoride (PVDF) membrane (Merck Millipore). Mouse anti-Flag antiserum (1:5000 dilution; Genscript), mouse anti-Pgk1 (1:10,000 dilution; Thermo Fisher Scientific), and anti-His (1:5000 dilution; Genscript) was used as the primary antibody. Horseradish peroxidase-conjugated anti-rabbit or anti-mouse antibody (1:10,000 dilution, Thermo Fisher Scientific) together with the Supersignal West Femto maximum sensitivity substrate (Thermo Fisher Scientific) was used to detect target proteins. Band intensities were quantified using Adobe Photoshop.

3.3.5 Fluorescence microscopy

For all localization studies, yeast cells co-expressing mC- and eGFP-tagged proteins were grown overnight in a synthetic defined medium containing 2% galactose as a carbon source at 30°C. From this starter culture, a subculture with an OD_{600} of 0.3 was initiated and grown in the galactose media for 6-7hours for fluorescence microscopic analysis.

3.4 Results and Discussion

To understand any potential role the linker region may have on the interactions between CAP and HEL-like domains, I constructed three plasmids capable of expressing three variants of the helicase-domain spanning different lengths of the C terminus of 1a. The HEL-like domain variants, HEL *1*, HEL *2*, and HEL *3* span aa 557-961, aa 487-961, aa 597-961, respectively (Fig 3.1). HEL *1* has the exact sequence of the predicted HEL-like domain with a molecular weight (MW) of 45 kDa. HEL *2* contains the linker region and the HEL-like domain, which I expect to test whether the linker region is required for the HEL-like domain to be targeted by the CAP to the nER membrane. An extra fragment (aa 557-596) from the HEL-like domain was deleted to serve as a negative control to directly target the HEL-like domain to the nER membrane so that the HEL-like and CAP domain may have a chance to interact.

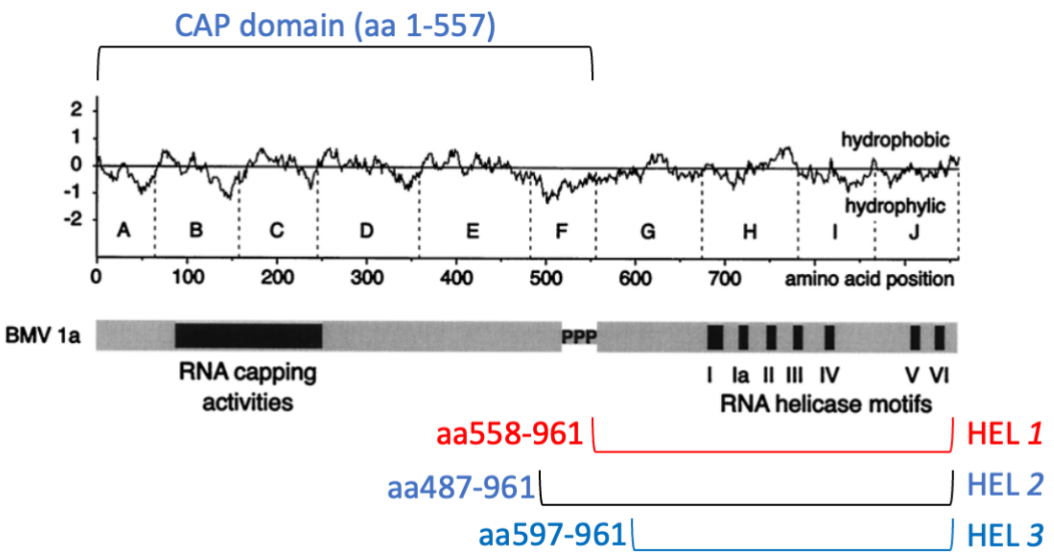

Fig. 3.1. Schematic of CAP domain and the HEL domain variants

The CAP and the HEL domain variants spanning various lengths of BMV 1a are indicated.

3.4.1. HEL domain variants with a fused helix B could associate with the nER

I first tested whether the helix B was able to target HEL-like domain variants to the nER. To do so, I co-expressed the mCherry-tagged HEL-like domain constructs with GFP-tagged Sec63, which is a marker protein for ER membranes, to check if any of the HEL-like domain variants were capable of associating with the membranes.

In agreement with a previous report (Diaz et al., 2012), none of the HEL-like domain variants could localize to nER membrane where BMV replicates (Fig 3.2B), suggesting that this domain was entirely dependent upon the N-terminal CAP domain for nER localization.

I next fused helix B to the three helicase-like domain variants at the N-terminus of each helicase-like domain variant. Since helix B has a demonstrated nER targeting activity (Chapter 2), I

anticipated that the HB-HEL domain variants localized at the nER independent will be able to interact with the CAP domain and support BMV replication.

The mCherry-tagged version of the HEL-like domain used in the study by Diaz et al. is represented by HEL *1* of this work and showed a strict cytosolic association.

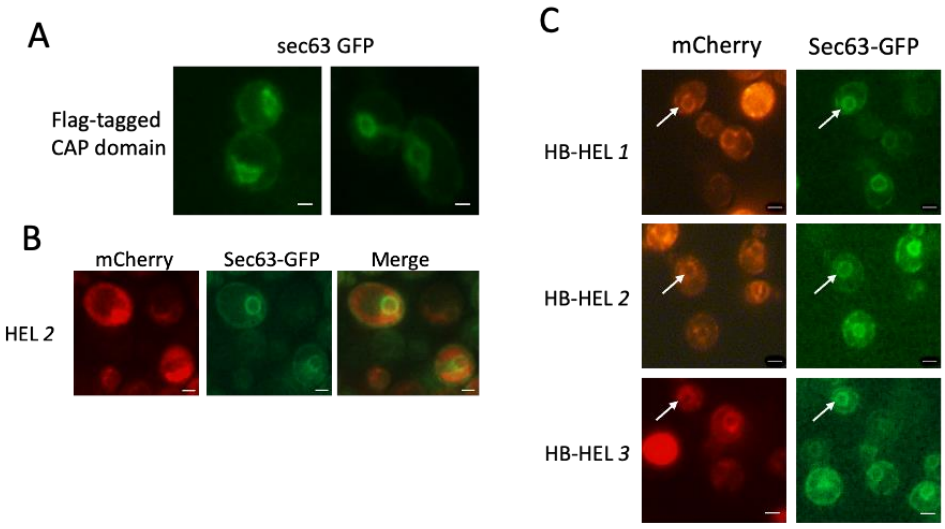

Fig. 3.2. Localization of mCherry-tagged HEL-domain variants

(A) Membrane remodeling observed in cells expressing the CAP domain. (B) A representative image of mCherry-tagged HEL domain variant, HEL *2*-mC is shown. GFP-tagged ER marker protein, Sec63, is also included. (C) HB-fused HEL domain variants coexpressed with GFP-–tagged ER marker protein, Sec63. Arrows indicate nER association in yeast cells. Scale bars: 2μm.

Although all three HB-HEL variants were detected in the nER regions (Fig 3.2C), HB-HEL *1* and *2* detected in the nER membranes at higher percentages of cells, approximately 64% and 57% respectively. HB-HEL *3*-mC was seen in nearly 26% of the cells.

3.4.2 HEL domain variants fail to replicate despite localizing to nER membranes

The CAP domain of BMV 1a is sufficient to induce nER remodeling even though the induced structures are quite different from spherules (Diaz et al., 2012) (Fig 3.2A). I performed a northern blot analysis to test replication of BMV in yeast cells co-expressing RNA3, $2a^{poll}$, FLAG-tagged CAP domain, the HEL domain variants fused with helix B (HB-HEL *1*, *2*, and *3*) that show a gain-of-function to associate with the nER regions. I reasoned that colocalization of the two domains at the nER may allow partial replication to occur. I, therefore, sought to study whether the nER targeted HB-HEL domain variants can successfully replicate in the presence of other necessary viral factors, $2a^{pol}$ and RNA3. I also coexpressed the three HEL-like domain variants without a helix B as controls.

Northern data (Fig. 3.3) showed that only full-length 1a is able to support BMV genome replication, with newly synthesized (-)RNA3 and (+)RNA4. No viral RNAs were detected when 1a was split into CAP and HEL domain. Moreover, no viral RNAs were detected when HB-HEL domain variants were used (Fig 3.3).

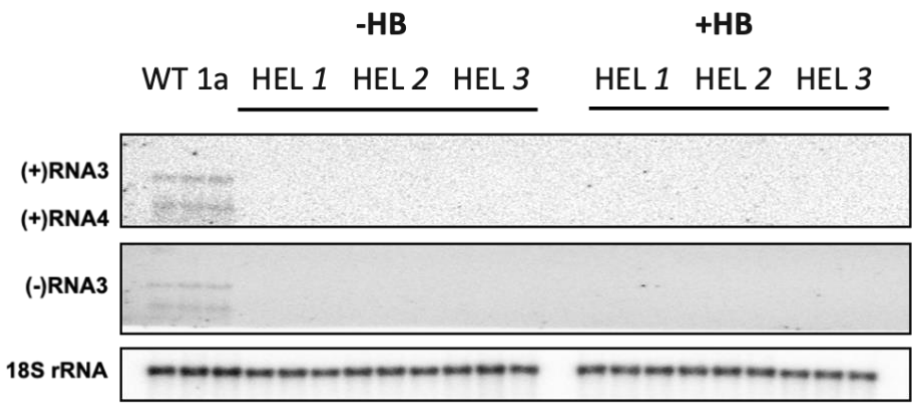

Fig. 3.3. Northern blotting analysis of the HEL domain variants

WT 1a, but not the split CAP and HEL domain variants indicate viral replication. 18S rRNA is used as loading control.

3.4.3 Expressing capping domain *in trans* has a dominant-negative effect on nER localization

I next tested the accumulation of HEL *2* variants in the absence and presence of HB and tested whether the association to the nER may affect their stability. As shown in Fig. 3.4, no significant differences of accumulated HEL 2 and HB-HEL 2 were observed. However, in the presence of CAP domain, the HEL *2* domain accumulated 30% more than that of HEL *2* expressed in the absence of CAP domain (Fig. 3.4A). I also noticed that the CAP domain affected the accumulation of HB-HEL *2* and HEL *2* with a 45% difference (Fig 3.4A).

I sought to further test why the accumulated levels of HEL *2* variant in the presence of CAP domain declined when it was fused to HB. I first checked the localization of the mCherry-tagged HEL domain variants expressed in the presence of CAP domain (Fig 3.4A).

In the presence and absence of CAP domain, the HEL *2* showed no changes in their localizations and were still cytosolically associated (Fig 3.4B). Surprisingly, in the presence of the CAP domain, the HB-HEL *1* and HB-HEL *2* variants were predominantly localized to vacuoles, where proteins are destined for degradation (Fig 3.4B). However, no significant vacuolar localization was observed for the HB-HEL *3* variant. It is not clear why the CAP domain promoted the vacuole-targeting of HB-HEL *1* and *2*.

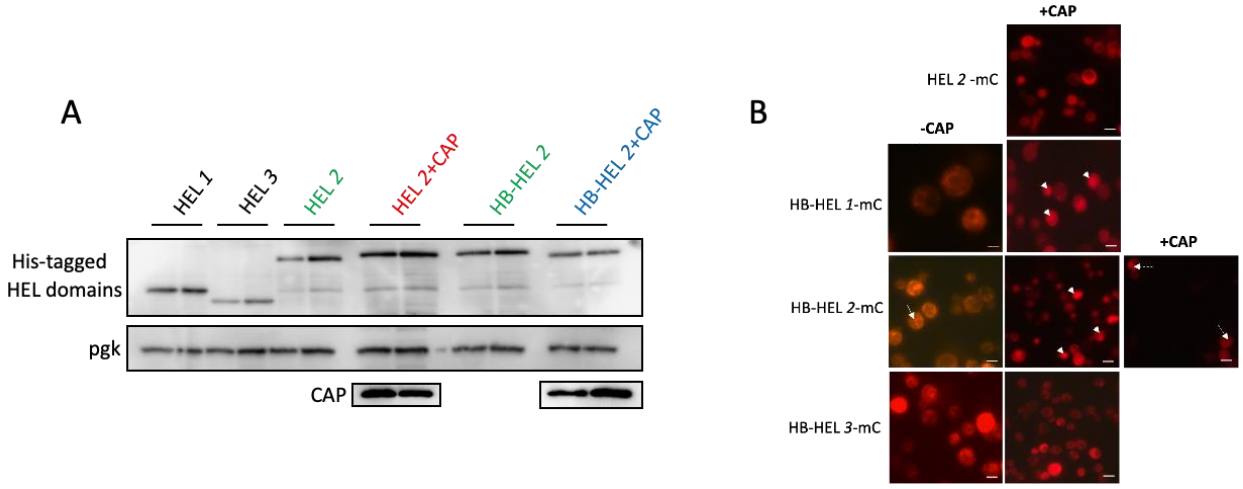

Fig. 3.4. HB-fused HEL domain variants coexpressed with or without the CAP domain
(A) Protein accumulation quantification shows HEL *2* and HB-Hel *2* accumulate to similar levels (green labels) whereas HEL *2* is expressed at higher levels than HB HEL *2* in the presence of the CAP domain. (B) Fluorescence microscopy images for HB fused HEL domain variants. Arrows indicate nER association, arrowheads indicate vacuolar localization, dotted arrows in the HB-HEL *2*-mC panel indicate the modified nER membranes in a few cells expressing CAP domain.

Since a previous study (Diaz et al., 2012) has shown that the CAP domain has a dominant-negative effect over WT 1a in BMV replication, I aimed to test the localization of 1a-mC in the presence of the CAP domain. It is possible that the WT 1a fails to replicate due to the remodeled nER regions, but we did not see any strikingly different nER remodeling of the yeast cells

expressing WT 1a in the presence of the CAP domain (Fig 3.5) nor did we notice any vacuolar localization as observed in HB-fused HEL *2*. The cells with WT 1a and CAP domain rather appeared to show an enriched localization at what appeared to be a likely peripheral ER region (Fig 3.5B). Further studies using electron microscopy and yeast two-hybrid assays could provide more insights into the likely mechanism of this replication inhibition by the dominant-negative effect of the CAP domain.

Interestingly, we also noticed that overexpression of the ER resident protein, Sec63 also tends to modify nER membranes (Fig 3.5C), and therefore it remains to be tested whether the nER remodeling activity by CAP domain is due to the recruitment and enrichment of some host genes capable of modifying the nER morphology upon CAP expression or whether it is an inherent characteristic of the CAP domain specifically.

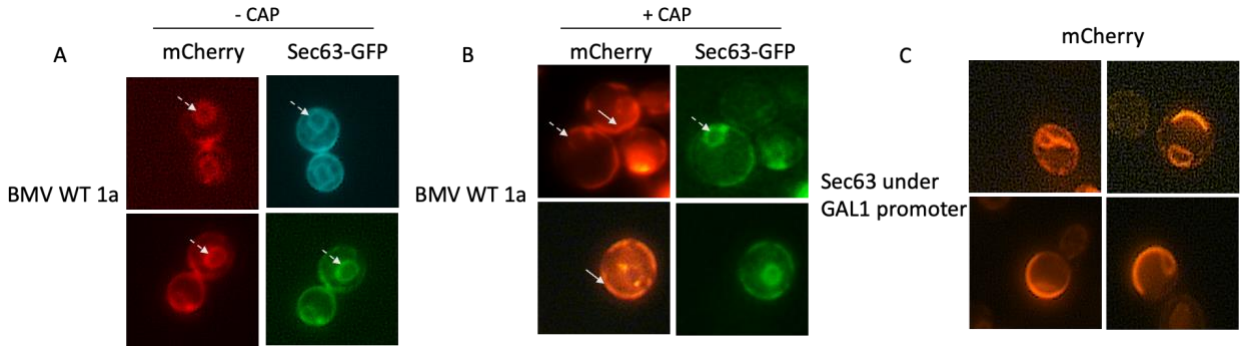

Fig. 3.5. Fluorescence microscopy images of WT1a coexpressed with or without the CAP domain

(A) The dotted arrows indicate the nER localization in yeast cells expressing WT1a protein and ER marker protein, Sec63 GFP. Note that the nER localization is preferred over peripheral ER localization in these cells. (B) In the presence of the CAP domain, the WT 1a preferentially

localizes to regions away from the nER. (C) modified nER membranes by overexpressing the ER resident protein Sec63.

I concluded that the two domains of BMV 1a were incapable of functioning when expressed separately, and further, the association of the Helicase-like domain at the nER regions was not sufficient for viral replication when co-expressed with the CAP domain.

3.5 References

Ahola, T., & Ahlquist, P. (1999). Putative RNA capping activities encoded by brome mosaic virus: methylation and covalent binding of guanylate by replicase protein 1a. *Journal of Virology*, *73*(12), 10061–10069.

Ahola, T., den Boon, J. A., & Ahlquist, P. (2000). Helicase and Capping Enzyme Active Site Mutations in Brome Mosaic Virus Protein 1a Cause Defects in Template Recruitment, Negative-Strand RNA Synthesis, and Viral RNA Capping. *Journal of Virology*, *74*(19), 8803–8811.

Ahola, T., & Kääriäinen, L. (1995). Reaction in alphavirus mRNA capping: formation of a covalent complex of nonstructural protein nsP1 with 7-methyl-GMP. *Proceedings of the National Academy of Sciences of the United States of America*, *92*(2), 507.

A.lemm, J., Rümenapf, T., Strauss, E. G., Strauss, J. H., & M.rice, C. (1994). Polypeptide requirements for assembly of functional Sindbis virus replication complexes: a model for the temporal regulation of minus- and plus-strand RNA synthesis. *The EMBO Journal*, *13*(12), 2925–2934.

Ali, A., Shafiekhani, M., & Olsen, J. (2011). Molecular characterization of the complete genomes of two new field isolates of Cowpea chlorotic mottle virus, and their phylogenetic analysis. *Virus Genes*, *43*(1), 120–129.

den Boon, J. A., Chen, J., & Ahlquist, P. (2001). Identification of Sequences in Brome Mosaic Virus Replicase Protein 1a That Mediate Association with Endoplasmic Reticulum Membranes. *Journal of Virology*, *75*(24), 12370–12381.

Diaz, A., Gallei, A., & Ahlquist, P. (2012). Bromovirus RNA Replication Compartment Formation Requires Concerted Action of 1a's Self-Interacting RNA Capping and Helicase Domains. *Journal of Virology*, *86*(2), 821–834.

Gomez De Cedrón, M., Ehsani, N., Mikkola, M. L., García, J. A., & Kääriäinen, L. (1999). RNA helicase activity of Semliki Forest virus replicase protein NSP2. *FEBS Letters*, *448*(1), 19–22.

Harris, K. S., Reddigari, S. R., Nicklin, M. J. H., Hammerle, T., & Wimmer', E. (1992). Purification and characterization of poliovirus polypeptide 3CD, a proteinase and a precursor for RNA polymerase. *Journal of Virology*, *66*(12), 7481–7489.

He, G., Zhang, Z., Sathanantham, P., Zhang, X., Wu, Z., Xie, L., & Wang, X. (2019). An engineered mutant of a host phospholipid synthesis gene inhibits viral replication without compromising host fitness. *Journal of Biological Chemistry*, *294*(38), 13973–13982.

Hellen, C. U. T., Kräusslich, H. G., & Wimmer, E. (2002). Proteolytic processing of polyproteins in the replication of RNA viruses. *Biochemistry*, *28*(26), 9881–9890.

Jore, J., de Geus, B., Jackson, R. J., Pouwels, P. H., & Enger-Valk, B. E. (1988). Poliovirus protein 3CD is the active protease for processing of the precursor protein P1 in vitro. *Journal of General Virology*, *69*(7), 1627–1636.

Kao, C. C., & Ahlquist, P. (1992). Identification of the domains required for direct interaction of the helicase-like and polymerase-like RNA replication proteins of brome mosaic virus. *Journal of Virology*, *66*(12).

Köhrer, K., & Domdey, H. (1991). Preparation of high molecular weight RNA. *Methods in Enzymology*, *194*(C), 398–405.

Kong, F., Sivakumaran, K., & Kao, C. (1999). The N-Terminal Half of the Brome Mosaic Virus 1a Protein Has RNA Capping-Associated Activities: Specificity for GTP and S-Adenosylmethionine. *Virology*, *259*(1), 200–210.

Li, J., Fuchs, S., Zhang, J., Wellford, S., Schuldiner, M., & Wang, X. (2016). An unrecognized function for COPII components in recruiting the viral replication protein BMV 1a to the perinuclear ER. *Journal of Cell Science*, *129*(19), 3597–3608. Linial, M. L. (1999). Foamy Viruses Are Unconventional Retroviruses. *Journal of Virology*, *73*(3), 1747–1755.

Nouri, S., Arevalo, R., Falk, B. W., & Groves, R. L. (2014). Genetic Structure and Molecular Variability of Cucumber mosaic virus Isolates in the United States. *PLOS ONE*, *9*(5), e96582.

O'Reilly, E. K., Wang, Z., French, R., & Kao, C. C. (1998). Interactions between the Structural Domains of the RNA Replication Proteins of Plant-Infecting RNA Viruses. *Journal of Virology*, *72*(9), 7160–7169.

Shirako, Y., & Strauss, J. H. (1994). Regulation of Sindbis virus RNA replication: uncleaved P123 and nsP4 function in minus-strand RNA synthesis, whereas cleaved products from P123 are required for efficient plus-strand RNA synthesis. *Journal of Virology*, *68*(3), 1874–1885.

Spall, V. E., Shanks, M., & Lomonossoff, G. P. (1997). Polyprotein Processing as a Strategy for Gene Expression in RNA Viruses. *Seminars in Virology*, *8*(1), 15–23.

Sullivan, M. L., & Ahlquist, P. (1999). A brome mosaic virus intergenic RNA3 replication signal functions with viral replication protein 1a to dramatically stabilize RNA in vivo. *Journal of Virology*, *73*(4), 2622–2632.

Vasiljeva, L., Merits, A., Auvinen, P., & Kääriäinen, L. (2000). Identification of a Novel Function of the AlphavirusCapping Apparatus: RNA 5′-triphosphatase activity of nsP2 *. *Journal of Biological Chemistry*, *275*(23), 17281–17287.

Wang, X., Lee, W.-M., Watanabe, T., Schwartz, M., Janda, M., & Ahlquist, P. (2005). Brome Mosaic Virus 1a Nucleoside Triphosphatase/Helicase Domain Plays Crucial Roles in Recruiting RNA Replication Templates. *Journal of Virology*, *79*(21), 13747.

Ypma-Wong, M. F., Dewalt, P. G., Johnson, V. H., Lamb, J. G., & Semler, B. L. (1988). Protein 3CD is the major poliovirus proteinase responsible for cleavage of the p1 capsid precursor. *Virology*, *166*(1), 265–270.

OVERALL SUMMARY

The replication protein 1a of brome mosaic virus has a strong affinity towards the perinuclear ER membrane (nER), however, the structural features in 1a that dictate its membrane association and thereby membrane remodeling activities are unclear. This study examined the following aspects. 1. the possible role of an amphipathic α-helix in BMV 1a's membrane association, 2. the functional conservation of the helix across different members of the alphavirus-like superfamily, 3. the possibility of separating the two functional domains and specifically targeting the helicase-like domain to the nER regions where the virus replicates, and 4. the role of a linker region that functionally separates the capping and the helicase-like domain for any contribution in domain interactions and viral replication. The results are summarized as follows.

Deletion or single substitution of multiple amino acids of helix B abolished BMV 1a's localization to nuclear ER membranes, indicating its necessary role in the nER membrane targeting. Additional reporter-based, gain-of-function assays showed that helix B is sufficient in targeting several soluble proteins to the nER membranes. Furthermore, we found that helix B-mediated organelle targeting is a functionally conserved feature among membranes of the alphavirus-like supergroup that includes notable human viruses as well as plant viruses s.

BMV 1a contains two functionally separable domains responsible for 1a's capping-related activities and helicase-like activities respectively. The concerted action of both capping and helicase-like domains is responsible for recruiting necessary viral factors to support viral replication. Although the capping domain alone is sufficient for establishing membrane remodeling activities, neither the capping domain nor the helicase-like domain is sufficient to induce spherules that are typically formed by WT 1a at the sites of replication. When the two domains are expressed separately, only the capping domain associates with the nER membranes

whereas the helicase-like domain is at the cytoplasm. BMV replication was not reconstituted even when the helicase-like domain was targeted to the nER membrane where the two domains may have a chance to interact, suggesting a yet unknown mechanism or likely involvement of viral/host factors that are essential for reconstituting replication processes. Additionally, no significant role of the linker region was observed when these domains were expressed separately.

Table 3.1 List of primers

	Sense	**Antisense**
BMV 1a-L32	GGTTCCGCAGGTGGTGGTTCCGGCGCGCCAATGTCTAAAGGTGAAGAATTA	TGGCGAAGAAGTCCAAAGCTGGATCCTTATTTGTACAATTCATCCATACC
BMV HA	ACTTTAACTGCAGTTTAATTAATGGTGGCCTTTGCTTTGACTTTG	CCACCTACATCGCGGCCGCAGGCCGTAAGCTTTTCGTACT
BMV HB	ACTTTAACTGCAGTTTAATTAATGTGGAAAGGTTGGTGCCATCA	CCACCTACATCGCGGCCGCATGAATCTCCACCCCACCAAAA
BMV HA+B	ACTTTAACTGCAGTTTAATTAATGGTGGCCTTTGCTTTGACTTTG	CCACCTACATCGCGGCCGCATGAATCTCCACCCCACCAAAA
BMV Frag E	ACTTTAACTGCAGTTTAATTAATGTCGTCGACTGTTATTATTAACGG	CCACCTACATCGCGGCCGCACGGTACAGAATCTTGCTCAAA
pgk	ATATACCTCTATACTTTAACTGCAGTTTAATTAATGTCTTTATCTTCAAAGTTGTCTGTCCAAG	ATTCTTCACCTTTAGACATTTTCTTTTCGGATAAGAAAGC
HB-pgk	TTTTGGTGGGGTGGAGATTCAATGTCTTTATCTTCAAAGTTG	CCTTCTGAACCACCACCACCTACATCGCGGCCGCATTTCTTTTCGGATAAGAAAG
CMV-HB	CTATACTTTAACTGCAGTTTAATTAATGGCTTCGAGTATTTCGAAGTGG	ACCACCACCACCTACATCGCGGCCGCAAAACACACGCAGCGGACGAGT
RuV-HB	ATGGACACCATTTGGGACGCCATTAAGCGGTTCCTCGGTTGCGGCCGCGATGTAGGTGGTGGTG	ATGGACACCATTTGGGACGCCATTAAGCGGTTCCTCGGTTGCGGCCGCGATGTAGGTGGTGGTG
CCMV-HB	CTATACTTTAACTGCAGTTTAATTAATGTGGAAGGGCTGGGTCAACCAC	ACCACCACCACCTACATCGCGGCCGCACGTACTTCCTCCCCACCAAAA
HEV-HB	TATACTTTAACTGCAGTTTAATTAATGCTCTACAGTTGGCTATTTGAGTGCGGCCGCGATGTAGGTGGTGGTTCA	TGAACCACCACCACCTACATCGCGGCCGCACTCAAATAGCCAACTGTAGAGCATTAATTAAACTGCAGTTAAAGTATAGAGGT
1a-W416A	CGCGATGGGATGGAAGCGAAAGGTTGGTGCCATCACTTCAAA	TTTGAAGTGATGGCACCAACCTTTCGCTTCCATCCCATCGCG
1a-K417A	CGCGATGGGATGGAATGGGCAGGTTGGTGCCATCACTTCAAA	TTTGAAGTGATGGCACCAACCTGCCCATTCCATCCCATCGCG

1a-G418A	CGCGATGGGATGGAATGGAAAGCTTGGTGCCATCACTTCAAA	TTTGAAGTGATGGCACCAAGCTTTCCATTCCATCCCATCGCG
1a-W419A	CGCGATGGGATGGAATGGAAAGGTGCGTGCCATCACTTCAAAACTAGG	CCTAGTTTTGAAGTGATGGCACGCACCTTTCCATTCCATCCCATCGCG
1a-C420A	GAATGGAAAGGTTGGGCCCATCACTTCAAAACTAGGTTTTGGTG	CACCAAAACCTAGTTTTGAAGTGATGGGCCCAACCTTTCCATTC
1a-H421A	GAATGGAAAGGTTGGTGCGCTCACTTCAAAACTAGGTTTTGGTG.	CACCAAAACCTAGTTTTGAAGTGAGCGCACCAACCTTTCCATTC
1a-H422A	GAATGGAAAGGTTGGTGCCATGCCTTCAAAACTAGGTTT	AAACCTAGTTTTGAAGGCATGGCACCAACCTTTCCATTC
1a-F423A	GGTTGGTGCCATCACGCCAAAACTAGGTTTTGGTGGGGTGGAGATTCA	TGAATCTCCACCCCACCAAAACCTAGTTTTGGCGTGATGGCACCAACC
1a-K424A	TGCCATCACTTCGCAACTAGGTTTTGGTGGGGTGGAGATTCA	TGAATCTCCACCCCACCAAAACCTAGTTGCGAAGTGATGGCA
1a-T425A	TGCCATCACTTCAAAGCTAGGTTTTGGTGGGGTGGAGATTCA	TGAATCTCCACCCCACCAAAACCTAGCTTTGAAGTGATGGCA
1a-R426A	CATCACTTCAAAACTGCGTTTTGGTGGGGTGGA	TCCACCCCACCAAAACGCAGTTTTGAAGTGATG
1a-F427A	CATCACTTCAAAACTAGGGCTTGGTGGGGTGGAGATTCA	TGAATCTCCACCCCACCAAGCCCTAGTTTTGAAGTGATG
1a-W428A	CATCACTTCAAAACTAGGTTTGCGTGGGGTGGAGATTCATCCAG	CTGGATGAATCTCCACCCCACGCAAACCTAGTTTTGAAGTGATG
1a-W429A	CATCACTTCAAAACTAGGTTTTGGGCGGGTGGAGATTCATCCAG	CTGGATGAATCTCCACCCGCCCAAAACCTAGTTTTGAAGTGATG
1a-G430A	AAAACTAGGTTTTGGTGGGCTGGAGATTCATCCAGGGC	GCCCTGGATGAATCTCCAGCCCACCAAAACCTAGTTTT
1a-G431A	AAAACTAGGTTTTGGTGGGGTGCAGATTCATCCAGGGC	GCCCTGGATGAATCTGCACCCCACCAAAACCTAGTTTT

1a-D432A	ACTAGGTTTTGGTGGGGTGGAGCATCATCCAGGGCGAAA	TTTCGCCCTGGATGATGCTCCACCCCACCAAAACCTAGT
1a-S433A	ACTAGGTTTTGGTGGGGTGGAGATGCTTCCAGGGCGAAA	TTTCGCCCTGGAAGCATCTCCACCCCACCAAAACCTAGT
HEL *1*	ACTTTAACTGCAGTTTAATTAATGTGGAAAGGTTGGTGCCATCA	CTCCGTGTCTAGATATGCCACGAGGGTCTGAATCTCCACCCCACCAAAACCTAGTT
HEL *2*	ACTTTAACTGCAGTTTAATTAATGTGGAAAGGTTGGTGCCATCA	TCCAGCCGGTCGAATAAGTCCTCTTCAGTTGAATCTCCACCCCACCAAAACCTAGT
HEL *3*	ACTTTAACTGCAGTTTAATTAATGTGGAAAGGTTGGTGCCATCA	TGCTCTTATTTGCGATCTCACTTCCGCGTGAATCTCCACCCCACCAAAACCTAGT
HB-HEL *1*	TACCTCTATACTTTAACTGCAGTTTAATTAATGGACCCTCGTGGCATATCTAGACACG	GACTTGACCAAACCTCTGGCG
HB-HEL *2*	TACCTCTATACTTTAACTGCAGTTTAATTAATGACTGAAGAGGACTTATTCGACCGGC	GACTTGACCAAACCTCTGGCG
HB-HEL *3*	TACCTCTATACTTTAACTGCAGTTTAATTAATGCGCGGAAGTGAGATCGCAAATAAG	GACTTGACCAAACCTCTGGCG
HB *11*	ACTTTAACTGCAGTTTAATTAATGTGGAAAGGTTGGTGCCATCA	CCACCTACATCGCGGCCGCACCTAGTTTTGAAGTGATGGCACCA
HB *7*	ACTTTAACTGCAGTTTAATTAATGTGGAAAGGTTGGTGCCATCA	CCACCTACATCGCGGCCGCAGTGATGGCACCAACCTTTCCA